

UCSF

UC San Francisco Electronic Theses and Dissertations

Title

Characterization of Dendrite Development and Regeneration

Permalink

<https://escholarship.org/uc/item/1fn3s6tx>

Author

Devault, Laura

Publication Date

2018

Peer reviewed|Thesis/dissertation

Characterization of Dendrite Development and Regeneration

by
Laura DeVault

DISSERTATION
Submitted in partial satisfaction of the requirements for degree of
DOCTOR OF PHILOSOPHY

in
Neuroscience

in the
GRADUATE DIVISION
of the
UNIVERSITY OF CALIFORNIA, SAN FRANCISCO

Approved:

DocuSigned by:
Eric Huang Eric Huang
9A805C3F0428410... Chair

DocuSigned by:
Jonah Chan Jonah Chan

DocuSigned by:
Aimee Kao Aimee Kao

DocuSigned by:
Yuh-Nung Jan Yuh-Nung Jan
D56D9EF9BC7E4B3...

Committee Members

Copyright 2018

by

Laura DeVault

Dedications and Acknowledgements

I want to thank my colleagues, friends and family for the help and support that I received while working on this dissertation. Without their kindness and support, none of this would have been possible.

It has been inspirational to work in the Jan lab. Yuh Nung and Lily have created a truly unique environment to study and work. Yuh Nung has been a very calm and kind mentor. Whenever I go to talk with him about a problem that I'm having in lab or a concern that I have, he's very patient and reasonable. I always leave his office with a feeling that my problem is entirely manageable. Thank you so much for letting me join the lab.

Yuh Nung and Lily have attracted wonderful people to the lab. The hard work of the professional staff makes the lab run smoothly. Sandy, Tong, Marena, Monica, Rose, Lani and Mariati are amazing resources and without them our experiments simply would not be possible.

Working in such a talented lab has been inspirational. There's such a wide range of expertise. Attending our lab meetings, I've learned so much. I'd like to extend a special thank you to the following Jan lab members:

Susan has taught me so much about genetics. Her patience and willingness to teach have helped me learn a great deal and made a good number of experiments possible.

Katie has taught me so much about how to be successful scientist. I appreciate all the time that she's taken to work with me. I've learned so much from her. She has an excellent sense for teaching and giving relevant feedback.

Tun's help with the functional experiments in my paper was invaluable. It is often the first question people ask when I describe my study. Thank you for helping answer it.

Caitlin, Smita, Shan, Maja and Jacob provided help editing my paper and dissertation. Their comments helped clarify my writing. Matt encouraged me to pursue difficult questions and tackle technical hurdles.

David G, Josh, Jason, Shan, Lynn, Mario and Hung, my fellow Jan lab graduate students, have provided scientific help and companionship. Josh's work in adult neurons helped me a great deal and I appreciate his willingness to answer my questions. Shan was such a good colleague and friend. Mario and Lynn, thank you for the baked goods.

My committee, Eric Huang, Jonah Chan and Aimee Kao, have been supportive and helpful. All of them care deeply about the students at UCSF. I couldn't have asked for a better committee.

I would like to thank my family for their support. My parents helped me develop a love of learning and reading. Thank you for the sacrifices that you made for my education that enabled me to be here today.

Chase, my partner, has been a constant source of support throughout this process. I appreciate the emotional support he gives me when I doubt myself. He helps put everything into perspective and reminds me what is important.

My friends in San Francisco have made my time here such fun. My graduate school classmates have been simply wonderful. A special thank you to Peter, Mihir, Karuna and Sarah.

Contributions

Yuh Nung Jan directed and supervised the research that forms the basis for this dissertation. Portions of this dissertation have been previously published. Chapter 1, 2 and 3 are unpublished material. Chapter 4 is a reprint of “Dendrite regeneration of adult *Drosophila* sensory neurons diminishes with aging and is inhibited by epidermal-derived matrix metalloproteinase 2” by Laura DeVault, Tun Li, Sarah Izabel, Katherine L. Thompson-Peer, Lily Yeh Jan and Yuh Nung Jan appearing in volume 32, issue 5-6 of *Genes & Development* (2018). Individual author contributions are noted at the end of each chapter.

This work is comparable to work for a standard dissertation awarded by the University of California, San Francisco.

Characterization of Dendrite Development and Regeneration

Laura DeVault

Abstract

Despite their key role in neuronal function, current understanding of dendrite development and regeneration are lacking. We focused on the class IV dendritic arborization (c4da) neuron of the *Drosophila* sensory system to address aspects of dendrite development and regeneration due to the complex dendritic arbor and peripheral location of these neurons. Although molecular motors are known to play a role in the development of the dendritic arbor, there was not a comprehensive understanding of kinesins in dendrite development. Therefore, a screen for kinesins which regulate dendritic arbor complexity was performed. Candidates for further study were identified. Aspects of dendrite development in adulthood were also examined, including the function of c4da neuron in the adult abdomen and the source of extracellular matrix in the abdomen. The focus of this work is on the ability of neurons to regenerate dendrites. This study characterizes the structural and functional capacity for dendrite regeneration *in vivo* in adult animals and examines the effect of neuronal maturation on dendrite regeneration. which has a dendritic arbor that undergoes dramatic remodeling during the first 3 d of adult life and then maintains a relatively stable morphology thereafter. Using a laser severing paradigm, we monitored regeneration after acute and spatially restricted injury. We found that the capacity for regeneration was present in adult neurons but diminished as the animal aged. Regenerated dendrites recovered receptive function. Furthermore, we found that the regenerated dendrites show preferential alignment with the extracellular matrix (ECM). Finally, inhibition of ECM degradation by inhibition of matrix metalloproteinase 2 (Mmp2) to preserve the extracellular environment characteristics of young adults led to increased dendrite regeneration. These results

demonstrate that dendrites retain regenerative potential throughout adulthood and that regenerative capacity decreases with aging.

Table of Contents

Chapter 1: Introduction.....	1
Dendrite Development.....	2
Regeneration.....	4
Dendrite Regeneration.....	9
Significance.....	10
Chapter 2: A genetic screen for kinesins involved in dendritic arborization.....	12
Introduction.....	12
Results.....	13
RNAi screen of 21 kinesins in the <i>Drosophila</i> genome.....	13
<i>unc-104</i> RNAi reduces dendritic arborization.....	13
Discussion.....	14
Materials and Methods.....	16
Acknowledgements	16
Chapter 3: Characterizing the development and function of class IV neurons in adult	
<i>Drosophila</i>	17
Introduction	17
Results.....	19
(1) What is the <i>in vivo</i> function of the c4da neurons in adults?.....	19

(2) What tissues secrete basement membrane in the adult abdomen?.....	21
Discussion.....	22
Materials and Methods	25
Acknowledgements.....	25
Chapter 4: Dendrite regeneration of adult Drosophila sensory neurons diminishes with aging and is inhibited by epidermal-derived Matrix-Metalloproteinase 2.....	27
Introduction.....	27
Results	29
Adult dendrites can regenerate, but incompletely.....	29
Injured dendrites recover functionality.....	32
Capacity for dendrite regeneration diminishes with age.....	33
Epidermal-derived Mmp2 mediates ECM reorganization and inhibits regenerative capacity.....	35
Dendrites preferentially regenerate into ECM-rich areas.....	36
Integrin-mediated adhesion to the ECM regulates dendrite regeneration.....	38
Discussion.....	40
Mature neurons regenerate dendrites.....	40
Comparison to juvenile dendrite regeneration.....	41
Tissue maturation impedes dendrite regeneration.....	42
Dendrite ECM interaction has the potential to guide regeneration.....	43

Materials and Methods.....	44
Acknowledgements.....	47
Chapter 5: Conclusion and Future Directions.....	48
What mechanism underlies <i>unc-104</i> 's dendritic arborization phenotype?.....	48
Do kinesins contribute to dendritic regeneration?.....	49
How does CO ₂ stimulate c4da neuron activity?.....	51
What functional and structural changes occur in regenerated dendrites?.....	52
How does aging affect the quality of regeneration?	53
What molecular pathways define dendrite regeneration?.....	54
How does the extracellular environment influence the extent of dendrite regeneration?..	55
References.....	85

List of Tables

Chapter 2.....56

Table 1: List of RNAi stocks used in kinesin screen

List of Figures

Chapter 2.....	58
Figure 2.1 Knockdown of <i>pavarotti</i> and <i>subito</i> in <i>c4da</i> neurons.....	58
Figure 2.2 Knockdown of <i>unc104</i> in <i>c4da</i> neurons decreases dendritic complexity.....	59
Chapter 3.....	60
Figure 3.1 Application of carbon dioxide stimulates neural activity in <i>c4da</i> neurons.....	60
Figure 3.2 Characterization of basement membrane in the adult <i>Drosophila</i> abdomen...	62
Figure 3.3 Characterization of basement membrane in the adult <i>Drosophila</i> abdomen...	63
Chapter 4.....	64
Figure 4.1 Dendrites regenerate 1 day after eclosion.....	64
Figure 4.2. Dendrites functionally recover after injury.....	66
Figure 4.3. Dendrites regenerate at 3, 7, 30 days after eclosion.....	67
Figure 4.4. Loss of <i>mmp2</i> increases dendrite regeneration.....	69
Figure 4.5. Regenerated dendrites associate with the ECM.....	71
Figure 4.6. During the 3 days period after eclosion, <i>mmp2</i> influences dendrite regeneration.....	72
Figure 4.7. Integrin expression alters dendritic crossings and dendrite outgrowth of regenerated dendrites.....	74
Figure 4.8. Images of disc for repeated imaging in adult <i>Drosophila</i>	76

Figure 4.9. Muscle damage occurred during dendrite injury.....	77
Figure 4.10. Effect of injured neighboring neurons on dendrite regrowth.....	78
Figure 4.11. Electrophysiological response of c4da neurons.....	79
Figure 4.12. GMR51F10 Gal4 is expressed in the epidermis of the abdomen.....	80
Figure 4.13. Dendrite length of uninjured neurons at 8 days after eclosion.....	81

Chapter 1: Introduction

The specialized morphology of neurons, estimated to have as much as 10,000 times the surface area of other cell types, allows communication over both long and short distances (Horton and Ehlers 2004). Polarized processes enable communication and are distinguished in the neuron as axons, transmitters of electrical and chemical information, and dendrites, receivers of information. There are similarities between axons and dendrites, but also striking differences in the way axons and dendrites develop, maintain and repair their structures.

The dendritic arborization (da) neurons of *Drosophila melanogaster* provide an excellent system to study the development, maintenance and repair of dendrites. As part of the peripheral nervous system (PNS), four types of da neurons grow dendrites near the epidermis. The class iv (c4da) da neuron has the most complex arborization pattern (Grueber et al., 2002). Much like their larval counterparts, adult *Drosophila* c4da neurons tile the dorsal and ventral abdomen in a non-overlapping manner, creating an ideal system for *in vivo* study. Once elaborated, c4da neurons persist throughout the life of the adult (Shimono et al., 2009).

Laser ablation studies have established that c4da neurons are capable of axon and dendrite regeneration in larvae (Song et al., 2012; Stone et al., 2014; Thompson-Peer et al., 2016). However, it was unknown if the same neurons are capable of regeneration throughout adulthood. Study of these neurons in adulthood furthers our understanding of neuronal maturation, maintenance and aging (Lee et al., 2011). This dissertation uses *Drosophila* c4da neurons to address unanswered questions about dendrite development and regeneration, especially focusing on developing c4da neurons as a model to study dendrite regeneration in adulthood.

Dendrite development

Dendrites contain distinct microtubule and secretory pathway structures.

Dendrites require the secretory pathway and microtubule structures to form the arborized processes (reviewed in Valenzuela and Perez 2015; Rao and Baas 2018). Secretory components, *rab1*, *sec23*, and *sar1*, were found to be required in a screen for dendrite elaboration phenotypes in the c4da neurons. These genes are critical to the formation of Golgi outposts, a highly polarized structure which predominantly populates dendrites (Ye et al., 2007). Golgi outposts contribute to the highly branched network of the dendritic arbor by providing acentrosomal microtubule nucleation sites (Ori-McKenney et al., 2012). Studies of hippocampal pyramidal neurons demonstrate that similar structures are observed in mammalian dendrites (Horton et al., 2005).

Microtubule polarity within processes also distinguishes dendrites from axons (reviewed in Barnes and Polleux 2009; Conde and Casceres 2009). Axons of both invertebrate and vertebrate neurons contain microtubules with a uniformly plus-end out orientation (Baas et al., 1988; Stepanova et al., 2003). Dendrites contain a different microtubule structure. Primary branches of invertebrate dendrites, including c4da neurons, have microtubules largely in the minus-end out orientation (Stone et al., 2008; Goodwin et al., 2012). Immature dendrites and higher order branches of invertebrate neurons have mixed microtubule polarity (Hill et al., 2012; Ori-McKenney et al., 2012; Yau et al., 2016). Distinct molecular motors drive differences in microtubule polarity. In *Drosophila*, loss of dynein, the minus-end directed motor protein, leads to a simplified dendritic arbor, mixed microtubule polarity throughout neurites, and Golgi outposts inclusion in the axon (Zheng et al., 2008). Loss of *kinesin-5*, a plus-end directed motor, shifts the polarity of microtubules in mammalian neurons. This results in a greater proportion of

minus-end microtubules in the dendrites, as well as thinner and shorter dendrites (Kahn et al., 2015).

Transcription factors regulate development of dendritic features.

Many transcription factors regulate dendrite arbor development (reviewed in Puram and Bonni 2013). Mechanistically, some of these transcription factors act through regulation of the microtubule cytoskeleton. The transcription factor, FoxO, regulates microtubule dynamics and polarity in both axons and dendrites (Sears et al., 2016; Nechipurenko et al., 2012). FoxO represses the kinesin, Pavarotti/MKLP1, an attenuator of microtubule dynamics (McLaughlin et al., 2016). Loss of the aptly named Dendritic arbor reduction 1 (Dar1) exerts more selective effects on dendrite, but not axon growth. Dendrite specific defects in growth are attributed to Dar1's suppression of Spastin, a microtubule severing protein and several dynein related genes (Ye et al., 2011; Wang et al., 2015).

Transcription factors also regulate neuronal type-specific dendritic features. In da neurons, the transcription factors, Cut and Knot, are combinatorially expressed by subtype (Hattori et al., 2007; Jinushi-Nakao et al., 2007; Crozatier et al., 2008). These transcription factors modulate cytoskeletal architecture including microtubule stabilization and f-actin organization which distinguish architectures between subtypes of neurons (Das et al., 2017).

Extracellular cues guide dendrite development.

External signals also drive dendrite development and maturation (reviewed in Dansie and Ethell 2011). Signaling from adjacent cells, such as the epidermis and glia, promotes dendrite development and dendritic boundary determination. Dendrite outgrowth and branching characteristics in larval c4da neurons are regulated by cell adhesion molecules present in the

epidermis (Jiang et al., 2014; Meltzer et al., 2016). Adult c4da neurons are also influenced by signaling in adjacent cells of the epithelium and sternites. In the abdomen, dendrite outgrowth is restrained by a Wnt5 boundary established by the sternites (Yasunaga et al., 2015). Epidermal cells participate in dendrite reorganization.

In the larval epidermis, the heparin chondroitin sulfate proteoglycans (HSPGs), Dally and Syndecan, promote dendrite growth and microtubule stabilization in c4da neurons (Poe et al., 2017). In adults, modification of extracellular proteins regulates dendrite shape. Epidermal cells secrete Matrix Metalloproteinase 2, which degrades basement membrane in abdomen and mediates reorganization of the dendrites into a lattice like structure (Yasunaga et al., 2010).

Within the neuron, interactions with surrounding tissues are defined by several transmembrane receptors. Dendrite attachment and outgrowth is guided by the interaction between the dendrite and the extracellular matrix. Integrin cues present in the dendrites play an important role in dendrite outgrowth (Han et al., 2012; Kim et al., 2012). Integrin signaling also acts downstream of other extracellular cues important to dendrite development. Receptors, identified in axon guidance studies, including Ret, guide dendrite adherence to the extracellular matrix, which acts through integrin signaling (Soba et al., 2015).

Regeneration

Axon Regeneration

Our understanding of neuronal capacity for regeneration primarily stems from studies of axon regeneration. In the PNS, axons are capable of robust regeneration (reviewed in Girouard et al., 2018; and Filous and Schwab 2018). The ability for axons to regenerate is largely confined to the PNS, although there are notable exceptions in the central nervous system (CNS) including

olfactory sensory neurons (Morrison et al., 1995), monoaminergic neurons of the mediobasal hypothalamus (Chauvet et al., 1998) and serotonergic neurons (Hawthorne 2011, Zhou et al., 1995; Sharma et al., 1990; Inman and Steward 2003). Studies of regenerating axons in the PNS have described axonal injury and regeneration, while identifying several pathways that influence the extent of regrowth.

Severing disrupts axonal structures.

After injury, axons undergo stereotyped changes resulting in degeneration and regeneration. After a severing event, the injured axon degenerates hundreds of micrometers within 30 minutes to several hours (Kerschensteiner et al., 2005). Recent work suggests that this period may be suitable for intervention. Although only observed in a fraction of axon injuries, spontaneous resealing of the axon prevented degeneration and facilitated functional recovery *in vivo* (Williams et al., 2014). In most severing events, in which resealing does not occur, degeneration proceeds.

Mechanistically, the stress of axon injury disrupts cytoskeleton and induces lipid second messengers. Dual leucine zipper kinase (DLK) is activated by cytoskeletal disruption after axon injury (Valakh et al., 2015). DLK acts as an early retrograde signal to the cell body (Shin et al., 2012; Huntwork-Rodriguez et al., 2013). DLK activates a MAP kinase cascade which is required for axon regrowth (Hammarlund et al., 2009; Ghosh-Roy et al., 2010). Activation of DLK promotes mitochondrial localization to the axon (Han et al., 2016), as well as mRNA stability and local translation (Yan et al., 2009). Interestingly, DLK activation has also been linked to apoptosis and neuronal degeneration, further establishing DLK's link to sensing neuronal injury (reviewed in Tedeschi and Bradke 2013).

Appropriate bundling and stabilization of microtubules occurs in regenerating axons. Disorganization and disassembly of microtubules drives axon degeneration and retraction (Ertürk et al., 2007). Pharmacological stabilization of microtubules after spinal cord injury, through application of Taxol or epothilone B, increased regrowth by promoting growth cone extension (Ruschel et al., 2015; Hellal et al., 2011). Interestingly, application of epothilone B also influences the extracellular environment, decreasing scarring and the infiltration of fibroblasts into the injury site (Ruschel et al., 2015).

Lipid second messengers also play a major role in axon injury and repair. Conversion of phosphatidylinositol biphosphate (PIP₂) to phosphatidylinositol triphosphate (PIP₃) by phosphoinositide 3-kinase (PI3K) occurs during axon injury. Phosphatase and tensin homolog (PTEN) catalyzes the reverse reaction, PIP₃ to PIP₂. Manipulating this pathway has been associated with major changes in regenerative potential of the axon (Reviewed in Zhang et al., 2018)

Molecular pathways are activated during axon regeneration.

Downstream of PI3K, the mammalian Target of Rapamycin (mTOR)/AKT pathway promotes growth. During peripheral nerve regeneration of sensory neurons, there is increased expression of Akt and PI3K (Christie et al., 2010). This reflects a shift in the balance of lipid second messengers in favor of PIP₃. Deletion of PTEN can also shift the balance of lipid second messengers to PIP₃ and induce downstream expression of Akt. Numerous studies have identified PTEN as a regeneration regulator (reviewed in Park et al., 2010). Pharmacological inhibition of PTEN can further increase regeneration in sensory neurons in the PNS (Christie et al., 2010). This pathway may also contribute to the failure of the CNS to regenerate. Deletion of PTEN in retinal ganglion cells (RGC) and the cortical spinal tract promotes axon regeneration in the CNS

after optic nerve crush or spinal cord injury, respectively (Park et al., 2008; Lui et al., 2010; Zukor et al., 2013). Neuronal intrinsic expression of this pathway may also account for cell type specific differences in regenerative capacity. Endogenous expression of mTOR in subtypes of retinal ganglion cells (RGC) correlates with their ability to regenerate (Duan et al., 2015).

Increases in regeneration observed upon PTEN deletion are further enhanced by modulation of Suppressor of Cytokine Signaling 3 (SOCS3) (reviewed in Luo and Park 2012). A negative regulator of the JAK/STAT pathway, deletion of *SOCS3* alone leads to increased neurite formation in RGCs after optic nerve injury (Smith et al., 2009). Deletion of both *SOCS3* and *PTEN* increases regeneration to a greater extent than either manipulation alone (Sun et al., 2011; Jin et al., 2015). This effect has been noted in a variety of cell types including dorsal root ganglia (Gallaher and Steward 2018), RGCs (Sun et al., 2011) and corticospinal tract neurons (Jin et al., 2015). Despite increased axon growth, studies of retinal injury in *SOCS3*, *PTEN* co-deletion models found that recovery was incomplete. Neurons failed to appropriately remyelinate the axon, contributing to the lack of functional recovery (Bei et al., 2016).

Another PI3K interactor, Glycogen synthase kinase 3 (GSK-3) has also been identified in regeneration studies (Saijilafu et al., 2013). Deletion of *GSK-3* enhances the speed and extent axon regrowth after axotomy (Liz et al., 2014; Barnat et al 2016; Gobrecht et al., 2016). Mechanistically, GSK-3 negatively regulates cytoskeletal assembly during regeneration, including microtubule assembly. Gsk-3 phosphorylates Map1B, stabilizing the balance of populations of tyrosinated and acetylated microtubules, preventing dynamic outgrowth after injury (Gobrecht et al., 2014; Barnat et al., 2016). Gsk-3 also phosphorylates Collapsin response mediator protein 2 (CRMP2), a microtubule interacting protein found in the axonal growth cone

during regeneration. Phospho-mimetic CRMP-2 is sufficient to decrease regeneration after axotomy (Liz et al., 2014).

These studies suggest that Gsk-3 negatively regulates multiple aspects of cytoskeletal assembly after injury. Despite the genetic evidence for *gsk-3* in regulating axon regeneration, it is unknown if the GSK-3 pathway is a pharmaceutical target for intervention. Pharmacological inhibition of Gsk-3 has produced mixed results. Systematic application of lithium, a Gsk-3 inhibitor, increased axon regeneration in the CNS (Dill et al., 2008). But other studies suggest that Lithium and a more specific Gsk-3 inhibitor may inhibit growth by decreasing microtubule and actin filament stability (Owen et al., 2003; Lucas et al., 1998; Krylova et al., 2002). This suggests our understanding of the GSK-3 pathway in axon regeneration is incomplete.

Extracellular cues influence regeneration.

Beyond the initial period, a second phase of degeneration takes place over several weeks. During this phase, macrophages and microglia invade the injury site and participate in further axon degeneration (Horn et al., 2008; Busch et al., 2009; Evans et al., 2014). Infiltration of the injury site by macrophages and microglia produces a dense scar in the mammalian CNS. This scar has a controversial role in influencing regeneration (reviewed in Cregg et al., 2014 and Sharma et al., 2012).

Growing over a several week period after injury, the glial scar consists of astrocytes and secreted proteoglycans, namely chondroitin sulfate proteoglycans (CSPGs), and HSPGs. The core of the scar contains primarily HSPGs, whereas the surrounding area of the scar primarily consists of CSPGs and keratin proteins (Moon et al., 2002). Although the presence of these secreted proteoglycans had historically been considered uniformly inhibitory to growth, recent

work suggests that the astrocytic scar aids axon regeneration. Genetically targeted strategies to prevent scar formation failed to improve axon outgrowth. The scar may act as scaffold to provide local delivery of growth factors aiding regrowth (Anderson et al., 2016). Some of the controversy may stem from opposing roles for HSPGs and CSPGs in outgrowth. HSPGs are permissive for axonal growth, during both development and regeneration (Gysi et al., 2013). Syndecan, an HSPG, is critical for axon growth cone stabilization in *C. elegans* (Edwards et al., 2014). But, other components of the scar have inhibitory effects on axon regeneration.

CSPGs inhibit axon myelination *in vivo* (Siebert et al., 2011). Cultured neurons in development and injury studies establish fewer neurites in the presence of CSPGs (McKeon et al., 1991; Snow et al., 1994). Removal of CSPGs has been shown to increase regeneration. Treatment of spinal cord injuries with chondroitinase ABC, which is known to cleave CSPGs, increased neuronal repair (Bartus et al., 2014; Yick et al., 2004; Steinmetz et al., 2005; Filiouis et al., 2010; Carter et al., 2011 reviewed in Zhao and Fawcett 2013). Other pharmacological inhibitors of CSPGs have been shown to improve myelination outcomes (Keough et al., 2016).

Dendrite Regeneration

Far less is known about dendrite regeneration. The difficulty of following a highly branched network during degeneration and regrowth *in vivo* has hindered study of dendrite regeneration. Studies of the c4da neuron of *Drosophila* promise to remedy this deficit. In the PNS of *Drosophila* larvae, severing a single branch of the dendritic arbor results in dendrite degeneration followed by regrowth, as measured by branching at the injury site and rearrangement of the existing arbor to cover the degenerated dendritic territory (Song et al., 2012). Regeneration can also be observed after the severing of all dendrite branches. From the

remaining cell body, new dendrite branches sprout and repopulate the dendritic field (Thompson-Peer et al., 2016; Stone et al., 2014).

Some molecular pathways identified in axon regeneration studies have been shown to also contribute to dendrite regeneration. Response to injury of a single dendrite of a c4da neuron during the larval stage requires PTEN (Song et al., 2012). Dendrite regeneration may also be increased by *SOCS3* deletion. In a spinal cord injury model, *SOCS3* deletion resulted in neurites positive for Map2, a dendrite marker (Park et al., 2015).

But there is also evidence for molecular pathways specific for dendrite or axon regeneration. Mechanisms required for sensing microtubule damage upon axon injury are not required for dendrite regeneration. DLK pathway genes, *dllk*, *jnk* and *fos* were dispensable for dendrite regrowth, suggesting that dendrite regeneration is DLK independent (Stone et al., 2014). Other genes associated with regrowth of the axonal cytoskeleton, including *spastin* and *atlastin*, which coordinate microtubule and ER concentration at the tip of regenerating axons, are dispensable for dendrite regrowth (Rao et al., 2016). This suggests that cytoskeletal damage in dendrites activates distinct pathways from those in axons or that dendrite damage is sensed by a cytoskeletal independent pathway.

Significance

The focus of this dissertation is dendrite regeneration. A thorough understanding of how dendrites grow and develop provides a foundation for understanding dendrite regeneration. In my effort to understand dendrite growth, I have filled in some of the gaps in our knowledge of dendrite development.

A screen for kinesins that contribute to dendrite elaboration and development of the c4da neurons is described in the second chapter of this study. Kinesins, a group of motor proteins, play a broad role in cell biology regulating processes including microtubule assembly to organelle trafficking. Many of these processes are important for dendrite development. But, at the time of the study, there was not a systematic evaluation of kinesin contribution to the dendritic development. Our study suggests that kinesins also contribute to the development of the dendritic arbor and identifies targets for future study.

In the third chapter, I describe two studies of adult c4da neurons. One explores the development of surrounding tissue, by identifying the source of the basement membrane in the abdomen. Cell type specific drivers point to hemocytes as a source of basement membrane in the abdomen. The other study examines the function of adult c4da neurons. Calcium imaging of the c4da neurons *in vivo* suggests that neurons are activated by the application of CO₂ to the abdomen.

The fourth and final chapter focuses on dendrite regeneration in adult c4da neurons. Previous studies of dendrite regeneration have focused on the larval period. It was unknown if dendrite regeneration occurred throughout adulthood. We establish that dendrite regeneration occurs in adulthood and establish a method for studying dendrites longitudinally during adulthood. Regenerated dendrites are characterized and compared to uninjured dendrites. This chapter also describes how extracellular signals, related to dendrite maturation influence regeneration. Taken together, these studies highlight how understanding dendrite development and regeneration are linked.

Chapter 2: A genetic screen for kinesins involved in dendritic arborization

Introduction

Structurally, neurons contain distinct polarity along axonal and somatodendritic domains with complex and potentially long processes. Within these processes, cellular components critical to neuronal function are transported to distant portions of the neuron and retained in those locations. Molecular motors, including dynein and kinesins, are critical to cargo transport as well as the development of the polarized cytoskeleton. Defects in microtubules, motor proteins, and motor adaptor proteins have been associated with neurological phenotypes ranging from defects in neuronal migration, vesicular transport, and neurodegeneration (reviewed in Franker et al., 2013, Dantas et al., 2016, Terenzio et al., 2017; Jaarsma et al., 2015).

The c4da neuron has a broad dendritic arbor located just under the surface of the epidermis of larvae which is amendable for studying neuronal polarity *in vivo*. Molecular motors are integral for the establishment of the dendritic arbor. Loss of dynein impairs dendrite arborization and microtubule polarity (Zheng et al., 2008; Satoh et al., 2008). Dynein co-factors, Lis1 and NudE, have also been implicated in dendritic arborization (Arthur et al., 2015).

Less is known about the role of kinesins in establishing the invertebrate dendritic arbor. In recent years, kinesins have been shown to play an important role in c4da neuron development. Kinesin-1 regulates Golgi outpost trafficking and microtubule sliding, drastically impacting dendritic arbor complexity (Kelliher et al., 2018; Winding et al., 2016). Other kinesins may also impact dendrite arborization but have not been systematically evaluated. To identify other kinesins important in arborization, we conducted an RNAi screen in c4da neurons.

Results

Our screen targeted the role of kinesins in *Drosophila* dendritic arbor development. There are 25 reported kinesins in the *Drosophila* genome (Goshima et al., 2003). We used 25 RNAi lines and one null mutant to target 21 kinesins (Table 1). Five kinesins (*costa*, CG10845, CG17461 and *no distributive disjunction*) were not assessed due to lack of available reagents. In addition, we decided to exclude *kinesin-1*, as it has been studied in the c4da neurons (Kelliher et al., 2018).

We speculated that loss of a kinesin could increase or decrease dendritic arbor branching and possibly shift the density of the dendrite arbor. To detect these shifts in the dendritic arbor, we used Sholl analyses to compare across three neurons from each RNAi line. We found that knock down of most kinesins did not alter dendritic arborization compared to wild type.

We selected three genes for further analysis based on a reduction in dendritic branching: *pavarotti*, *subito* and *unc-104*. Knockdown of *subito* and *pavarotti* caused a mild reduction in branching (Figure 2.1). The greatest reduction in dendritic arbor was observed upon knockdown of *unc-104* (Figure 2.2). This phenotype occurred in 50% of larvae, which may be explained by the presence of TM3, Sb in BL28951, a non-larvae balancer. Upon knockdown of *unc-104* (BL28951), neurons extended primary branches of similar length to wild-type arbors but failed to extend secondary and tertiary branches like wild-type neurons. Unlike knockdown of *dhc64c*, which produced many branches near the cell body, knockdown of *unc-104* did not increase branching near the cell body. Throughout the length of the primary branches, we observed short secondary branches. The total dendritic length and branch number were reduced upon *unc-104* knockdown. Sholl analysis also reflected the smaller and less branched dendritic arbor.

Discussion

Our screen of 25 RNAi lines identified 6 RNAi lines affecting the dendritic arbor. Three of these lines were for *dhc64c*. The identification of *dhc64c* confirms that our screen can identify motor proteins that contribute to the complexity of the dendritic arbor. Dynein plays a well-established role in building the dendritic arbor (Zheng et al., 2008; Satoh et al., 2008).

We noted a slight decrease in arborization upon knockdown of kinesin-6 family members, *pavarotti* and *subito*. These results should be confirmed through use of MARCM mutants as use of RNAi may result in incomplete or off target knockdown of the protein. Other published works suggest that kinesin-6 family members, including *pavarotti*, play a role in dendrite development through regulating microtubule dynamics. In *Drosophila*, Pavarotti and binding partner, RacGAP50C, regulate neuroblast proliferation and neurite outgrowth (Goldstein et al., 2005; del Castillo et al., 2015). RacGAP50C has also been identified as a regulator of sensory dendrite branching (Gao et al., 1999). Additionally, the mammalian homolog, CHO1/MKLP1, has been shown to be critical for the development and maintenance of dendrites through the regulation of minus-end microtubules (Lin et al., 2012).

The most striking result of our screen was the identification of *unc-104*, a kinesin-3 family member, as a potential contributor to dendrite development. Previous studies also observed that expression of *unc-104* RNAi reduces dendritic complexity in c4da neurons (Chen et al., 2012). Loss of function studies should be used to confirm this phenotype. Below, we explore the possibility that *unc-104* contributes to the dendritic arbor through either regulation of the cytoskeleton or trafficking of a molecular cargo.

Differences in cytoskeletal structure and microtubule dynamics were previously linked to *unc-104*. In *unc-104* mutants, structural defects occurred in the neuromuscular junction (NMJ) and in actin rich branches of class III da neurons (c3da). C3da neuron branch distribution was shifted distally compared to controls. The NMJ was also compromised. Synaptic vesicle and boutons failed to develop (Medina et al., 2006; Kern et al., 2013). Structurally, the NMJ contained a decreased presence of stabilized microtubules (Pack-Chung et al., 2007). Previous work has shown highly ordered microtubule structure in the c4da neurons, which may be sensitive to deficiencies in microtubule assembly. Primary branches have the strongest presence of stabilized microtubules, secondary branches have lesser amounts of stabilized microtubules and tertiary branches have little to no stabilized microtubules (Ferreira et al., 2014; Sears et al., 2016). Further evidence for an altered cytoskeletal structure comes from c4da neurons. Microtubule dynamics changed upon *unc-104* knockdown, dramatically increasing EB1 comets in the dendritic arbor (Chen et al., 2012). Linking the changes in microtubule dynamics to the cytoskeletal structure may provide a mechanistic understanding of *unc-104*'s role in dendrite development.

A second mechanistic explanation for the dendritic branching phenotype observed may relate to a defect in endo-lysosomal trafficking. It is not known what role the endo-lysosomal pathway plays in dendrite development, but there is evidence that *unc-104* participates in endo-lysosomal trafficking. Mammalian Kinesin-3 family members traffic lysosomes into the periphery of cells along a tyrosinated microtubule network in HeLa cells (Guardia et al., 2016). Dendrites are also rich in tyrosinated microtubules (Baas et al., 1988) and mammalian Kinesin-3 family members facilitate trafficking into dendrites along these microtubules (Lipka et al., 2016; Tas et al., 2017). More recently, studies in the c4da neurons, suggest that Unc-104 interacts with

clathrin adaptor protein, α -Adaptin, to regulate the endo-lysosomal pathway during dendritic pruning (Zong et al., 2018). Evaluating other endo-lysosomal proteins during the course of dendrite development will provide insight into the importance of these pathways for dendrite growth.

Materials and Methods

To visualize c4da neurons and knockdown specific kinesin proteins, we crossed *w; ppk-cd4-tdGFP, UAS-dcr; ppk-gal4^{1a}* (Han et al., 2011) flies to RNAi lines available from the Bloomington stock center (Table 1). Larvae from this cross were raised to the third larval instar. To image c4da neurons, larvae were mounted on a SP5 confocal microscope system at 40x magnification. Dendrite length and sholl analysis were semi-automatically traced and quantified using the Simple Neurite Tracer plug-in for Image J.

Acknowledgements

We thank Dr. Kassandra Ori-McKenney for her help designing these experiments and Susan Younger for her help with fly genetics.

Chapter 3: Characterizing the development and function of c4da in adult *Drosophila*

Introduction

Sensory dendritic arborization (da) neurons of *Drosophila* larvae have been characterized and studied for almost 20 years. The majority of these studies have focused on larvae. More recent studies have demonstrated that a subset of these neurons survive larval metamorphosis and persist during the adult stage of the *Drosophila* life cycle. C4da neurons, v'ada and ddaC, populate the ventral and dorsal abdomen, respectively (Kuo et al., 2005; Shiono et al., 2009; Satoh et al., 2012). Due to the heavy pigmentation of the dorsal, but not ventral abdomen, v'ada, is the most accessible for and therefore is the focus of this chapter. Here, I address two outstanding questions about v'ada neurons in the adult:

(3) What is the *in vivo* function of the c4da neurons in adults?

In larvae, c4da neurons have been implicated in a wide range of nociceptive behaviors, including activation by intense short-wave length light, harsh touch and heat (Hwang et al., 2007; Mauthner et al., 2014; Tracey et al., 2003; Xiang et al., 2010; Gorczyca et al., 2014; Guo et al., 2014). In electrophysiological preparations, larval c4da neurons can be activated with an acidified solution (Bioko et al., 2012). Further characterization suggests that these neurons play a role in larval escape behaviors. Optogenetic stimulation of the c4da larval neurons initiates larval rolling. Buzzing, reminiscent of the sound of parasitic wasps which target *Drosophila* larvae, can also elicit rolling. Thus, these sensory neurons may initiate the rolling behavior to escape approaching wasps (Hwang et al., 2007).

It is not known if c4da neurons serve a similar function in adults or what physiological circumstances activate the c4da neurons in adults. In the 4th chapter of this dissertation, we

demonstrate that the adult neurons, much like the larval c4da neurons, respond electrophysiologically to stimulation by acidified solutions (Boiko et al., 2012). It is not known what the endogenous source of acid may be. Further study is needed to understand the physiological function of these neurons. To this end, we applied a calcium imaging approach to look at c4da neuron function in the adult.

Calcium based imaging approaches have been applied to the larval c4da and c3da neurons to study function *in vivo*. The c3da neurons respond to gentle touch through the channel *nompc*, which initiates calcium transients in the neuron's dendrites. While calcium imaging has not been used to assay larval c4da neuron function, ectopic expression of *nompc* also induced calcium transients after gentle touch in larval cd4a neurons (Yan et al., 2013). Calcium imaging approaches have not been successfully used to study endogenous stimuli in c4da neurons. In this set of experiments, I sought to identify stimulation paradigms using calcium imaging to study the function of c4da neurons in adult *Drosophila*.

(4) What tissues secrete basement membrane in the adult abdomen?

Our study of regeneration in adult *Drosophila* suggests that remodeling of the surrounding environment, including the basement membrane regulates the potential for regrowth as the fly ages. A more thorough understanding of the source of basement membrane in the adult will aid future studies.

During metamorphosis, tissue remodeling, and programmed cell death shape the abdomen of the emerging fly. Larval epidermal cells, a subset of larval muscles, and certain classes of da neurons undergo programmed cell death. Other da neurons drastically remodel by pruning and regrowing dendrites (Kuo et al., 2005; Williams and Truman 2005; Kuo et al., 2006). During this

time, histoblasts generate adult epithelial cells which migrate into and populate the abdomen. The adult epithelial cells, as well as remodeled neurons and muscle repopulate the abdomen (Kuleesha et al., 2016; Madhavan et al., 1980; Ninov et al., 2007; Bischoff et al., 2009).

When the adult emerges from the pupal case, the abdomen consists of a layer of epidermal cells, a layer of basement membrane and a deeper layer of lateral abdominal muscles. The c4da neurons are located in the basement membrane layer. It is unknown what the initial sources of basement membrane in the adult abdomen are. Basement membrane protein production has been associated with a wide range of tissues, ranging from the fat body (Pastor-Pareja et al., 2011), and hemocytes (Matsubayashi et al., 2017; Van De Bor et al., 2015). Basement membrane remodeling has also been associated with epithelial cells in the abdomen (Yasunaga et al., 2010). We therefore evaluated epithelial cells and hemocytes as sources of basement membrane in the abdomen.

Results

(1) What is the *in vivo* function of c4da neurons?

Initial attempts to assess the activity of the c4da neurons *in vivo* focused on spontaneous activity in restrained, but unanesthetized flies, using the imaging chamber described in the following chapter (Figure 4.8). In these preparations, the abdomen could freely contract, as well as move laterally. Vertical movement was largely prohibited by the presence of foam padding. The limited vertical movement facilitated sustained proximity to the cover slip and imaging of the neurons during movement. There were instances of increased GCaMP6f signal during movement or spontaneous contraction in individual dendrites, but these were transient in nature (Figure 3.1 B, +9s frame). This activity was not uniform, and movement was mostly not

synchronized with GCaMP6f transients in the dendrites. Little to no GCaMP6f signal was observed in the cell body.

More sustained GCaMP6f activity was observed upon application of CO₂ to the imaging chamber (Figure 3.1 A). In the same preparation, application of CO₂ resulted in sustained GCaMP6f signaling throughout the dendritic arbor and cell body. Upon application of CO₂, there was a 567% increase in GCaMP6f signal in the cell body (n=6). Without application of CO₂, there was a 6% increase in GCaMP6f signaling in the cell body over a comparable period (n=5) (Figure 3.1 D). The GCaMP6f response did not diminish during stimulation (Figure 3.1 C).

To address age dependent changes in neurons, 21-day old flies were assessed. There was a 403% (n=4) increase in GCaMP6f activity after exposure to CO₂ in the cell body of c4da neurons. This suggests that neurons maintain their responsiveness to this stimulus as the animal ages. Animals older than 21 days were not assessed.

Expression of the DEG/ENaC ion channels, *ppk1* and *ppk26*, are required for many c4da neuron driven larval behaviors. Response to mechanical stimuli, but not thermal stimuli, requires heteromeric expression of *ppk1* and *ppk26* (Zhong et al., 2010; Guo et al., 2014; Gorczyca et al., 2014; Mauthner et al., 2014). Proprioceptive properties of c4da neurons have also been linked to both *ppk1* and *ppk26* (Ainsley et al., 2003; Gorczyca et al., 2014). To better understand the nature of this stimulus, I sought to look at this response in *ppk1* and *ppk26* null backgrounds.

Loss of *ppk26*, did not alter the response to CO₂. Upon application of CO₂ to *ppk26*⁴²⁹ flies, there was a 415% (n=6) increase in GCaMP6f signaling in the cell body (Figure 3.1 E). The prolonged response during CO₂ exposure was also observed in these flies.

At the time of these studies, there was not an available GCaMP6f reagent on the III chromosome. To study *ppk1*, which is located on the II chromosome, we used the UAS-GCaMP6m reagent, which was available on III. We did not observe the same dramatic increase in signal with the 6m reagent as compared to use of the 6f reagent. Upon CO₂ application to GCaMP6m expressing flies, there was an 82% (n=3) increase in signal. In *ppk1*^{Δ16} animals, there was a 7% decrease in GCaMP6m signal upon CO₂ application (Figure 3.1 F). Due to the relatively small increase observed in these neurons, we discontinued experiments with the 6m reagent. Future experiments with GCaMP6f may provide more information.

(2) What is the primary source of the basement membrane in the adult abdomen?

In the abdomen of adult *Drosophila*, there is developmentally regulated distribution of Collagen IV. Previous studies have used an endogenously tagged *viking*, a Collagen IV α chain, to study localization (Figure 3.2 A). Collagen IV initially surrounds the lateral tergo-sternal muscles (LTM) of the abdomen. Within three days of eclosion, epidermally derived Matrix Metalloproteinase 2 degrades Collagen IV between the muscle and epidermis. In older animals, thin strips of Collagen IV are relegated to the space between muscles (Yasunaga et al., 2010).

To understand the source of basement membrane in the abdomen, we used tissue specific Gal4 lines for hemocytes and epithelium and UAS expression lines for GFP tagged secreted forms of CollagenIV α chains, *vkg* and *cg25c*. Epithelial cell driven expression of *vkg* was punctate in nature, with a mixture of small and large GFP particles. Epithelial cell driven expression of *cg25c* was diffuse with some amorphic shapes (Figure 3.3 C). The pattern of epithelial driven expression of *vkg* and *cg25c* does not match the endogenous pattern of *vkg* expression.

Hemocyte driven expression of *vkg* and *cg25c* mimicked the endogenously tagged expression pattern for *vkg*. There were lateral stripes of GFP that extended ventrally towards the sternites (Figure 3.2 B). The spacing of these stripes was consistent with the spacing of LTM muscles of the abdomen. Dendrites of the *c4da* neurons largely corresponded with these stripes. The correlation between the Gal4 driven expression pattern and the endogenous expression pattern of Collagen IV suggest that hemocytes are a source of basement membrane in the *Drosophila* abdomen.

Discussion

***In vivo* function of *c4da* neurons**

Calcium imaging suggests that application of carbon dioxide can induce neuronal activity in the adult *c4da* neurons. Dramatic increases in GCaMP signal throughout the dendritic arbor and cell body were observed when CO₂ was administered to the adult fly. This response was also observed in 21-day old flies, suggesting that these neurons are responsive to carbon dioxide throughout adulthood. However, it is unknown how this stimulus induces neuronal activity. Carbon dioxide has a complex effect on *Drosophila* and further study will be required to determine the mechanism that mediates neuronal response upon introduction of CO₂.

Carbon Dioxide may directly stimulate *c4da* neurons. Studies of the larvae establish that *c4da* neurons act as nociceptors (Boiko et al., 2012; Hwang et al., 2007; Mauthner et al., 2014; Tracey et al., 2003; Xiang et al., 2010). It is possible that CO₂ is noxious to *Drosophila*. At low concentrations, CO₂ is an aversive stimulus to walking *Drosophila*. Stressing *Drosophila* causes secretion of CO₂, which has been shown to repel other flies through chemosensory receptors expressed in olfactory sensory neurons (Suh et al., 2004; Jones et al., 2007; Kwon et al., 2007). The aversive nature of the stimulus is consistent with the role of *c4da* larval neurons as

nociceptors. However, additional studies suggest the attractive or aversive nature of CO₂ may be context dependent. Attractive qualities have been associated with CO₂ during flight and feeding behaviors. In flight, obligate olfactory receptors expressed in coelomic sensilla neurons mediate attraction to CO₂ (Wasserman et al., 2013). A subset of gustatory neurons in the taste peg also detect CO₂, which may function to test nutrient value from microorganisms such as yeast (Fischler et al., 2007). Because the valence of this stimulus is unknown, we cannot conclude that the c4da neurons are acting as nociceptors in this instance. Chemosensory receptors, Gr63a and Gr21a, have been shown to mediate the molecular responsiveness to CO₂ in *Drosophila* (Kwon et al., 2007). Presence of these chemosensory receptors in the c4da neurons would support direct detection of CO₂ by the c4da neurons.

An alternative explanation is that CO₂ indirectly stimulates c4da neurons, either through changes in the hemolymph or muscle contraction. Changes to the hemolymph may directly stimulate these neurons through changes in pH. Interestingly, c4da neurons are responsive to changes in pH (Boiko et al., 2012). In adults, c4da neurons can be stimulated at pH 3.0 as described in chapter 4. Studies of CO₂ as an anesthetic in *Drosophila* describe physiological effects include a rapid drop in pH of hemolymph, and increased heart rate followed by cardiac arrest (Badre et al., 2005). However, previous studies suggest that the change in hemolymph acidity upon CO₂ exposure may be outside of this range demonstrated to stimulate c4da neurons. Twenty minutes of 100% CO₂ exposure only lowers HL3, a hemolymph like solution, to pH 5.0 (Badre et al., 2005). It is possible that a greater change in pH is observed *in vivo* or that the drop to pH 5.0 is sufficient to prime neurons for further stimulation. A more thorough understanding of how CO₂ alters hemolymph will be required to understand this response.

Indirect stimulation may also occur through muscle contraction. Initial application of CO₂ results in abdominal contraction preceding the GCaMP activity observed in neurons. Larval studies posit that the c4da neurons act as proprioceptors, gathering information about muscle contraction and abdominal movement. Loss of c4da neuron specific ion channels, Ppk1 and Ppk26, results in uncharacteristically straight and fast crawling behavior, indicative of proprioceptive defects (Ainsley et al., 2003; Gorczyca et al., 2014; Fushiki et al., 2016). While these studies have not been expanded to adulthood, the positioning of the adult c4da neuron indicates that muscle contraction may be important to the function of these neurons. Early in adulthood, the c4da neurons reorganize to largely align with abdominal muscles (Yasunaga et al., 2010). Although this reorganization has not been linked to c4da function, it is reasonable to speculate that form and function are related. Further study of GCaMP activity in Mmp2 deficient *Drosophila*, in which neurons do not align with the lateral muscles of the abdomen, may offer insight into this possibility. Understanding if dendritic realignment facilitates neuronal activity of c4da neurons will clarify if muscle contraction is the underlying stimuli for these neurons.

Source of adult basement membrane

Basement membrane provides developmental cues to surrounding tissues. Basement membrane stiffness shapes organ morphogenesis (Crest et al., 2017; Bunt et al., 2010) and composition affects stem cell niches (Van De Bor et al., 2015). The maturation of the c4da neuron dendritic arbor is shaped by the presence of basement membrane in abdomen (Yasunaga et al., 2010). However, little is known about the source of basement membrane in the abdomen.

Our results suggest that hemocytes are an important source of basement membrane in the adult abdomen. Tissue specific expression of these genes in the hemocytes matched the

endogenous localization of GFP tagged *vkg*. Epithelial specific expression of secreted Vkg and Cg25c did not match the endogenous localization of Vkg. This suggests that epithelial cells are not a major source of these proteins. Hemocyte originated basement membrane is consistent with studies from embryonic *Drosophila*, in which hemocytes contribute Collagen IV, Laminin A and Perlecan (Matsubayashi et al., 2017; Kushche-Gullberg et al., 1992). It is possible that other sources contribute to basement membrane development in abdomen, specifically the fat body and muscles, which are known to synthesize Collagen IV (Yasothornsrikul et al., 1997; Pastor Pareja et al., 2011; Matsubayashi et al., 2017). Assessing the contribution of the fat body and muscles will be an interesting avenue for future exploration.

Materials and Methods

Fly Stocks

To perform calcium imaging in *c4da* neurons, we used flies heterozygous for *UAS-tdTomato*, *UAS-GCaMP6f*; *ppk-gal4* (Chen et al., 2013). To perform calcium imaging in a *ppk26* null fly, we used *UAS-tdTomato*, *UAS-GCaMP6f*; *ppk26^{Δ29}* crossed to *ppkgal4*; *ppk26^{Δ29}*. To perform calcium imaging in a *ppk1* null fly, we used *ppk1^{Δ16}*; *ppkgal4* crossed to *ppk1^{Δ16}*; *UAS-tdTomato*, *UAS-GCaMP6m*. We evaluated *ppkgal4* and *UAS-tdTomato*, *UAS-GCaMP6m* heterozygotes as a control.

To evaluate the potential source of basement membrane in the adult abdomen, we used expressed GFP-tagged inducible forms of Collagen IV subunits, Viking and Cg25c (Van De Bor et al., 2015). We used *GMR51F10-Gal4* (Losick et al., 2013) to express in the adult epithelium and *VT050116-Gal4* to express in the hemocytes (line identified by Sarah Headland).

Calcium Imaging

Calcium imaging was performed in the adult anesthetization chamber described in Chapter 4. Flies were mounted in the chamber as previously described in an area with less foam, where the fly's movement was somewhat, but not entirely constricted. No CO₂ was applied initially. Time of CO₂ application was noted, and experiments were aligned to the initial application time. After initial application, CO₂ exposure was sustained. Controls, in which no CO₂ was applied, were also performed. Quantification of GCaMP activity was performed in the cell body. Images were corrected for drifting across stacks by using the StackReg plugin in Image J. An area that encompassed the cell body was measured for both tdTomato and tdGFP fluorescence. To normalize GCaMP activity, a ratio of average GCaMP fluorescence to tdTomato fluorescence in the area surrounding the cell body was calculated (GCaMP_N). To calculate an average, 10 frames were selected starting 15 frames after the stimulus was applied. The Baseline activity was calculated 15 frames from the application of the stimulus. Data was aligned to initial application of CO₂.

$$\Delta\text{GCaMP} = (\text{GCaMP}_N - \text{GCaMP}_{N\text{-baseline}}) / \text{GCaMP}_{N\text{-baseline}}.$$

Acknowledgements

We thank Susan Younger for her help with genetics, Sarah Headland for her identification of a Hemocyte Gal4 driver, and Beverly Piggott for her help quantifying calcium imaging.

Chapter 4: Dendrite regeneration of adult *Drosophila* sensory neurons diminishes with aging and is inhibited by epidermal-derived Matrix-Metalloproteinase 2

Laura DeVault, Tun Li, Sarah Izabel, Katherine L. Thompson-Peer, Lily Yeh Jan, Yuh Nung Jan

Introduction

Dendrite injury can result from acute injury to the neuron or from progressive degeneration of the neuron. Alzheimer's disease, depression and stroke are associated with loss of dendrite complexity, spine loss and dendritic withering (Koleske, 2013; Vickers et al., 2016). Indeed, the severity of dendrite loss may correlate with the severity of behavioral deficits (Falke et al., 2003). Whereas the importance of dendrite loss in these conditions is well recognized, dendrite recovery and regeneration remain unstudied, and dendrite regeneration also takes place in young adult *Drosophila* and *C. elegans* (Oren-Suissa et al., 2017; Stone et al., 2014). It will be important to examine the quality of the regenerated dendrite and to determine whether dendritic regenerative capacity persists throughout adulthood. However, these inquiries have been hampered by the difficulty of following the progression of dendrite regeneration over time. To further our understanding of dendrite regeneration in adults, we establish a system to study dendrite regeneration in the peripheral nervous system of adult *Drosophila*.

Drosophila dendritic arborization (da) neurons are well suited for studying the mechanisms of dendrite regeneration. Adjacent neurons non-redundantly cover the epithelium of the larval body wall and the adult abdomen. Their dendritic arbors are primarily restricted in a two-dimensional space by the surrounding epithelia (Grueber et al., 2002). The position and elaborate morphology of the dendritic arbor has facilitated many *in vivo* studies of dendrite

development (Dong et al., 2015; Jan & Jan, 2010). Interestingly, these neurons develop and elaborate a dendritic arbor twice, once during the larval stage, and again during metamorphosis (Kuo et al., 2005; Kuo et al., 2006; Williams et al., 2005; Williams et al., 2005). The dendritic arbor of the c4da neuron that degenerated during the early pupal stage is then re-elaborated subsequently during the pupal phase and extends into the space between the lateral abdominal muscles and the epithelium. Initially, the arbor extends radially from the center of the abdominal segment. Within the first 3 days after eclosion, the orientation of the dendritic arbor matures, taking a lattice like orientation, which aligns with the lateral muscles of the abdomen. This change in orientation depends on tissue remodeling after eclosion, which is specifically mediated by Mmp2 secretion from the epidermal epithelial cells (Yasunaga et al., 2010). The arbor remains stable in orientation and dendrite length after this change for at least 21 days (Shimono et al., 2009), presenting the opportunity to study adult dendrites *in vivo* as the animal ages.

Previously, it was reported that the c4da neuron in newly eclosed *Drosophila* is capable of regenerating dendrites following injury (Stone et al., 2014). This raised several interesting questions: (1) Does the neuron's ability to regenerate dendrites change with aging? (2) What is the quality of the regenerated dendrites in terms of their morphology and function? (3) What regulates the capacity of dendrite regeneration? We were particularly interested in finding ways by which to enhance a neuron's ability to regenerate dendrites, which might lead to therapeutic applications. To examine injury and regeneration of dendrites, we chose to focus on v'ada, a c4da neuron with favorable location for our experiments in the adult *Drosophila*. We first developed a novel method to follow changes in individual, identifiable neurons *in vivo* at multiple time points in adult flies. Without the ability to repeatedly image the same animal as the adult fly ages, previous studies of c4da neurons in *Drosophila* adults had relied on imaging the

mounted abdomens of dissected animals in terminal experiments or were limited to the period immediately after eclosion (Shimono et al., 2009; Stone et al., 2014). While protocols have been developed to mount legless adults for time lapse imaging sessions of up to 12 hours (Yasunaga et al., 2010), this approach was terminal. To study dendrite recovery from injury, we needed to enable animals to survive multiple imaging sessions and fully recover. Whereas it is possible to repeatedly image the wings of intact adults to study the regeneration of axons of wing neurons after injury (Brace et al., 2017; Soares et al., 2014), those wing neurons are unsuitable for examining dendrite architecture because they lack complex dendritic arbors.

Using the adult c4da neuron system, we characterized the recovery from injury and examined how tissue remodeling affects regenerative growth of the dendrites. Here, we show that adult neurons can regenerate dendritic arbors after injury. Regenerated dendrites have structural features that are less complex than those of uninjured neurons, as indicated by the total dendritic length, territory coverage and the presence of stabilized microtubules. Nevertheless, the regenerated dendrites recovered their ability to respond to sensory stimuli. Regenerative capability of the dendrites declined with the age of the fly, starting at 3 days after eclosion. This decline corresponded with the period of dendritic remodeling. Preventing dendritic remodeling through knockdown of *mmp2* preserved the ECM and increased dendrite regeneration.

Results

Adult dendrites can regenerate, but incompletely

To examine the response of adult dendrites to injury, we established a novel method to repeatedly image the same identified neuron in anesthetized adult *Drosophila*. To achieve this, we developed a padded chamber for mounting adult flies, exposed to a carbon dioxide source as

an anesthetic, where the abdomen is positioned so that it is suitable for confocal imaging (Figure 4.1A, Figure 4.8). Flies were anesthetized only during the injury procedure and subsequent imaging sessions and were otherwise housed in individual vials.

Adult flies were initially anesthetized on ice. Once the fly was placed into the padded chamber, we severed the dendrites of individual neurons using a two-photon laser (Figure 4.1B). Using the laser mediated focal injury, all dendrites were severed at the first branch point, as described in previous studies of larval dendrite regeneration (Stone et al., 2014; Thompson-Peer et al., 2016).

Having established a technique that allows us to image as well as injure the dendrites of c4da neurons *in vivo* in adult flies, we then tested if dendrites had the ability to regenerate by following dendritic growth of the same neurons after injury in the same fly. We chose to perform our experiments on v'ada neurons, because this subset of c4da neurons are situated at the ventral surface of the abdomen and not obscured by dark pigment making them particularly well suited for our experimental protocol. Laser mediated focal injury to v'ada was performed at 1 day after eclosion (@1 Day). Imaging 1 day after severing all dendrites, we found that dendrites distal to the site of injury had degenerated. For all experiments, we imaged neurons at 1 day after injury to confirm that all dendrites had been fully severed and subsequently degenerated (+1 Day, Figure 4.1C, top left). At 7 days after injury, neurons were again imaged to assess dendrite regrowth (+7 Days, Figure 4.1C top right). Although focal in nature, laser injury of the abdomen also injured surrounding tissues. We noted injury and subsequent degeneration of the lateral muscle of the abdomen, typically one or two muscle fibers (Figure 4.9). The dendrite arbor of each neuron covers a defined territory of the body wall. We quantified regeneration as the total change in dendrite length in μm between +1 and +7 days after injury and as the fraction of the

total territory that is covered by regenerated dendrites at +7D after injury (Figure 4.1C, D, 4.3C). For all experiments, control uninjured neurons were also mounted during injury and imaged at all time points.

We found that, after injury at 1 day after eclosion (@1D), most neurons of the adult fly did regrow dendrites by 7 days after injury. Adjacent uninjured control neurons did not grow in length between +1 and +7 days after injury. By contrast, neurons whose dendrites had been severed demonstrated significant increases in dendrite length and territory coverage over this time (Figure 4.1D). Although regenerated dendrites displayed significant regrowth, the regenerated arbors failed to occupy the same area or regrow to the same total dendrite length as uninjured neurons. Between +1 day and +7 days after injury, we observed an increase of $250 \pm 300 \mu\text{m}$ in uninjured neurons compared to an increase of $2700 \pm 900 \mu\text{m}$ in injured neurons (Figure 4.1D). The arbor of injured neurons was also more compact and smaller than that of uninjured neurons, occupying only $33 \pm 13\%$ of the territory occupied by control, uninjured neurons (Figure 4.1E, 4.3C). Neighboring neurons did not influence the extent of dendrite regeneration. Injured neurons with intact, uninjured neighbors regenerated dendritic arbors with dendritic lengths and coverage areas statistically indistinguishable from injured neurons with injured or absent neighboring neurons (Figure 4.10).

In addition to assessing the length and coverage of the regenerated dendrites, we wanted to examine the structural integrity of the dendrites. To assess the cytoskeletal structure of regenerated dendrites, we examined microtubule stability in the injured and uninjured arbors. Futsch, the *Drosophila* homolog of Map1B, is associated with stabilized microtubules and is found in the axon, cell body and dendrites of neurons (Hummel et al., 2000). Previous studies have shown that Futsch is highly expressed in primary branches and at lower levels in secondary

branches, but is rarely detectable in tertiary branches (Ferreira et al., 2014; Sears et al., 2016). In uninjured neurons, we observed strong Futsch staining along primary branches and weaker staining of higher order branches. In injured neurons, we observed patchy and weaker Futsch staining in the primary branches and throughout the regenerated dendritic arbor (Figure 4.1F). We selected the most intensely stained Futsch branches for comparison to primary branches in injured and uninjured neurons and found that regenerated dendrites had significantly weaker Futsch intensity compared to uninjured neurons (Figure 4.1G). This suggests that regenerated dendrites are different from uninjured dendrites.

Injured dendrites recover functionality

We next tested whether regenerated dendritic branches could also functionally recover. Larval c4da neurons are polymodal; they respond to light, thermal, chemical and mechanical stimuli (Boiko et al., 2012; Hwang et al., 2007; Mauthner et al., 2014; Tracey et al., 2003; Xiang et al., 2010; Gorczyca et al., 2014; Guo et al., 2014; Mauthner et al., 2014). Delivery of an acid stimulus is sufficient to drive larval c4da neurons to threshold and evoke a burst of action potentials (Boiko et al., 2012). To test the ability of regenerated neurons to functionally respond, we performed electrophysiology experiments using acidified solutions to stimulate injured neurons 7 days after injury as well as uninjured neurons in age matched flies as a control. Neurons were injured at 1 day after eclosion. At 1 day after injury, balded neurons, namely neurons whose dendrites have all been severed and subsequently degenerated after injury, but have not yet regenerated, did not respond to an acid stimulus (Figure 4.11). At 7 days after injury, injured and uninjured neurons were indistinguishable in their response to acid stimulation. To better characterize the response to acidified stimulation, we performed a dose response curve, using solutions with acidity ranging from pH 3 to pH 7. Maximal response was observed at pH 3,

and the response declined at pH 4. No substantial response was observed at pH 5 or higher. Uninjured neurons had a firing rate of 14.9 ± 6.9 Hz and injured neurons had a firing rate of 10.1 ± 4.0 Hz at pH 3 (Figure 4.2A, B).

Response to mechanical stimuli depends on the presence of Ppk26 in larvae (Gorczyca et al., 2014; Guo et al., 2014; Mauthner et al., 2014). While no studies have yet demonstrated that adult neurons respond to mechanical stimuli, adult c4da neurons express Ppk26 (Figure 4 2C). Appropriate expression and trafficking of ion channels is a minimal requirement for neuronal function. Presence of neuron specific ion channels suggests that neurons are competent to respond to stimuli. To test for expected ion channel presence, we performed immunohistochemistry using a Ppk26 antibody. We found that Ppk26 was present at the cell surface in both injured and uninjured v'ada dendrites (Figure 4.2C). This suggests that regenerated v'ada dendrites could be competent to respond to mechanical stimuli in addition to chemical stimuli. We also tested if Ppk26 was required for the response to acid stimulation and found that Ppk26 is not required. We tested adult c4da neurons in *ppk26^{Δ11}/Df(3L) Exel⁸¹⁰⁴* flies, which are null for *ppk26*, and observed bursting action potentials similar to those observed in wild-type flies (Figure 4.11).

Capacity for dendrite regeneration diminishes with age

After observing that dendrites of v'ada neurons are capable of regrowth at 1 day after eclosion, we wanted to determine if regeneration was possible in older adults. Dendrites undergo extensive remodeling and rearrangement around 2 days after eclosion (Shimono et al., 2009; Yasunaga et al., 2010), so it was especially important to determine if these neurons could regenerate dendrites after this reshaping was complete and they had achieved a stable morphology. To assess the potential and quality of regeneration as a function of age, we severed

all dendrites in the neurons of adults that were either 3, 7, or 30 days old (@ 3 Days, @ 7 Days, @ 30 Days), confirmed injury 1 day later (+1D), and assessed regeneration 7 days later (+7D). Animals more than 30 days old were too frail to survive the injury experiment and subsequent imaging.

We found that neurons in animals at all ages tested could regenerate after injury (Figure 4.3A, B). However, the extent of regenerative capacity diminished in older animals. In terms of dendrite length, neurons injured at 3, 7, or 30 days only regrew half as much as neurons injured in 1-day old adults. Neurons injured in 3, 7- and 30-day old adults regrew $1400 \pm 700 \mu\text{m}$, $1300 \pm 600 \mu\text{m}$ and $1400 \pm 500 \mu\text{m}$ of dendritic length respectively over the 7-day period after injury, compared to neurons injured at 1 day which regrew $2700 \pm 900 \mu\text{m}$. Uninjured controls from 1, 3, 7 and 30 days respectively grew $250 \pm 300 \mu\text{m}$, $150 \pm 350 \mu\text{m}$, $-400 \pm 600 \mu\text{m}$ and $200 \pm 530 \mu\text{m}$ between +1 and +7 days after injury of adjacent neurons (Figure 4.3B). In terms of the area of territory covered by regenerated dendrites, the area covered by 1 day old and 3-day old adult neurons, $33 \pm 13\%$ and $27 \pm 17\%$, was comparable (Figure 4.3C). But neurons injured in 7-day old adults recovered $17 \pm 12\%$, approximately half the territory of neurons injured in 1-day old adults, while neurons injured in 30-day old adults could only cover $11 \pm 6\%$, approximately a third of the area of neurons injured in 1-day old adults. Thus, we found that the ability to regrow dendrite in length declined between 1- and 3-day old animals, but then remained stable, whereas the ability to recover body wall territory with regenerated dendrites gradually decreased with age.

Dendrite structure was disorganized in all regenerated neurons at all time points. One measure for dendrite disorganization is the number of dendritic crossing events. These dendrites normally display self-avoidance, where the sister branches of the same neuron do not cross one

another. To account for the reduced size of injured dendritic arbors, crossing events are normalized to dendritic length. We examined crossing events in neurons injured at 3 and 30 days after eclosion (Figure 4.3E). At both times points, injured neurons had a greater number of self-crossing defects than that of uninjured neurons (Figure 4.3F).

Epidermal-derived Mmp2 mediates ECM reorganization and inhibits regenerative capacity

Adult c4da neurons undergo a dramatic transformation after eclosion. Neurons from animals that have just eclosed have a radial orientation which is then reorganized into a lateral or lattice-like orientation within 3 days after eclosion. This period corresponds with the decline in dendrite regenerative capacity. Our data above demonstrate that neurons can regrow dendrites after injury before and after this transition. We hypothesized that neuronal remodeling might influence the extent of dendrite outgrowth after injury. Remodeling depends on epidermal secretion of Mmp2 (Yasunaga et al., 2010). To address the role of neuronal remodeling in dendrite regeneration, we examined regeneration in *mmp2* mutants. We measured the regenerative ability of dendrites in *Drosophila* trans-heterozygous for an allele of *mmp2*^{M100489} and a deficiency for *mmp2*, *Df(2R) BSC132*. After confirming dendrite degeneration + 1 day after injury, we measured dendrite regrowth and coverage at +7 days after injury (Figure 4.4A, B, C). We found that, compared to injured wild-type neurons, injured neuron regrowth and coverage was greater in *mmp2* mutants. While wild-type neurons regrew $2700 \pm 800 \mu\text{m}$ of dendrite length and recover $31 \pm 3\%$ of their territory, *mmp2* mutants regrew $4200 \pm 800 \mu\text{m}$ and recovered $47 \pm 9\%$ of their territory, an increase of approximately 50% over wild-type (Figure 4.4B, C). Total dendrite length of uninjured neurons was also greater in *mmp2* mutants than in

wild-type (Figure 4.13). This suggests that *mmp2* inhibits dendrite outgrowth as well as dendrite regeneration after injury.

In the adult abdomen, the expression of *mmp2* is restricted to transient expression in the epidermal epithelial cells during a period directly after eclosion (Yasunaga et al., 2010). In addition to the role for matrix metalloproteinases in tissue remodeling, MMPs have been shown to facilitate wound healing and axon guidance in *Drosophila* (Huang et al., 2011; Miller et al., 2007; Stevens et al., 2012). To determine from which cells *mmp2* inhibits dendrite regeneration, we examined the effect of tissue specific expression of *mmp2*-RNAi in the epidermal cells and in c4da neurons. Epidermal expression of GMR51F10 (Epidermal) Gal4 was confirmed using UAS-Red Stinger (Figure 4.12). Expression of *mmp2*-RNAi in either the epidermis (Figure 4.4D) or the c4da neurons (Figure 4.4G) did not affect total dendrite length of uninjured neurons (Figure 4.13). We found that dendrite regeneration was enhanced by expressing *mmp2*-RNAi in the epidermis (Figure 4.4E, F) but not in the c4da neurons (Figure 4.4H, I). Knockdown of *mmp2* in epidermal cells increased dendrite growth and coverage in injured neurons (Figure 4.4E, F). Epidermal knockdown of *mmp2* doubled the increase in dendrite length from $2700 \pm 1200 \mu\text{m}$ to $5500 \pm 800 \mu\text{m}$ and increased the area covered from $24 \pm 13\%$ to $53 \pm 9\%$ for injured neurons compared to controls. This suggests that *mmp2* derived from the epidermal cells limits dendrite regeneration in adults.

Dendrites preferentially regenerate into ECM-rich areas

Neuronal maturation and the transition from radial to lattice-like dendrites is associated with local degradation of the ECM surrounding the dendrites in the area between the epidermal and muscle cells of the abdomen. Young neurons grow into an environment enriched with Basement Membrane, BM, as marked by collagen IV, known in *Drosophila* as *viking* (*vkg*).

After Mmp2 expression in the epidermis during the 3 days after eclosion, the abdominal BM is degraded and there are stripes of collagen IV between lateral muscles in the abdomen, but the BM no longer completely surrounds the muscles (Yasunaga et al., 2010). Visualizing collagen IV through a vkgGFP tag, we confirmed that expressing *mmp2* RNAi in the epidermis inhibited collagen IV degradation to an extent at 3 days after eclosion (vkgGFP, Figure 4.5A, B).

To explore the importance of ECM remodeling in the 3 days after eclosion and dendrite regeneration, we performed a series of dendrite injury experiments using a temperature sensitive allele of *mmp2*, Y53N (Page-McCaw et al., 2003, Wang et al., 2014). Trans-heterozygous flies for *mmp2*^{Y53N} and *Df(2R) BSC132* were lethal when raised at the non-permissive temperature of 29°C and viable at the permissive temperature of 25°C. Flies were viable when moved to the non-permissive temperature after eclosion. Raised at the permissive temperature, wild-type and *mmp2*^{Y53N}/*Df(2R) BSC132* flies were either kept at 25°C, 29°C or shifted from 25°C to 29°C 3 days after eclosion. All injuries occurred at 3 days after eclosion, at which time all remodeling should be complete (Figure 4.6 A, B, C). When moved to the non-permissive temperature at eclosion, we found that dendrites of *mmp2*^{Y53N}/*Df(2R) BSC132* neurons regrew to a greater extent than wild-type neurons, reaching a length of $2574 \pm 612 \mu\text{m}$ and $1523 \pm 312 \mu\text{m}$ and covering $30 \pm 9\%$ and $22 \pm 5\%$ of their territory (Figure 4.6 D, E). We observed no difference in total dendrite length in uninjured *mmp2*^{Y53N}/*Df(2R) BSC132* neurons and wild-type neurons raised at 29°C (Figure 4.13). At the permissive temperature, *mmp2*^{Y53N}/*Df(2R) BSC132* neurons and wild-type neurons regrew to comparable lengths, $1834 \pm 802 \mu\text{m}$ and $1744 \pm 593 \mu\text{m}$, and areas $23 \pm 11\%$ and $21 \pm 8\%$, respectively. No difference in regrowth was noted between neurons in flies shifted from the permissive to non-permissive temperature; *mmp2*^{Y53N}/*Df(2R) BSC132* neurons regrew to $1928 \pm 381 \mu\text{m}$, covered $21 \pm 3\%$ of their territory and wild-type neurons regrew to

1874 ± 628 μm and covered 23 ± 4% (Figure 4.6 D, E). This suggests that the primary influence of *mmp2* in dendrite regeneration occurs during the 3 days after eclosion.

To further examine the importance of ECM in regeneration, we wanted to determine if the presence of ECM was favorable for growth of regenerating dendrites. To limit our study to neurons that had already undergone dendrite realignment, we injured neurons at 3 days after eclosion and looked at co-localization of collagen IV and dendrites 7 days after injury (Figure 4.5C). In uninjured neurons, 58 ± 3% of the dendritic arbor co-localized with collagen IV by 10 days after eclosion. After injury at 3 days after eclosion, approximately 78 ± 12% of regenerated dendrites co-localized with collagen IV, more than what was observed for uninjured dendrites (Figure 4.5D). Thus, after injury, dendrites grow in ECM rich regions. This may be due to either preferential growth on ECM or selective elimination from non-ECM rich areas. We note that ECM may be altered in injured abdomens, particularly in areas corresponding to muscle or epidermal damage incurred during the dendrite injury procedure (Figure 4.9; Figure 4.5C).

Integrin-mediated adhesion to the ECM regulates dendrite regeneration

Given these observations of dendrite co-localization with collagen IV in adult flies and previous observations about dendrite disorganization of injured larval neurons (Thompson-Peer et al., 2016), we hypothesized that adhesion to the ECM could affect regenerative potential and influence the increased crossing behavior of regenerated dendrites (Figure 4.3E, F). Adherence to the ECM is influenced by neuronal expression of integrin, a heterodimeric cell surface receptor consisting of an α subunit and a β subunit. Neuron-specific overexpression of *mysospheroid* (*mys*), a β integrin subunit and *multiple edematous* (*mew*), an α integrin subunit, increases dendrite adhesion to the ECM. Uninjured dendrites of c4da neurons generally avoid dendrites of the same neuron. Without proper ECM attachment, dendrites fail to properly avoid

each other. Forcing adhesion to the ECM influences the crossing behavior of dendrites. Integrin overexpression reduces the length of dendrites detaching from the ECM, thereby reducing the number of non-contacting self-crossing events, defined as events where dendrites cross over sister branches of the same neuron without direct contact. Upon integrin overexpression, dendrites are forced into the same plane as other dendrites and can no longer avoid each other by growing into a different plane (Han et al., 2012; Kim et al., 2012; Meltzer et al., 2016). In regenerated larval dendrites, increased adhesion to the ECM through overexpression of *mys* and *mew* increased the number of contacting crossings, defined as events where dendrites directly touched the dendrite they are crossing over (Thompson-Peer et al., 2016). Similarly, in adults, we found that overexpression of the integrin subunits, *mys* and *mew*, caused the contacting crossings of regenerated dendrites to increase from 8.7 ± 1.8 to 14 ± 3 per 1000 μm . In contrast, expression of *mew* or *mys* RNAi in neurons decreased contacting crossings in regenerating dendrites to 4.1 ± 1.9 and 5.7 ± 2.3 per 1000 μm , respectively (Figure 4.7A, B). Overexpressing integrin did not promote dendrite outgrowth. There was no difference in the growth of either control uninjured neurons or injured neurons overexpressing *mys* and *mew* as compared to neurons expressing *mCherry*. RNAi knockdown of *mew* or *mys* decreased dendritic growth after injury and decreased the total dendritic length of uninjured neurons (Figure 4.7C; Figure 4.13). These results demonstrate that in regenerating a dendritic arbor after injury, integrins have somewhat opposing roles in terms of dendritic length and organization. Loss of integrin subunits, *mys* or *mew*, decreases the dendritic length of the arbor, but increases the organization of the arbor, as measured through contacting crossing events.

Discussion

Mature neurons regenerate dendrites

Here, we characterize dendrite regeneration in adult animals. Regeneration of dendrites in adult animals has previously been shown for the PVD neuron of *C. elegans* (Kravtsov et al., 2017; Oren-Suissa et al., 2017) and immediately after eclosion in adult *Drosophila* (Stone et al., 2014). Our study is a significant advance in the study of dendrite regeneration in adult *Drosophila*, because previous studies examined only the youngest possible adult *Drosophila* injured at the time of eclosion, for the reason that adults mounted at any time after eclosion did not survive (Stone et al., 2014). For the first few days after eclosion, these neurons display a highly dynamic dendrite morphology (Shimono et al., 2009; Yasunaga et al., 2010), and then achieve a stable dendrite shape. We confirm that neurons in the young adult fly can regenerate their dendrites. We further characterize the regenerated dendrites. Regenerated dendrites have altered structure compared to uninjured dendrites, as indicated through reduced Futsch staining in primary branches. This could indicate that regenerated dendrites are more comparable to higher order dendritic branches or they fail to build structurally sound primary branches. We also establish that dendrite regeneration can occur in flies up to 30 days after eclosion and possibly even older in age. The persistence of regenerative capacity is reminiscent of studies of axon regeneration in adult *Drosophila*, in which sprouting after injury to the wing margin is observed at 14 days. Older neurons regenerate axons at a slower rate than young neurons (Soares et al., 2014). These results suggest that neurons retain the ability to sprout dendrites and axons late in adult life, although at a diminished capacity compared to neurons in young animals.

Comparison to juvenile dendrite regeneration

Parallel studies in *Drosophila* larvae offer a point of comparison between regeneration during development and adulthood. The most apparent difference between neurons injured in adulthood and neurons injured during the larval period is the extent of regeneration, which is greater in larvae. In larval neurons injured at 48 hours after egg laying, dendrites recover almost 80% of dendrite length and approximately 50% of the area that is normally covered by an uninjured neuron within 3 days after injury (Thompson-Peer et al., 2016). Adult dendrites regrow to a much lesser extent. Even neurons injured at 1 day after eclosion only recover, 7 days after injury, one third of the dendrite length and the area normally covered by an uninjured neuron. Despite these differences, many of the features of regenerated dendrites are shared between the adult and larval neurons.

One striking feature of regenerated dendrites is the disorganization and loss of regular structure. Both larval *Drosophila* da neurons and PVD neurons of *C. elegans* display a loss of self-avoidance in regenerated dendrites (Oren-Suissa et al., 2017; Thompson-Peer et al., 2016). We found that adult *Drosophila* c4da neurons also display self-avoidance defects of their regenerated dendrites, when injured at 3 days or 30 days after eclosion.

We also demonstrate the functionality of regenerated dendrites in adults. In larvae, regenerated c4da neurons appropriately traffic Ppk26, a channel essential to neuronal function, and the regenerated class III da neurons show partial response to gentle touch after injury (Thompson-Peer et al., 2016). We demonstrate that regenerated adult neurons retain functional properties; they exhibit not only appropriate trafficking of Ppk26 but also electrophysiological responses to acid stimuli. This is the first demonstration of functional regeneration of adult dendrites.

Tissue maturation impedes dendrite regeneration

Our results suggest that degradation of the ECM creates a less permissive environment for dendrite outgrowth and regeneration. In *Drosophila* larvae, dendrite outgrowth is regulated in two phases. The initial stage of outgrowth, in which the dendrites must extend to cover the body wall, occurs when ECM has low attachment to the epithelium. Increased ECM attachment to the epithelium, regulated by the epidermally derived microRNAi *bantam*, decreases plasticity and elaboration of dendrite growth (Jiang et al., 2014; Parrish et al., 2009). ECM regulation in adulthood also appears to have two phases. Young adults, during the phase in which the dendrites re-elaborate to cover the body wall, have an ECM rich environment, permissive to dendrite outgrowth (Sato et al., 2012). The extracellular matrix degrades within 3 days of eclosion (Yasunaga et al., 2010). We found that there was a pronounced difference between dendrite regeneration during the early period with rich ECM and the period after ECM remodeling, suggesting that the completion of tissue remodeling may decrease dendrite regeneration. Thus, in both larvae and adults, the status of ECM influences the ability of dendrites to grow and regenerate.

In support of the dependence of dendrite regeneration on the ECM, we found that *mmp2* mutants have increased dendrite regeneration. MMPs have a broad role in injury response including breaking down the blood brain barrier, glial scar formation, breakdown of inhibitory molecules, and proteolytic activation of trophic cues (Page-McCaw et al., 2007; Andries et al., 2017). Our results suggest that increased dendrite regeneration stems from the role for *Mmp2* in remodeling the ECM. *Mmp2* has been distinctly associated with basement membrane (BM) remodeling during fat body remodeling and abdominal maturation (Llano et al., 2002; Jia et al., 2015; Yasunaga et al., 2010). Increased dendrite regeneration was specific to epidermal

knockdown of *mmp2* and associated with partial preservation of the BM between muscle and the epidermis. This suggests that inhibiting tissue remodeling can aid the regenerating dendritic arbor and partially rescue defects in dendrite regeneration in adult animals.

Dendrite ECM interaction has the potential to guide regeneration

We observed preferential placement for regenerating dendrites on collagen IV, an ECM component. ECM cues may be derived from a combination of endogenous ECM patterning and changes in the extracellular environment observed after injury. Injury is a complex process which affects both the neuron and surrounding tissues, including the ECM. Studies of axon re-innervation of the neuromuscular junction after injury similarly suggest that existing extracellular cues guide regeneration. Regenerated synapses almost exclusively repopulate pre-existing synapse locations which are rich in basal lamina, and the cues necessary for synapse maturation (Sanes & Chiu, 1983). Moreover, therapeutic interventions have been proposed through the introduction of collagen scaffolds as a tool for delivery of growth cues and structural preservation (Cholas et al., 2012). Pro-regenerative qualities have been ascribed to exogenous Collagen XII in zebrafish spinal cord regeneration (Wehner et al., 2017). Our experiments suggest that the ECM plays an important role in dendrite outgrowth after injury. It will be of interest to characterize the precise cues that are instructive for dendrite regrowth in future studies.

Another interesting avenue for future studies concerns how neuronal regulation of ECM interaction influences dendrite regeneration. Integrin has been proposed as a target for increasing neurite regrowth (Platman 2012). Studies of axon regeneration have linked integrin activation to improved outgrowth in dorsal root ganglion neurons (Ekström et al., 2003; Tan et al., 2012; Tan et al., 2011; Hu et al., 2008; Vogelezang et al., 2001; Andrews et al., 2009). In retinal neurons,

treatments to increase integrin expression enabled neurons to increase neurite outgrowth in laminin poor environments, which are typically unfavorable to growth (Ivins et al., 2000). Older cultured neurons have also shown increased neurite growth upon increasing integrin expression (Condic 2001; Lemons et al., 2008). We did not observe an increase in dendrite regeneration upon integrin overexpression *in vivo*, while decreasing integrin expression caused a decrease of dendrite regeneration. This suggests that integrin expression is important to regeneration but is insufficient to increase dendrite outgrowth after injury in mature animals.

This study provides a platform for future exploration of the molecular mediators of dendrite regeneration. Here, we establish that dendrite regeneration in adult *Drosophila* occurs throughout adulthood. The regenerated dendrites have impaired growth, microtubule stability and self-avoidance when compared to dendrites of uninjured neurons. Moreover, our studies indicate that the capacity for regeneration decreases with age and the maturation of surrounding tissues and identify ECM that is subject to remodeling and the ability of neurons to adhere to the ECM via integrins as factors important for dendrite regeneration.

Materials and Methods

Dendrite Injury

We designed a disc to image adult flies (Figure 4.1A; Figure 8). The disc was cut from 1/8-inch acrylic plastic by a ULS laser cutter. A circle of a 2.25 diameter with a rectangular groove and a hole offset in the center was cut. The center of the rectangular groove was filled with foam to cushion the adult fly. Magnetic strips with adhesive 1 x 0.5 x 0.06 in (Magnet Source) were used to secure coverslips in place. The small hole was used to facilitate attachment to a carbon dioxide line. Flies were temporary anesthetized on ice and then mounted in this chamber, using water as

a mounting media. During imaging sessions, a light flow of carbon dioxide was used to anesthetize and immobilize the flies. Flies were injured using a custom build Zeiss microscope using a Chameleon laser (Coherent) set at 930nm as previously described (Song et al., 2012; Thompson-Peer et al., 2016). After injury, flies were individually housed in food vials with yeast. Subsequent imaging was performing on an SP5 confocal microscope. All experiments were performed using male flies.

Fly Stocks

We used *ppkCD4tdGFP* lines (Han et al., 2011) to visualize the c4da neurons in adult *Drosophila*. *Mef2 Gal4* was used to mark muscles in the adult abdomen. Studies of *ppk26* were performed using *ppk26^{Δ11}* and *Df(3L) exel⁸¹⁰⁴* (BL 7929) Studies of *mmp2* were performed using *y¹ w**; *Mi {MIC}Mmp2^{M100489}/CyO* (BL 31026), *w¹¹¹⁸ Df(2R) BSC132/SM6a* (BL 9410), *mmp2* RNAi line (v107888), *mmp2^{Y53N}* (Page-McCaw et al., 2003; Wang et al., 2014). *UAS-Dcr2* was used in combination with *mmp2* RNAi to knockdown *mmp2*. Knockdown studies in the epithelial cells were done using *GMR51F10 Gal4* (Losick et al., 2013). To visualize the BM, we used endogenously tagged Collagen IV, *vkgGFP*. Overexpression studies were performed using *ppkCD4tdGFP^{1b}*; *ppkGal4^{1a}* crossed to *w*; *UAS-mys*, *UAS-αPS1 / TM6B*, *Tb* (Han et al., 2012). We used *mew* RNAi (BL44553) and *mys* RNAi (BL33642); knockdown of *mew* and *mys* were confirmed by expression in the wing disk and observation of a failure for the wing to fuse (Goulas et al., 2012).

Quantitative Analysis

Dendrite length was calculated by tracing dendritic arbors using the Simple Neurite Tracer plugin in Image J 1.51n (NIH). Dendrite area was calculated by outlining the neuron and

measuring dendrite coverage area. This measurement was normalized to the area of the segment, as defined by the width and height of the segment. For all graphs, open circles represent uninjured neurons, solid squares represent injured neurons.

Colocalization was analyzed in Imaris (Bitplane). Leica files were deconvoluted with Autoquant (Media Cybernetics) and processed using parameters previous described (Han et al., 2012; Meltzer et al., 2016). Neurons were traced in the GFP channel and the co-localization channel. The ratio of co-localized dendrite to GFP dendrite was compared.

XZ projections were generated in Image J. Images were rotated to align muscles perpendicularly for and cropped to comparable areas.

Immunohistochemistry

Adult abdomens were dissected (Krupp & Levine, 2010) and fixed for 30 minutes in 4% Paraformaldehyde. Antibodies used were Ppk-26, rabbit, 1: 10,000 (Gorczyca et al., 2014) and Futsch 22C, mouse, 1:50 (Hummel et al., 2000) (Developmental Studies Hybridoma Bank).

Using the measure tool of Image J, Futsch intensity was quantified by measuring Futsch intensity in primary branches over 3 lines (width=3) proximal to the cell body and normalized to GFP in that branch. All images were acquired with the same settings. These areas were averaged for each neuron and the averages were compared between neurons.

Electrophysiological recordings

Fillet preparations were made by dissecting male flies 8 days after eclosion in hemolymph-like saline containing (in mM): 103 NaCl, 3 KCl, 5 TES, 10 trehalose, 10 glucose, 7 sucrose, 26 NaHCO₃, 1 NaH₂PO₄ and 4 MgCl₂, adjusted to pH 7.25 and 310 mOsm. 2mM Ca²⁺ was added

to the saline before use. C4da neurons in segments A2, A3 and A4 were exposed by gently removing muscles with fine forceps. v'ada neurons were visualized and identified by green fluorescent protein driven by *ppk* promoter. Glass electrodes for electrophysiological recording were pulled with a P-97 puller (Sutter instruments) from thick wall borosilicate glass and filled with external saline solution. Action potentials were recorded extracellularly with a sample rate of 10 kHz and low-pass filtered at 1 kHz. Multiclamp 700B amplifier, DIGIDITA 1440A and Clampex 10.3 software (Molecular Devices) were used to acquire and process the data. A train of action potentials were induced by 1 second puff application of acidified external saline (pH=3,4,5,6,7) at the distal dendritic area through a glass electrode attached to Picospritzer III (Parker Hannifin Precision Fluidics Division). Firing frequency within 2 seconds before and after the puff was calculated, and the change in firing frequency was used to quantify the intensity of the response to low pH stimulation.

Acknowledgments

We thank Caitlin O'Brien, Jacob Jaszczak, Smita Yadav, Shan Meltzer, Maja Petkovic and Mihir Vohra for critical reading of the manuscript and Matt Klassen and Susan Younger for technical help. Andrea Page-McCaw provided stocks for this study. Supported by K99NS097627 to KTP, NIH grant number R37NS040929 and R35NS097227 to Y.-N.J. L.Y.J and Y.-N.J. are investigators of the Howard Hughes Medical Institute.

Conclusion and Future Directions

This dissertation explores unanswered questions about dendrite development and regeneration. These topics are conceptually linked by growth, but distinct in their context. Development occurs as tissues move from immature to mature states, surrounded by other tissues dividing and growing in parallel. Programed regeneration can occur during the course of development, including examples from *Drosophila*'s transition from larvae to adults. For example, the mushroom body and c4da neurons prune dendrites during the pupal phase and regrow dendrites during the development of the adult fly (Lee et al., 2000; Kuo et al., 2005; Williams and Truman 2005; Satoh et al., 2012). Our study specifically addresses regeneration after injury. Regeneration after injury requires a mature or maturing tissue to respond to an unexpected insult and initiate growth in a matured environment in the presence of inflammation and damaged tissue.

What mechanism underlies *unc-104*'s dendritic arborization phenotype?

Molecular motors drive growth of the cytoskeletal network and movement of molecular cargo. Loss of the molecular motor, dynein, drastically reduces dendritic arborization, neuronal polarity, and localization of organelles including Golgi outposts (Ye et al., 2007; Satoh et al., 2008). Our screen identified 3 kinesins which may play a role in dendritic elaboration. While knock-down of kinesin-6 family members, *pavarotti* and *subito*, had a mild effect on dendritic elaboration, knock-down of kinesin-3 family member, *unc-104* had a dramatic effect on dendritic elaboration. Further work will be required to describe the contribution of *unc-104* to dendrite development and maintenance.

Two mutually nonexclusive hypotheses exist for *unc-104*'s role in dendrite development and are discussed in the second chapter of this dissertation. The first postulates that Unc-104 regulates microtubule dynamics leading to structural deficiencies in cytoskeletal structure. The second postulates that Unc-104 transports elements of the endo-lysosomal pathway that contribute to dendrite development. It is not known if *unc-104* contributes to dendritic maintenance. Examining knockdown of *unc-104* in adult c4da neuron over time will determine if *unc-104* is relevant for dendritic maintenance, as well as development. It is also unknown if *unc-104* is important for dendrite regeneration but given the importance in dendrite elaboration seems likely to play a role.

Do kinesins contribute to dendritic regeneration?

Other kinesins are likely important for regeneration of the dendritic arbor, as cytoskeletal assembly and cargo transport are also critical to regrowth (reviewed in Bradke et al., 2012; Gordon-Weeks et al., 2013; Li et al., 2014). Studies of axon regeneration have demonstrated that several kinesins regulate microtubule dynamics during regrowth.

Axon injury induces local microtubule depolarization. Downregulation of kinesins that stabilize microtubules at the dynamic injury site facilitates neurite outgrowth. In adult axons, knockdown of KLP-7, a kinesin-13 family member that stabilizes microtubules, promotes microtubule growth in the period immediately following axotomy in *C. elegans* (Ghosh-Roy et al., 2012). Similarly, chemical inhibition of Kinesin-5 also aids regeneration, releasing inhibition of advancing microtubules during axon growth (Liu et al., 2011; Xu et al., 2015; Baas et al., 2015).

Other kinesins aid axon regeneration. In both mammalian hippocampal and *Drosophila* neuron cultures, Kinesin-1 promotes axon elongation through driving actively sliding microtubules into outgrowing neurites (Lu et al., 2014; Watt et al., 2015). In rat sensory neurons, kinesin-2 family member, KIF3C, positively regulates microtubule dynamics during regeneration. Local translation of KIF3C promotes more dynamic populations of microtubules after injury and increases regrowth when compared to neurons from null rats (Gumy et al., 2013).

Cargo transport by molecular motors is critical during regeneration. Injury initiates transport of retrograde signals to the cell body (reviewed in Shah et al., 2018). These signals provide the cell body with information about the timing and extent of the insult (reviewed in Rishal and Fainziber 2010). The Wallenda/DLK pathway plays a central role in relaying the retrograde injury signal (Shin et al., 2012). Interestingly, dendrite regeneration has been decoupled from Wallenda/DLK signaling in larval c4da neurons (Stone et al., 2014). It is not known how injury is communicated from the dendrites to the cell body during dendrite injury. One direction for future study will include understanding how dendrite injury is communicated to the cell body and regeneration programs are initiated.

Anterograde transport of mitochondria and mRNA to the axonal injury site is also critical to regrowth (reviewed in Shah et al., 2018). Rebuilding the damaged neuron requires energy. Failure to traffic mitochondria and maintain mitochondrial density at the injury site leads to axon regeneration failure in *C. elegans* (Han et al., 2016). Mammalian studies confirm the importance of mitochondria transport during regeneration. *Armcx1*, a mitochondrial protein upregulated with injury, regulates mitochondrial transport during regrowth (Cartoni et al., 2016). Local translation of proteins relevant to regeneration requires mRNA trafficking to injury site

(reviewed in Yoo et al., 2010). Shifts in mRNA populations after axotomy suggest that mRNAs related to axon targeting and synaptic development are actively trafficked (Taylor et al., 2009). Differences in the capacity of CNS and PNS neurons to traffic mRNA have been suggested to account for the failure of CNS axons to regenerate (Kalinski et al., 2015). Although studies have not examined mitochondria or mRNA after dendrite injury, both are likely to be important contributors to rebuilding the dendritic arbor.

How does CO₂ stimulate c4da neuron activity?

The behavioral significance of c4da neurons in adults remains unknown. Larval c4da neurons respond to various sensory stimuli including light, heat, mechanical and chemical stimulation. But these studies have not been expanded to adult c4da neurons. In electrophysiological studies, larval c4da neurons can be stimulated by application of low pH solutions to the distal dendrites (Boiko et al., 2013). Our study establishes that this stimulus also activates the adult c4da neurons. To identify sensory stimuli for adult c4da neurons, this dissertation explores c4da neurons function *in vivo* using calcium imaging.

We found that c4da neurons are stimulated by application of CO₂ to the adult abdomen. This stimulus may be driven by muscle contraction or acidification of the abdomen after CO₂ application. The first possibility, muscle contraction, suggests that these neurons function as sensors of body wall position and peripheral movement. This is consistent with evidence that larval c4da neurons act as proprioceptors (Adams et al., 1998; Ainsley et al., 2003; Gorczyca et al., 2014).

It is also possible that CO₂ drives acidification of the abdomen leading to stimulation. Larval and adult c4da respond to stimulation by low pH solutions (Boiko et al., 2012; chapter 4).

But it is unknown if application of CO₂ results in a decrease in pH sufficient to stimulate the c4da neurons *in vivo*. These scenarios are not mutually exclusive. Evaluating these two mechanisms will aid our understanding of the adult c4da neurons.

What functional and structural changes occur in regenerated dendrites?

There remain unanswered questions about the function and structure of regenerating dendrites. Our work suggests that functional recovery of these neurons occurs. We observed dendritic competency to respond to stimulation in electrophysiological preparations, as well as appropriate trafficking of Ppk26, an ion channel associated with neuronal function. These results are consistent with functional recovery in regenerating neurons. Future work could expand our understanding of functional recovery in these neurons by focusing on *in vivo* calcium imaging using the functional study described above.

Our study described the structure of regenerated dendrites. We observed a reduction in the presence of stabilized microtubules. This suggests that regenerating dendrites are not competent to form primary branches and the regenerated branches more closely resemble higher order branches. Further assessing the diameter and microtubule dynamics of regenerating dendrites will provide more insight. It is unknown if the microtubule polarity of regenerated dendrites is different from uninjured primary branches, which are uniformly minus- end out in orientation (Stone et al., 2008; Rolls et al., 2007; Zheng et al., 2008; Satoh et al., 2008). Regenerating branches may resemble higher order branches, which have mixed microtubule polarity (Yau et al., 2016).

How does aging affect the quality of regeneration?

Our study finds that neurons retain the ability to regrow until at least midlife, suggesting an intrinsic ability to regrow dendrites. There may, however, be a decline in *Drosophila* older than 30 days. Assessing older animals may require developing additional imaging methods, as older flies are more fragile.

The quality of regeneration in older animals has not been systematically characterized. Our characterization studies primarily focused on young adult animals. But we were able to compare the extent of outgrowth and crossing behavior in both populations. Very young adult *Drosophila* regenerated better than all other age groups, but outgrowth rapidly declined in the first week of adulthood. Regrowth observed in 7-day old animals and 30-day old animals was roughly comparable in terms of length.

Increased crossing behavior in regenerating dendrites was observed in both young and old animals. There was a trend towards fewer crossing events in older animals that may warrant additional study. We linked the crossing behavior in younger neurons to integrin signaling. But we did not study the signaling pathways related to crossing behavior in older animals. It is not known if known self-avoidance cues, including integrins, are altered in older animals. It will be interesting to assess integrin expression throughout the lifespan and understand if augmenting expression in aged animals can increase regeneration outcomes.

Our characterization studies of structure and function should also be expanded to older regenerated dendrites. We have not assessed the microtubule structure of regenerated neurons at this age. Older regenerated dendrites appear more frail than younger regenerated dendrites.

Stabilized microtubules may also be further reduced in this population and microtubule dynamics may be changed.

We also know nothing of the functional recovery of older neurons. It is not known if older regenerated neurons traffic the appropriate ion channels to the distal dendrites or are functional competent to respond to electrophysiological stimulation. Coupling these studies to calcium imaging may aid understanding of functional recovery in older animals.

What molecular pathways define dendrite regeneration?

Our study of dendrite regeneration provides a platform for understanding the molecular pathways which guide dendrite regeneration in mature neurons. It is not known if dendrite severing produces the same downstream signals that axon severing produces. Cytoskeletal disruption to the axon results in a retrograde signal to the cell body initiating axon repair pathways. Studies of larval dendrite regeneration suggest that this pathway may not be important for dendrite regeneration. RNAi knockdown of the DLK/JNK pathway did not prevent dendrite regeneration in larvae (Stone et al., 2014). As regrowth during the larval life phase may be coupled to developmental growth, it will be important to confirm these results in adult neurons. There is the possibility that DLK may be required during adult dendrite regeneration. If these results are confirmed in adult neurons, understanding how cytoskeletal disruption in dendrites is conveyed to the cell body will be important to understand.

Lipid second messengers likely convey dendritic severing. Although it is unknown if the balance of PIP₂ and PIP₃ change upon dendrite severing, there is evidence suggesting that downstream targets influence regeneration. Dendrite recovery after injury to a single branch requires the PTEN/AKT pathway during the larvae life stage (Song et al., 2012). Observing

increased regeneration upon PTEN knockdown in adulthood would strengthen the argument for the importance of this pathway for dendrite regeneration. It will also be interesting to look at SOCS3 and GSK-3 in the context of dendrite regeneration.

How does the extracellular environment influence the extent of dendrite regeneration?

In our study of adult dendrites, we found that expressing RNAi for *mmp2* in epidermis significantly increased regeneration. This manipulation also inhibited reorganization of the extracellular matrix in the abdomen, suggesting that the state of the extracellular matrix influences the extent of dendrite regeneration. It is not known which cues in the extracellular matrix are important for this response or which tissues secrete the extracellular matrix.

Our developmental studies of the adult abdomen describe the incorporation of extracellular matrix protein, Collagen IV, into the space between the epithelial layer and muscle. We found a clear contribution of hemocytes to the extracellular matrix. It is possible that the muscles and fat body contribute to the endogenous basement membrane of the abdomen but will require additional study. It is not known if these tissues can contribute extracellular matrix beyond the pupal phase. Promoting secretion of extracellular matrix beyond this phase may prove therapeutic.

Other extracellular matrix proteins, including Laminin, may have different sources and localization in the adult abdomen. We do not know the importance these proteins for dendrite regeneration. Understanding the relative importance of extracellular proteins will require the development of additional reagents to further our understanding of the microenvironment. A more thorough understanding of the elaboration and maturation of the dendritic arbor will provide new testable hypotheses about the regeneration of the mature dendritic arbor.

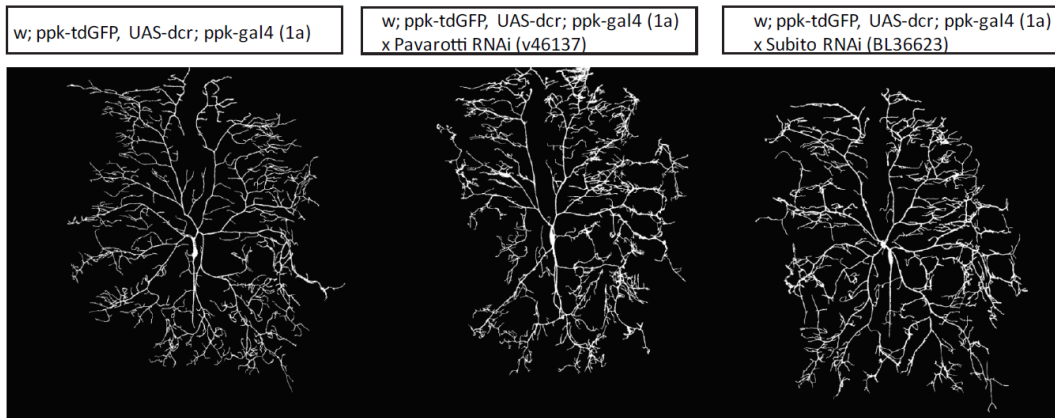
Table 1. List of RNAi stocks used in kinesin screen

Stock	Reagent	CG #	Gene	kinesin family	mammalian
35475	RNAi	CG33694	CENP-ana	CENP-E	CENP-E
35816	RNAi	CG6392	CENP-meta	CENP-E	CENP-E
36583	RNAi	CG7507	Dynein heavy chain 64C	Cytoplasmic DHC	DHC1
36698	RNAi	CG7507	Dynein heavy chain 64C	Cytoplasmic DHC	DHC1
28749	RNAi	CG7507	Dynein heavy chain 64C	Cytoplasmic DHC	DHC1
35472	RNAi	CG9913	Kinesin family member 19A		
36733	RNAi	CG8183	Kinesin heavy chain 73	Unc-104	KIF13
33963	RNAi	CG1453	Kinesin-like protein at 10A	Kin1	KIF2
35473	RNAi	CG5300	Kinesin-like protein at 31E	Chromo-K	KIF21
35975	RNAi	CG8590	Kinesin-like protein at 3A	Chromo-K	KIF4
36577	RNAi	CG43323	Kinesin-like protein at 54D	KIF12	KIF12
35596	RNAi	CG3219	Kinesin-like protein at 59C	Kin1	KIF2
35474	RNAi	CG12192	Kinesin-like protein at 59D	Kin1	KIF2
33685	RNAi	CG9191	Kinesin-like protein at 61F	BimC/Eg5	Eg5
40945	RNAi	CG10642	Kinesin-like protein at 64D	Kin-II	KIF3A
27549	RNAi	CG10923	Kinesin-like protein at 67A	Kip3	KIF18
35606	RNAi	CG10923	Kinesin-like protein at 67A	Kip3	KIF18
36268	RNAi	CG10923	Kinesin-like protein at 67A	Kip3	KIF18
29410	RNAi	CG7293	Kinesin-like protein at 68D	Kin-II	KIF3B
29410	RNAi	CG7293	Kinesin-like protein at 68D	Kin-II	KIF3B
39037	RNAi	CG5658	Kinesin-like protein at 98A	Unc-104	KIAA1590
28897	RNAi	CG10718	nebbish	Unc-104	KIF14
2243	mutant	CG7831	non-claret disjunctional	Kin C	KIFC1
46137	RNAi	CG1258	pavarotti	MKLP1	MKLP1

Table 1. List of RNAi stocks used in kinesin screen

Stock	Reagent	CG #	Gene	kinesin family	mammalian
36623	RNAi	CG12298	subito	Kinesin-6	KIF20A
28951	RNAi	CG8566	uncoordinated-104	Kinesin-3	KIF1A

A



B

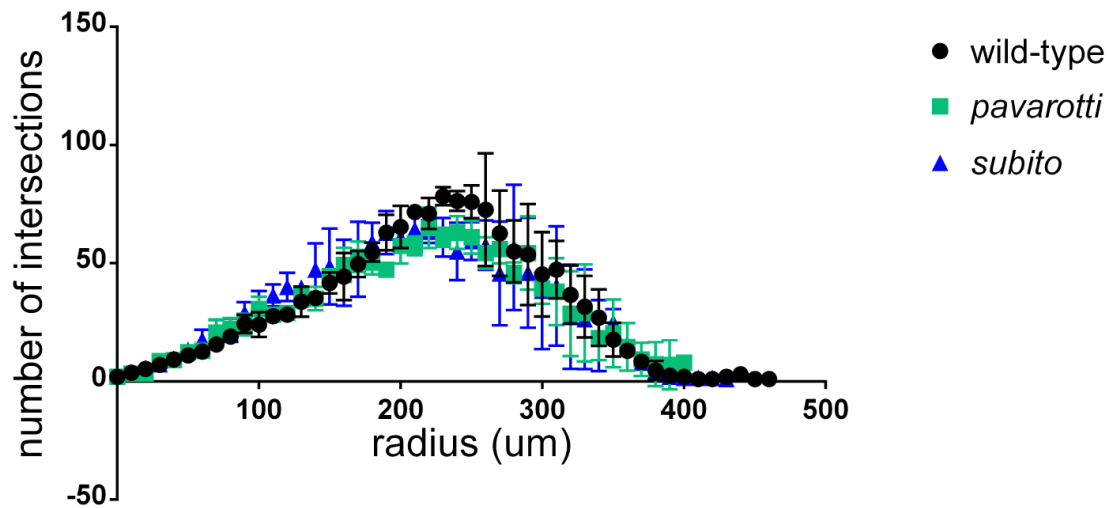
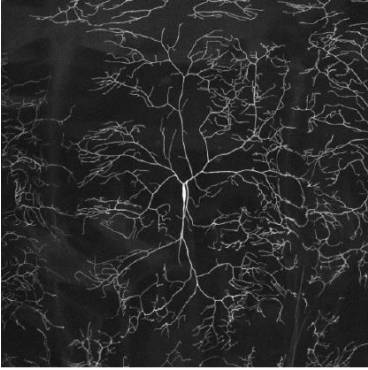


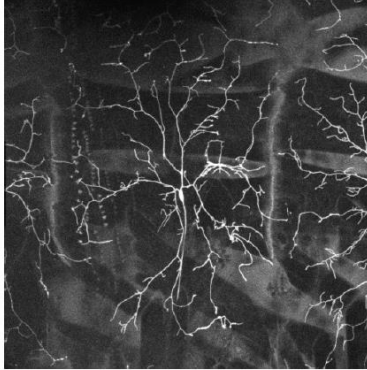
Figure 2.1 Knockdown of *pavarotti* and *subito* RNAi in *c4da* neurons. A. *Ppk-tdGFP*; *Ppk Gal4* drives expression of *pavarotti* RNAi (v46137) and *subito* RNAi (BL36623). B. Sholl analysis of dendritic arbor complexity for wild-type, *pavarotti* and *subito* RNAi neurons. The number of intersections of the dendritic arbor at intervals of 10 μm from the center are plotted. Mean \pm SD is plotted (N=3).

A

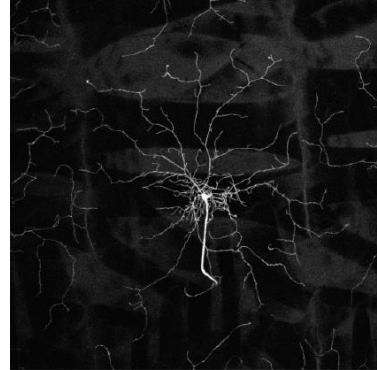
w; ppk-tdGFP, UAS-dcr; ppk-gal4 (1a)



w; ppk-tdGFP, UAS-dcr; ppk-gal4 (1a)
x *unc-104* RNAi (BL28951)



w; ppk-tdGFP, UAS-dcr; ppk-gal4 (1a)
x *Dhc64c* RNAi (BL36583)



B

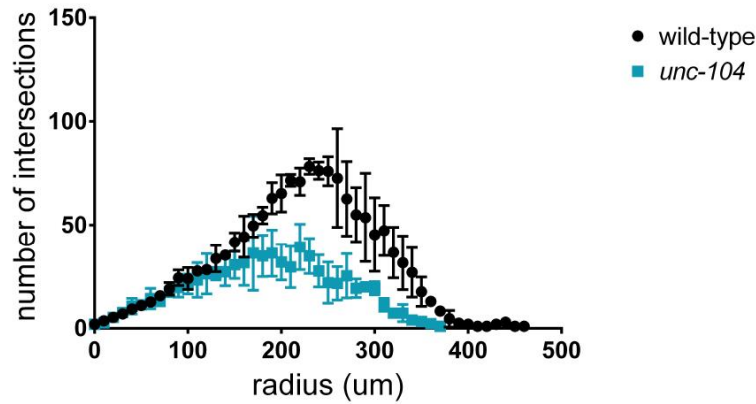


Figure 2.2 Knockdown of *unc-104* in *c4da* neurons decreases dendritic complexity. A. *Ppk-tdGFP*; *Ppk Gal4* drives expression of *UAS-dcr2* and RNAi for *unc-104* (BL28951) and *Dhc64c* (BL36583). B. Sholl analysis for dendritic arbor complexity of wild-type and *unc-104* RNAi neurons. The number of intersections of the dendritic arbor at intervals of 10 μm from the center are plotted. Mean \pm SD is plotted (N=3).

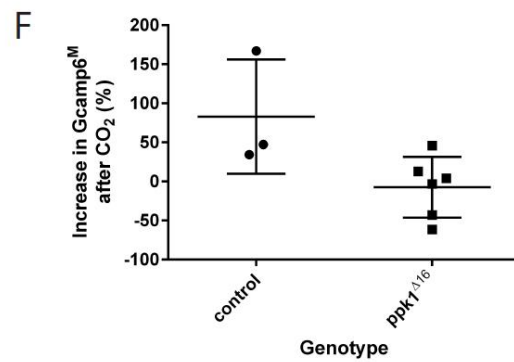
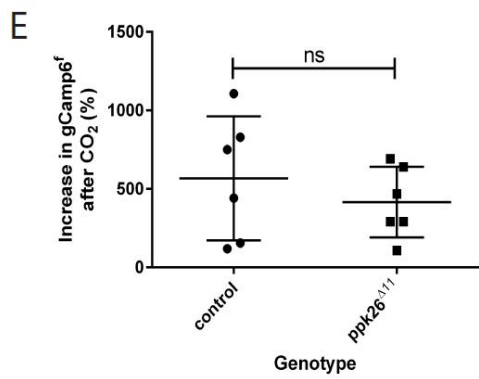
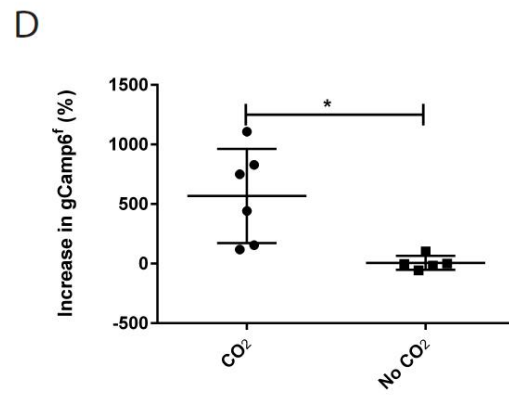
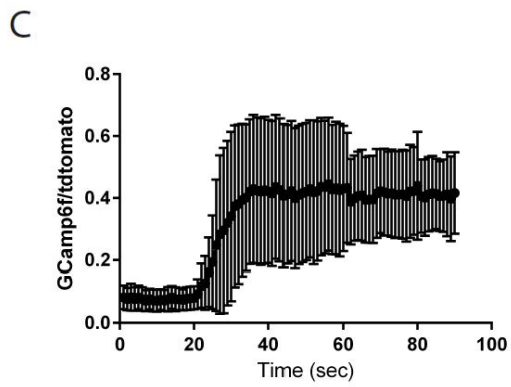
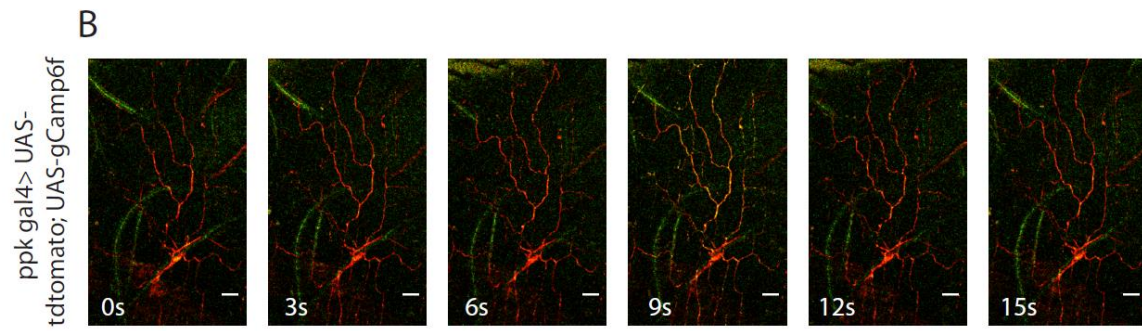
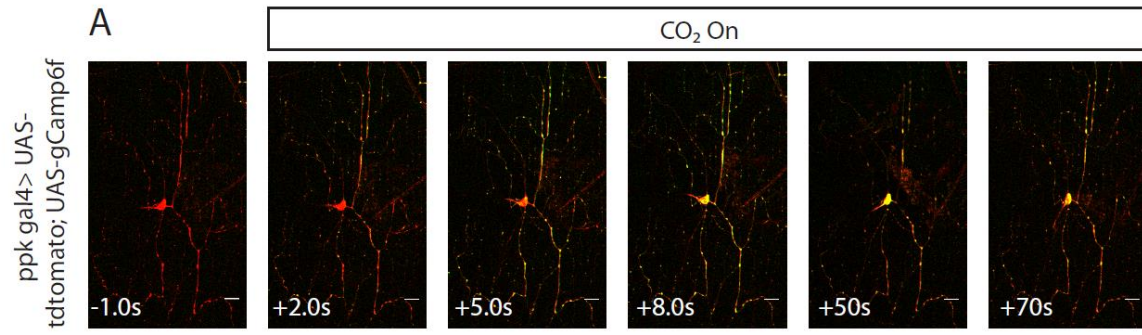


Figure 3.1 Application of carbon dioxide stimulates neural activity in c4da neurons. A. *Ppk* Gal4 drives expression of UAS-*tdtomato* and UAS- *GCaMP6f*. CO₂ stimulus was delivered at 0 sec. Scale bar represents 20 μ m. A representative time course of response to stimulation is shown before and after stimulation. B. *Ppk* Gal4 drives expression of UAS-*tdtomato* and UAS-*GCaMP6f*. No stimulation is applied. Abdomen is largely restrained, but some movement occurs. C. The ratio of *GCaMP6f*/*tdtomato* is plotted over time. Stimulation was delivered at 20 seconds (N=6). D. Increase in neuronal activity in the cell body is plotted. A 10 second window ending 5 seconds before stimulus delivery was averaged to calculate baseline *GCaMP6f*/*tdtomato*. A 10 seconds window starting 15 seconds after stimulus delivery was averaged to calculate response. An unpaired t-test revealed a statistically significant difference between neurons that had been stimulated and those that had not $t(9) = 3.121$, $p = 0.0123$. E. Increase in neuronal activity in control and *ppk26^{Δ11}* flies is plotted. An unpaired t-test revealed no difference between stimulation of control and *ppk26^{Δ11}* flies $t(10) = 0.8165$, $p = 0.4332$. F. Increase in neuronal activity in control (*GCaMP6m*) and *ppk1^{Δ16}* flies is plotted. An unpaired t-test revealed a difference between stimulation of control and *ppk1^{Δ16}* flies $t(7) = 2.505$, $p = 0.04508$.

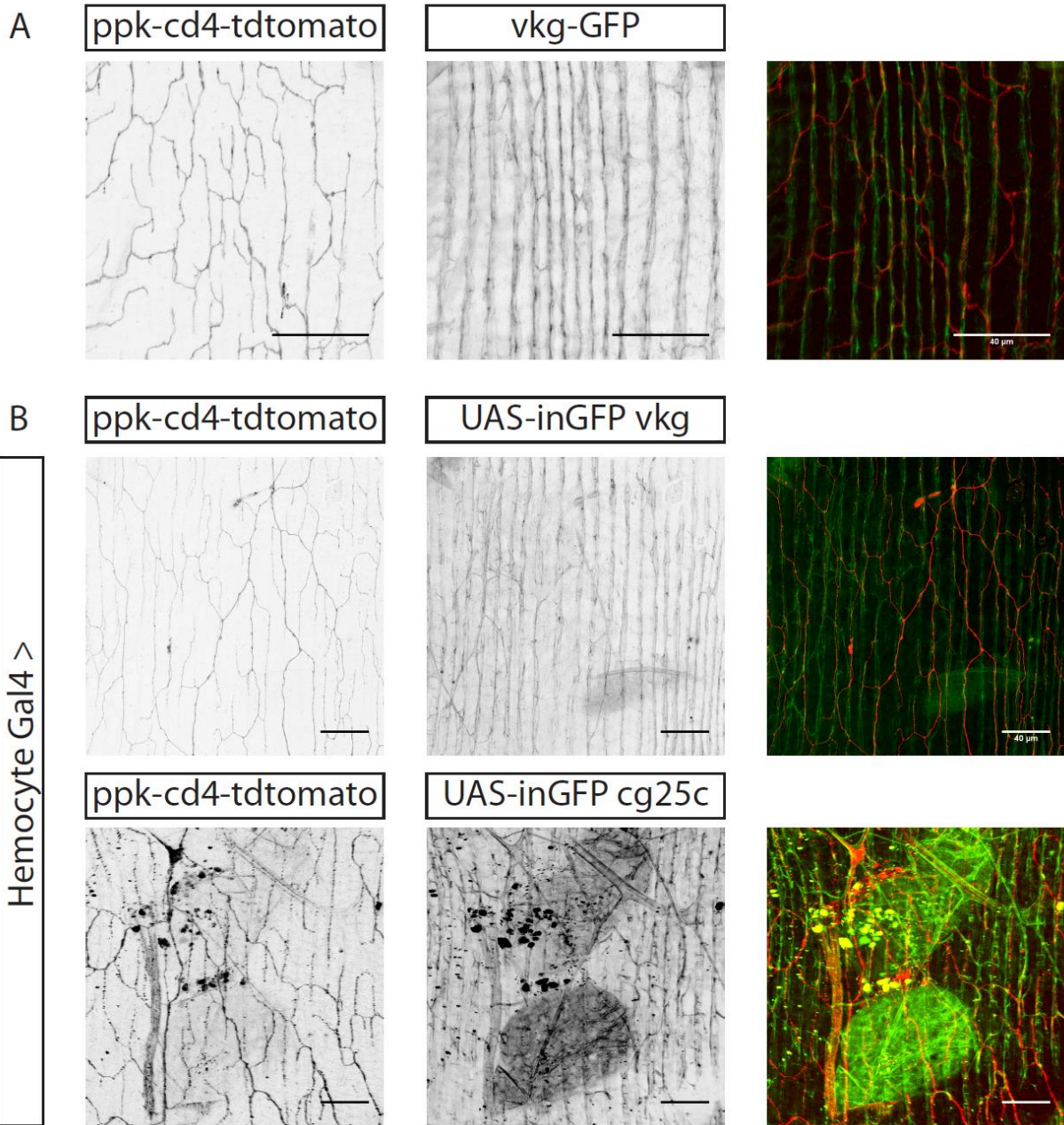


Figure 3.2 Characterization of basement membrane in the adult *Drosophila* abdomen. A. Endogenously tagged Collagen IV co-localizes with dendrites of c4da neurons. C4da neurons are marked by tdTomato. Collagen IV is marked by vkg-GFP. Scale bar represents 40 μm. **B.** Hemocyte driven expression of Collagen IV α chain proteins, *vkg* and *cg25c* mimics endogenous expression. Hemocyte Gal4 drives expression of *UAS-inGFP vkg* and *UAS-inGFP cg25c*.

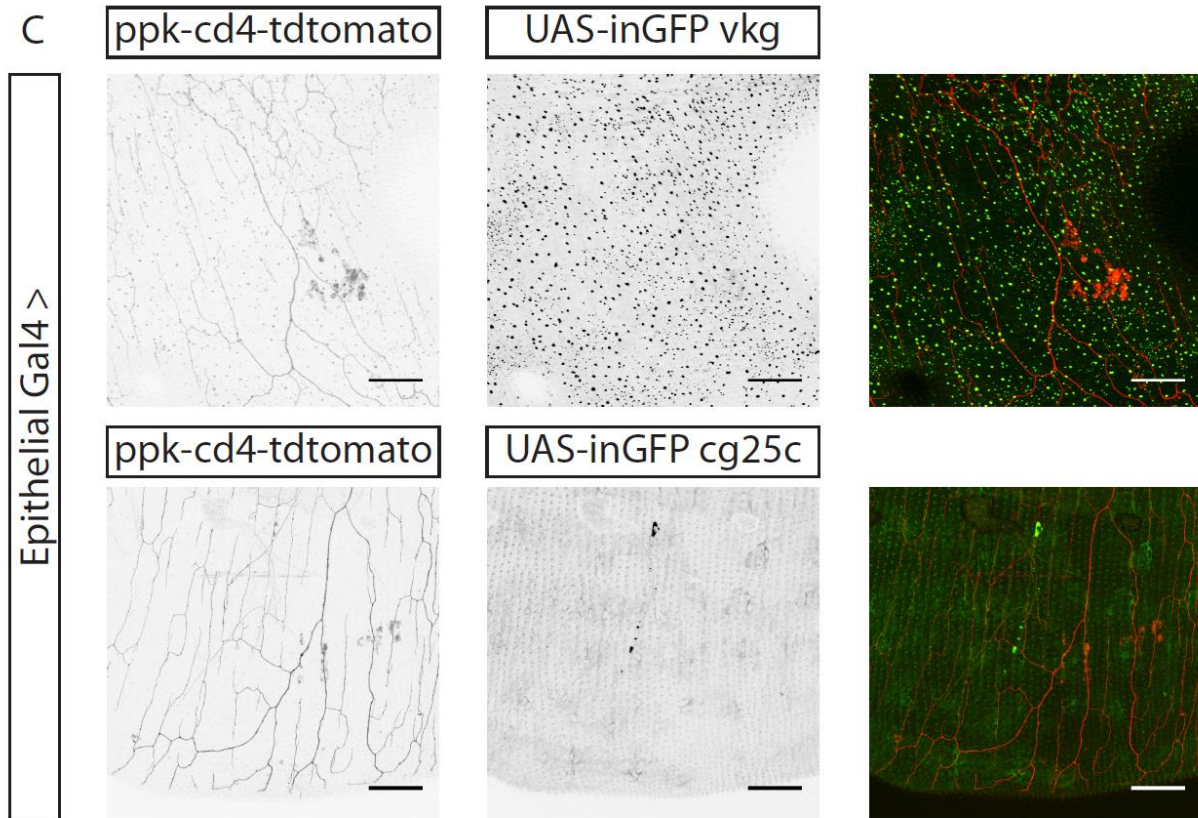


Figure 3.3 Characterization of basement membrane in the adult *Drosophila* abdomen. C. Epithelial driven expression of Collagen IV α chain proteins, *vkg* and *cg25c* is shown. Epithelial Gal4 drives expression of *UAS-inGFP vkg* and *UAS-inGFP cg25c*. Scale bar represents 40 μ m.

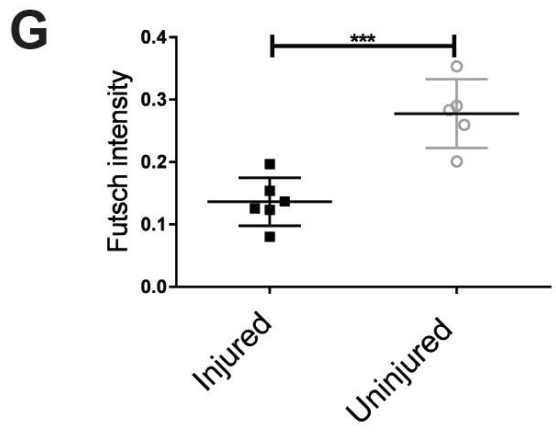
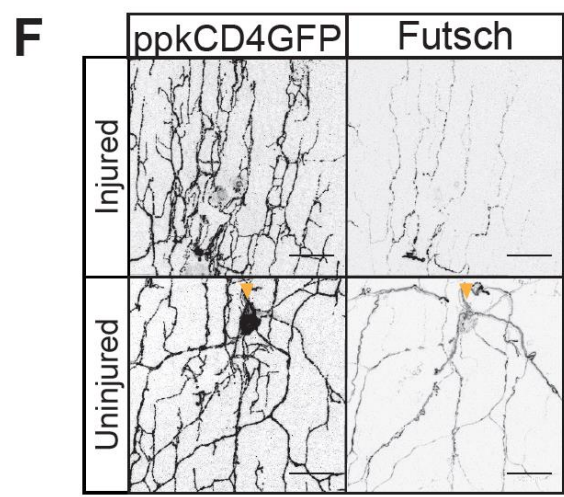
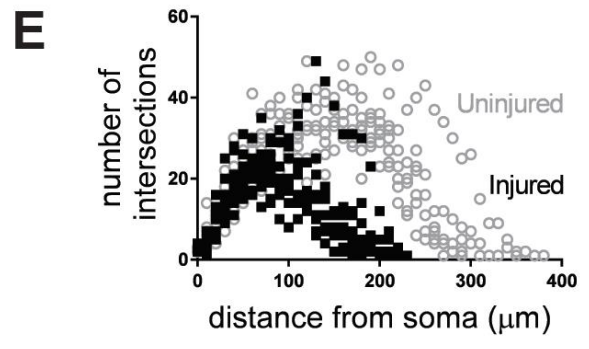
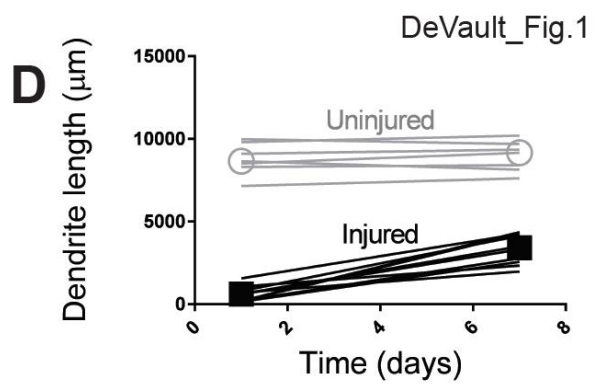
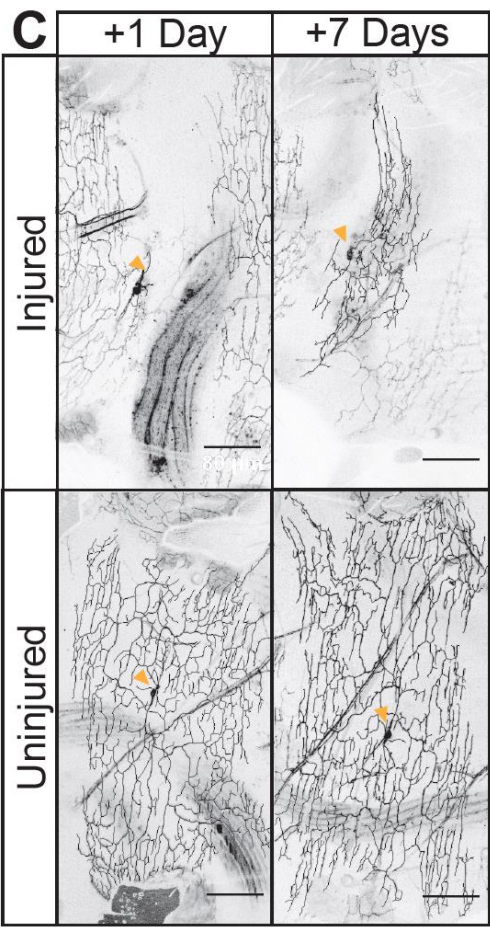
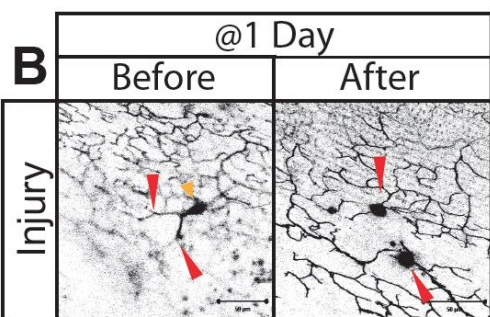
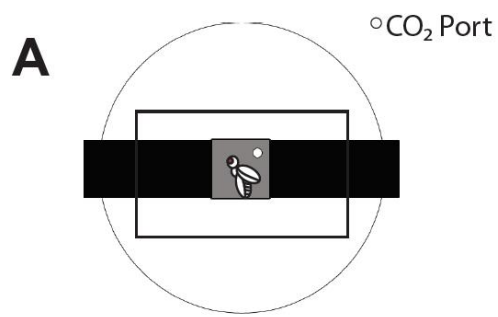


Figure 4.1 Dendrites regenerate 1 day after eclosion. A. Chamber to image anesthetized adult *Drosophila*. B. V'ada neurons in the adult abdomen are injured at the first branching points in the dendritic arbor 1 day after eclosion. Scale bar represents 50 μm . Red arrowheads indicate the injury location. Orange arrowheads indicate the cell body of the neuron when visible in the plane of the image. C. Top panels: neurons at 1 and 7 days after injury. Bottom panels: uninjured control neurons. Scale bar represents 80 μm . D. Total dendrite length at 1 and 7 days after injury. Injured neurons ($M=2738$; $SD=880$) had a greater change in dendrite length than uninjured neurons ($M=255$; $SD=306$), $t(15) = 7.11$, $p < 0.0001$; $n=10$ injured, 7 uninjured. For all graphs, open circles represent uninjured neurons, solid squares represent injured neurons. E. Sholl analysis of injured and uninjured neurons at 7 days after injury. F. Injured and uninjured dendrites are stained for Futsch. G. Average intensity along primary branch is plotted. Uninjured neurons had greater intensity ($M=0.28$; $SD=0.055$) than injured neurons ($M=0.14$; $SD=0.038$), $t(9) = 5.0$, $p=0.0007$. $n= 6$ injured, 5 uninjured. Scale bar represents 20 μm .

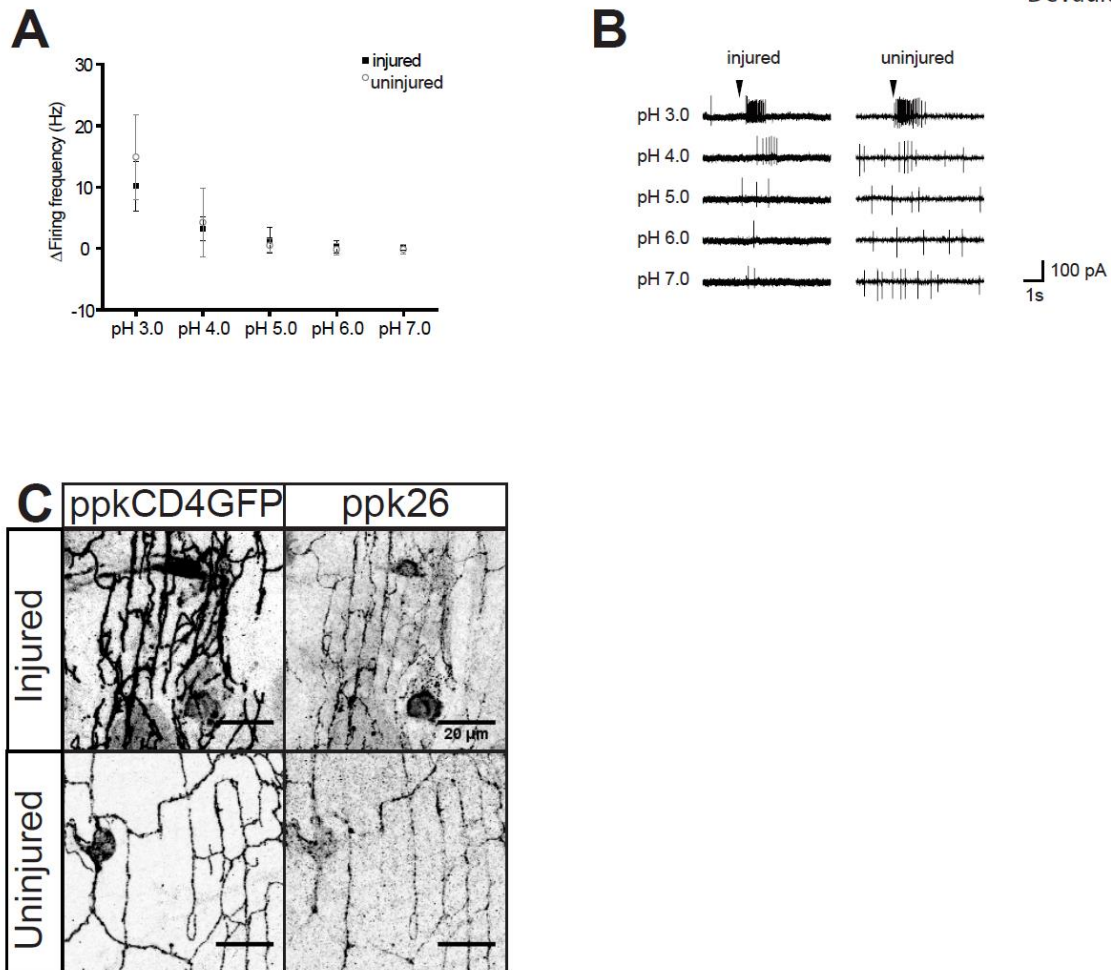


Figure 4.2. Dendrites functionally recover after injury. A. Average firing frequency (Hz) in response to acidified solutions between pH 3-7 in injured and uninjured neurons. At pH 3, There was no statistical difference between uninjured (M=14.9; SD=6.9) and injured neurons (M=10.14; SD= 4.0), $t(15) = 1.63, p=0.12; n=7$ injured, 10 uninjured. B. Representative recordings trace from stimulation of uninjured and injured neurons by an acidified solution at pH 3-7. C. Ppk26 is present in the dendrites of injured and uninjured dendrites. Scale bar represents 20 μm .

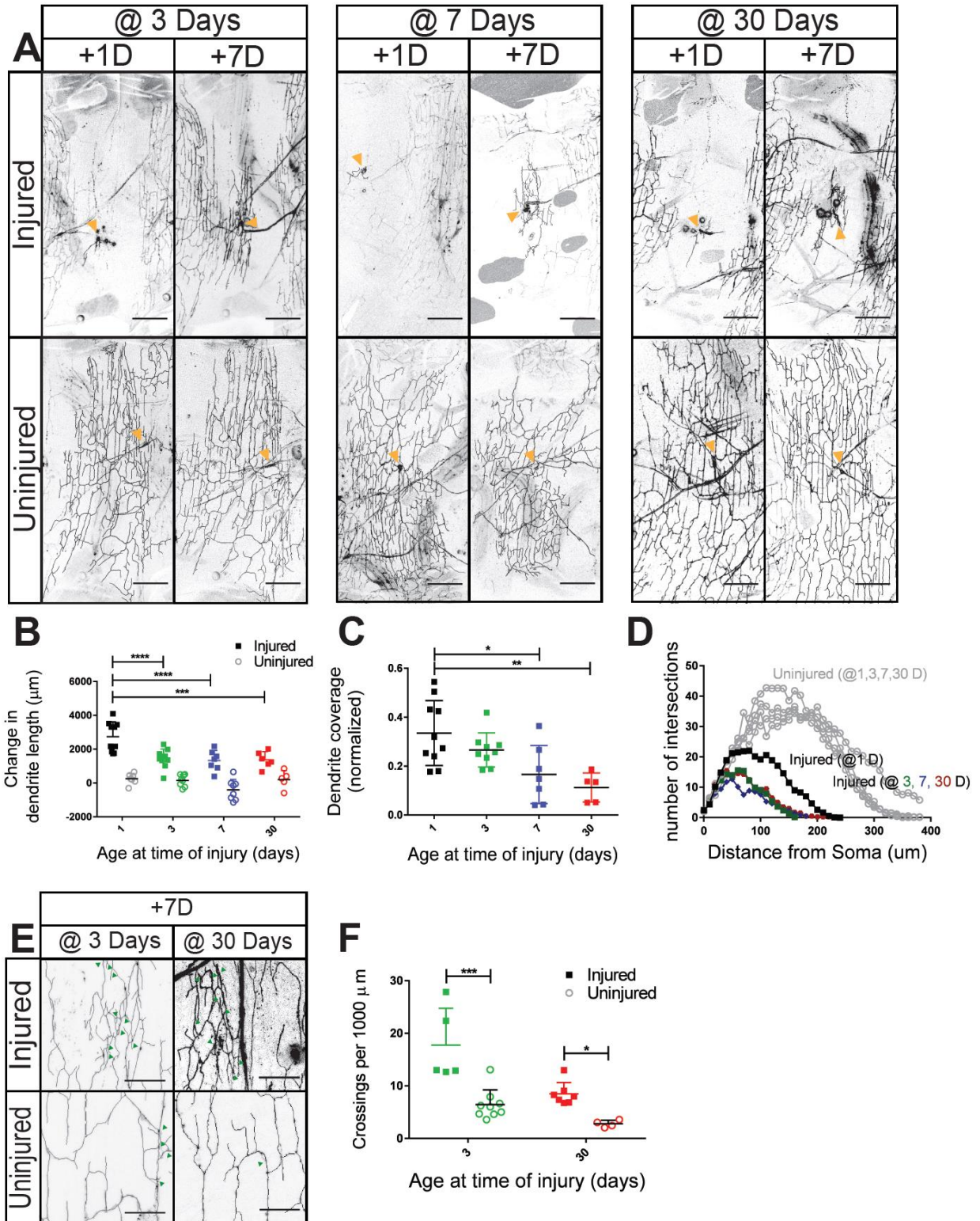


Figure 4.3. Dendrites regenerate at 3, 7, 30 days after eclosion. A. Neurons were injured at 3, 7 and 30 days after eclosion. The dendritic arbor is shown 1 and 7 days after injury. Orange arrowheads indicate the cell body of the neuron when visible in the plane of the image. Scale bar represents 80 μm . B. Difference in dendrite length between 1 and 7 days after injury for neurons injured at 1, 3, 7, and 30 days after eclosion. Measured differences in dendrite length were subjected to a two-way ANOVA. Injury, $F(1, 53) = 119.2$, $p < 0.0001$, and age, $F(3, 53) = 8.757$, $p < 0.0001$, were statistically significant. The interaction effect was significant $F(3, 53) = 3.880$, $p = 0.0140$. Sidak's post hoc test revealed that neurons injured at 1 day after eclosion ($M=2738$; $SD=880$) had greater dendrite length than neurons injured at 3 days after eclosion ($M=1393$; $SD=710$), 7 days after eclosion ($M=1333$; $SD=598$) and 30 days after eclosion ($M=1375$; $SD=479$) $n=10$ injured, 8 uninjured neurons 1 day after eclosion; 10 injured, 8 uninjured 3 days after eclosion; 7 injured, 8 uninjured 7 days after eclosion; 5 injured, 5 uninjured 30 days after eclosion. C. Dendrite coverage of injured neurons measured 7 days after injury. Area coverage by dendrite was subjected to a one-way ANOVA. $F(3, 27) = 6.575$, $p = 0.0018$. Sidak's post hoc test revealed that neurons injured at 1 day after eclosion ($M=0.33$; $SD=0.13$) covered greater area than neurons injured at 7 ($M=0.17$; $SD=0.12$) and 30 days after eclosion ($M=0.11$; $SD=0.06$) D. Sholl analysis of regenerated neurons and uninjured controls for neurons injured at 1, 3, 7 and 30 days after eclosion. E. Injured and uninjured dendrites of neurons injured at 3 and 30 days. Scale bar represents 20 μm . Green arrows represent crossing events. F. Dendritic crossing events per 1000 μm . Dendritic crossing events were analyzed with a two-way ANOVA. Injury, $F(1,21) = 30.03$, $p < 0.0001$, and age, $F(1,21) = 17.34$, $p = 0.0004$ were significant. $n= 5$ injured, 9 uninjured neurons at 3 days after eclosion; 7 injured, 4 uninjured at 30 days after eclosion.

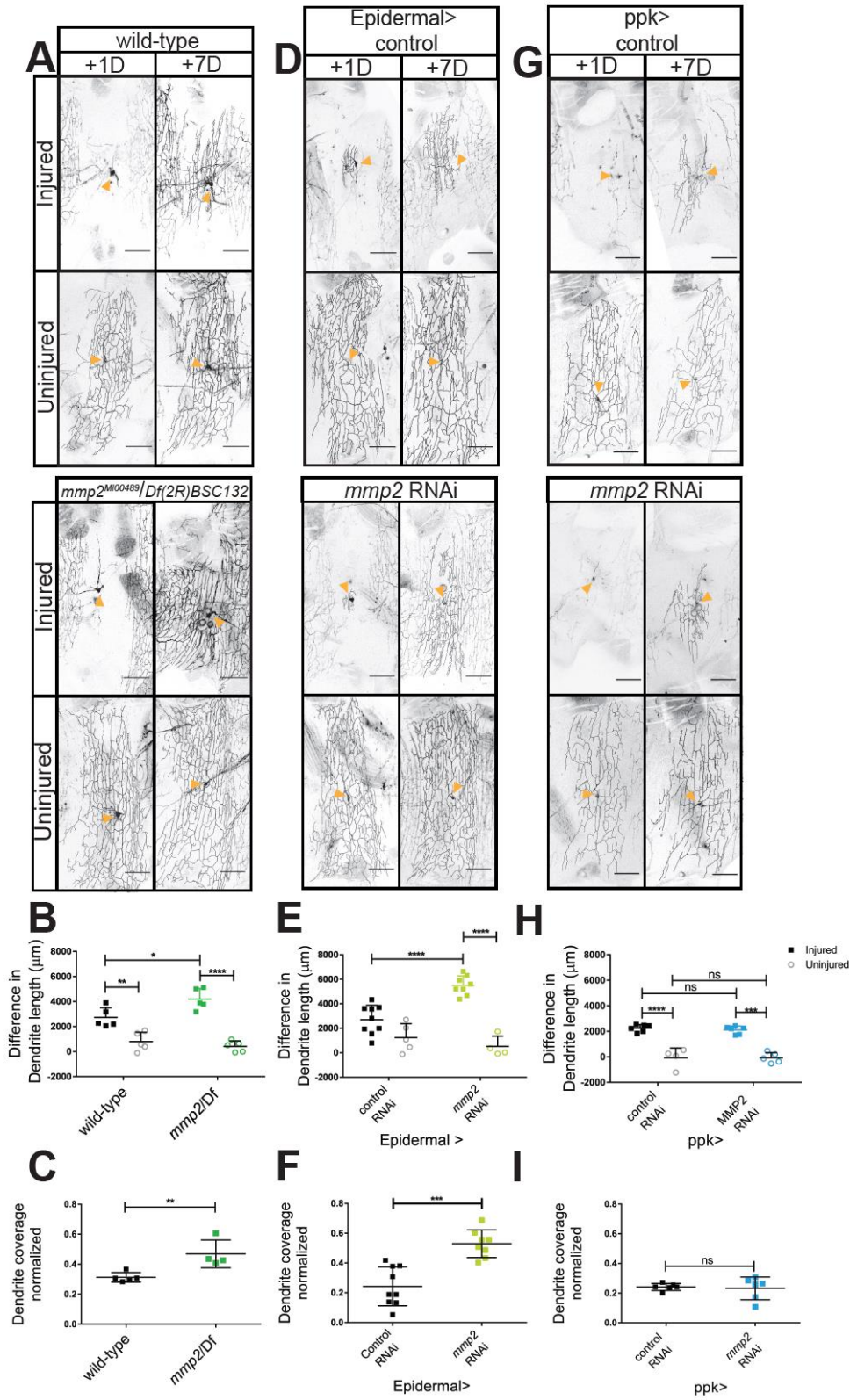


Figure 4.4. Loss of *mmp2* increases dendrite regeneration. A. Wild-type and *mmp2*^{MI00489}/*Df(2R) BSC132* neurons 1 and 7 days after injury. Orange arrowheads indicate the cell body of the neuron. B. Change in dendritic length 7 days after injury. Dendrite lengths were subjected to a two-way ANOVA. Injury increased the difference in dendrite length $F(1, 16) = 78.65, p < 0.0001$. Genotype was not statistically significant $F(1, 16) = 2.8394, p = 0.11$. The interaction effect was significant $F(1, 16) = 8.394, p = 0.0105$. Tukey's post hoc test revealed that *mmp2* injured neurons (M= 4199; SD =835) grew more than wild-type injured neurons (M=2722; SD=790) Uninjured *mmp2* neurons (M=412; SD=439) were not different from wild-type uninjured (M= 800; SD=746). $n = 5$ injured, 5 uninjured wild-type; 5 injured, 5 uninjured *mmp2* mutants. C. Coverage of dendritic area at 7 days after injury. There was a significant difference between wild-type (M =0.3126; SD =0.31) and *mmp2* (M =0.4693; SD =0.093) $t(7) = 3.580, p = 0.0090$ D. Epidermal Gal4 drives expression of control (UAS-Dcr2) and *mmp2* (V107888) RNAi at 1 and 7 days after injury. E. Change in dendritic length 7 days after injury. Changes in dendrite length were subjected to a two-way ANOVA. Injury, $F(1, 22) = 58.05, p < 0.0001$, and *mmp2*, RNAi $F(1, 22) = 6.035, p = 0.0224$ were significant. The interaction effect was significant $F(1, 22) = 17.14, p = 0.0004$. Sidak's post hoc test revealed that *mmp2* RNAi (M =5495; SD=787) increased dendrite length compared to control RNAi (M=2703; SD=1188) injured neurons. There was no difference between uninjured neurons in control RNAi (M=1230; SD=1147) and *mmp2* RNAi (M =518; SD =837) neurons. $n = 9$ injured, 5 uninjured control RNAi; 8 injured, 4 uninjured *mmp2* RNAi neurons. F. Dendritic area 7 days after injury There was a significant difference between control (M= 0.2436; SD=0.13) and *mmp2* RNAi (M=0.5295; SD=0.092) $t(15) = 5.137, p = 0.0001$. G. Neuronal Gal4 (Ppk Gal4) drives expression of control (UAS-Dcr2) and *mmp2* (V107888) RNAi. H. Change in dendrite length 7 days after injury. Changes in dendrite length were subject to a two-way ANOVA with two injured conditions (injured, uninjured) and two RNAi conditions (control, *mmp2*). There was a significant effect of injury $F(1, 13) = 92.12, p < 0.0001$. There was not a significant effect of RNAi $F(1, 13) = 0.1814, p = 0.67$ or an interaction effect $F(1, 13) = 0.56, p = 0.47$. $n = 6$ injured, 4 uninjured control RNAi, 6 injured, 5 uninjured *mmp2* RNAi neurons. I. Regenerated dendrite area 7 days after injury. There was not a significant difference between *mmp2* RNAi and control neurons $t(8) = 0.9867, p = 0.3527$.

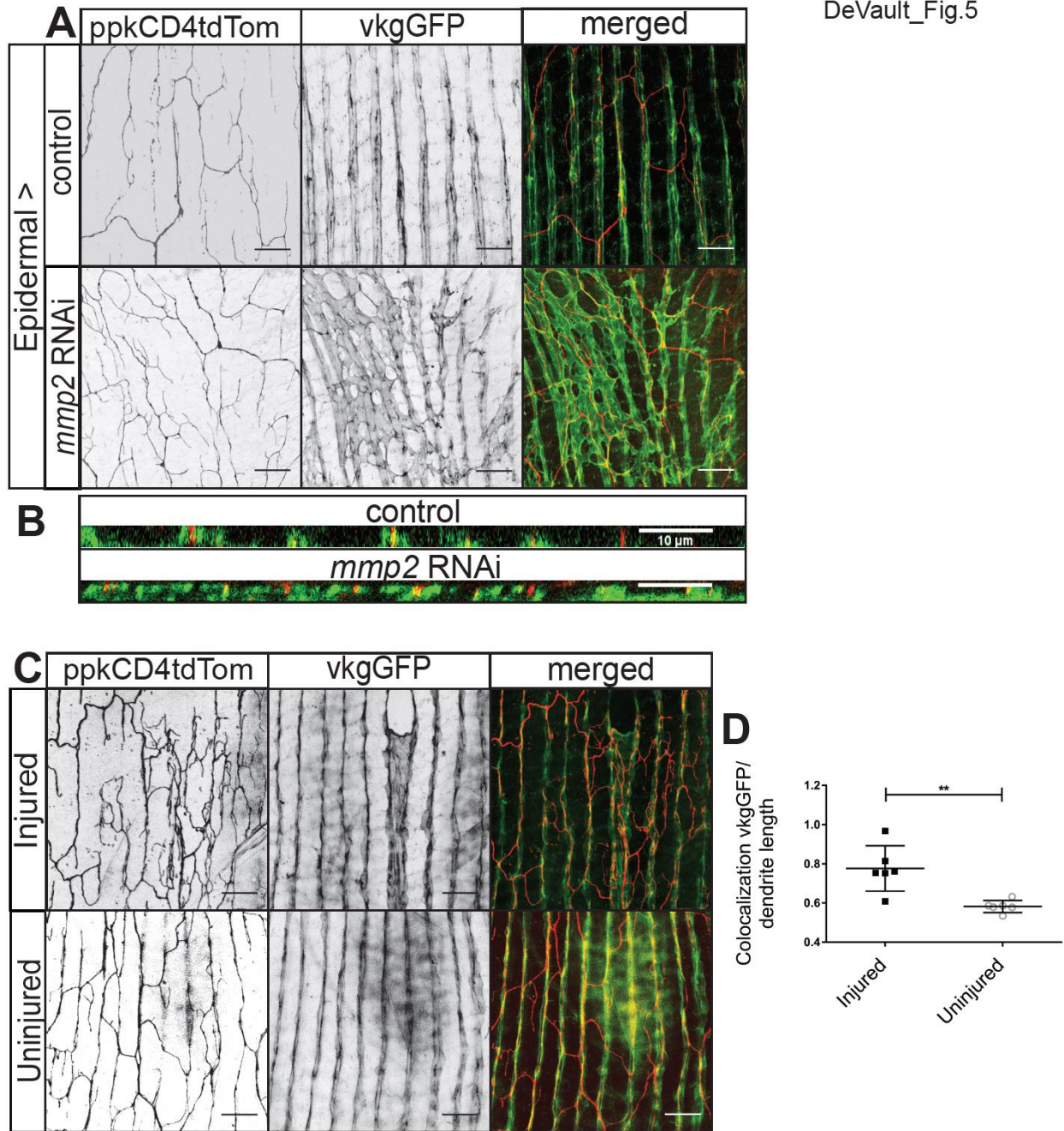


Figure 4.5. Regenerated dendrites associate with the ECM. A. Epidermal expression of *mmp2* RNAi partially preserves ECM at 3 days after eclosion. Collagen IV (vkgGFP) marks ECM. B. XZ view of ECM and dendrite co-localization. C. Co-localization of neuron (ppkCD4tdTom) and Collagen IV (vkgGFP) in injured and uninjured neurons at 7 days after injury. D. Proportion of the dendritic arbor that co-localizes with Collagen IV. There was a significant difference between injured (M=0.7762, SD=0.12) and uninjured neurons (M=0.5828, SD=0.031) $t(10) = 3.940$, $p=0.0028$. $n= 6$ injured, 6 uninjured neurons.

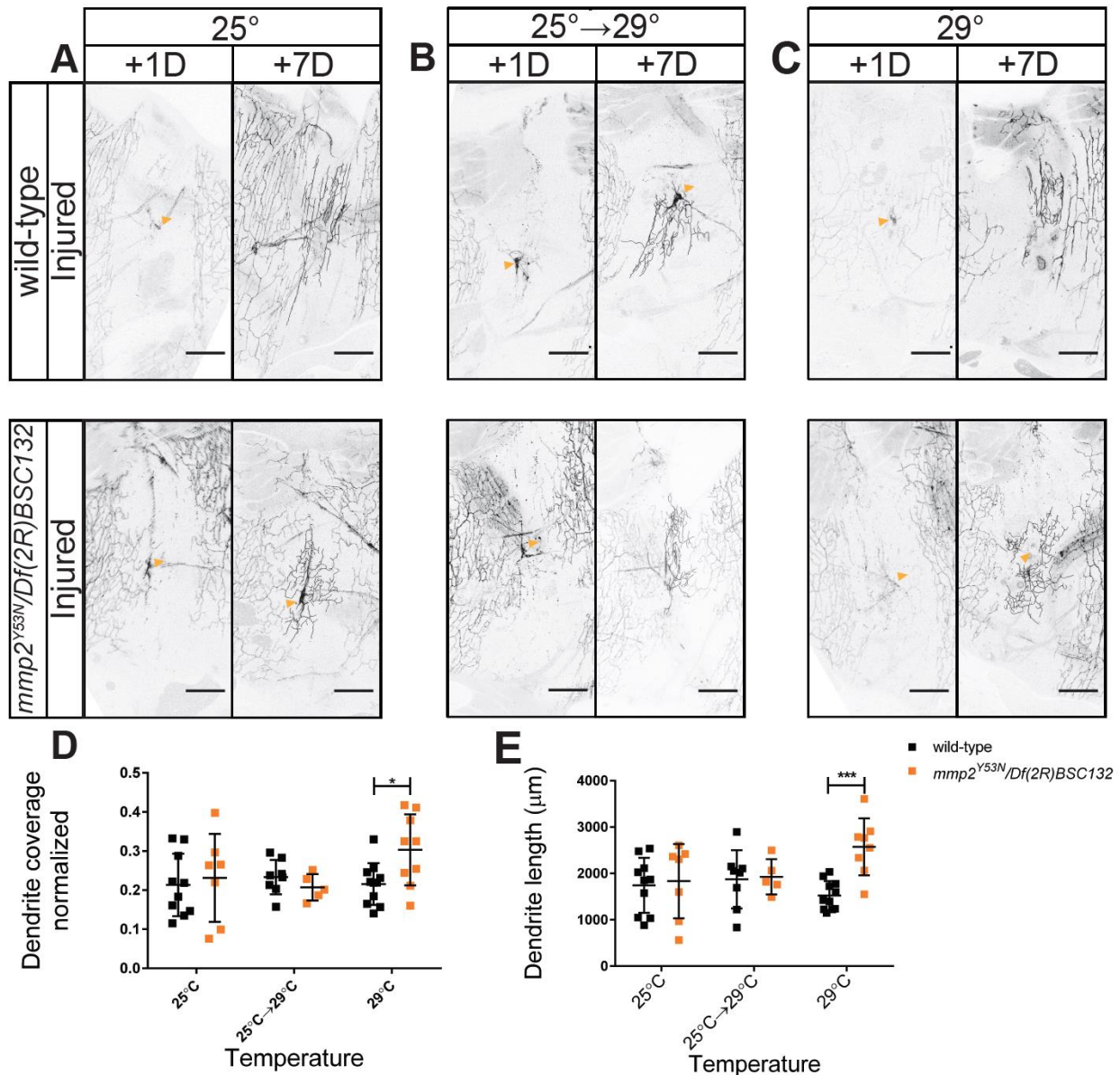


Figure 4.6. During the 3 days period after eclosion, *mmp2* influences dendrite regeneration. Wild-type and *mmp2^{Y53N}/Df(2R) BSC132* neurons were injured at 3 days after eclosion. Neurons were imaged at 1 and 7 days after injury. A. Flies were kept at 25°C. B. Flies were raised at 25°C and shifted to 29°C at 3 days after eclosion C. Flies eclosed at 25°C and were shifted to 29°C within 1 day of eclosion. D. Regenerated dendrite area after 7 days is plotted. Area coverage was subject to a two-way ANOVA. There was not a significant effect of temperature $F(2, 44) = 1.513$, $p=0.2314$, genotype $F(1, 44) = 1.464$ or interaction $F(2, 44) = 2.364$, $p=0.1058$. Sidak's post hoc test revealed at 29°C, a difference between *mmp2^{Y53N}/Df(2R) BSC132* and wild-type neurons. E. Dendrite length 7 days after injury. Dendrite length was subject to a two-way ANOVA. The effect of temperature was not significant $F(2, 43) = 0.9129$, $p=0.4090$. Genotype, $F(1, 43) = 5.612$, $p=0.0224$ and interaction, $F(2,43) = 4.139$, $p=0.0227$, were significant. Sidak's

post hoc test revealed that at 29°C, *mmp2^{Y53N}/Df(2R) BSC132* regenerated neurons (M=2574, SD= 612) had greater dendrite length than wild-type neurons (M=1523, SD=312). *n*= 10 wild-type, 7 *mmp2^{Y53N}/Df(2R) BSC132* neurons at 25°C, 8 wild-type, 5 *mmp2^{Y53N}/Df(2R) BSC132* neurons shifted from 25°C→29°C, 11 wild-type, 8 *mmp2^{Y53N}/Df(2R) BSC132* neurons at 29°C.

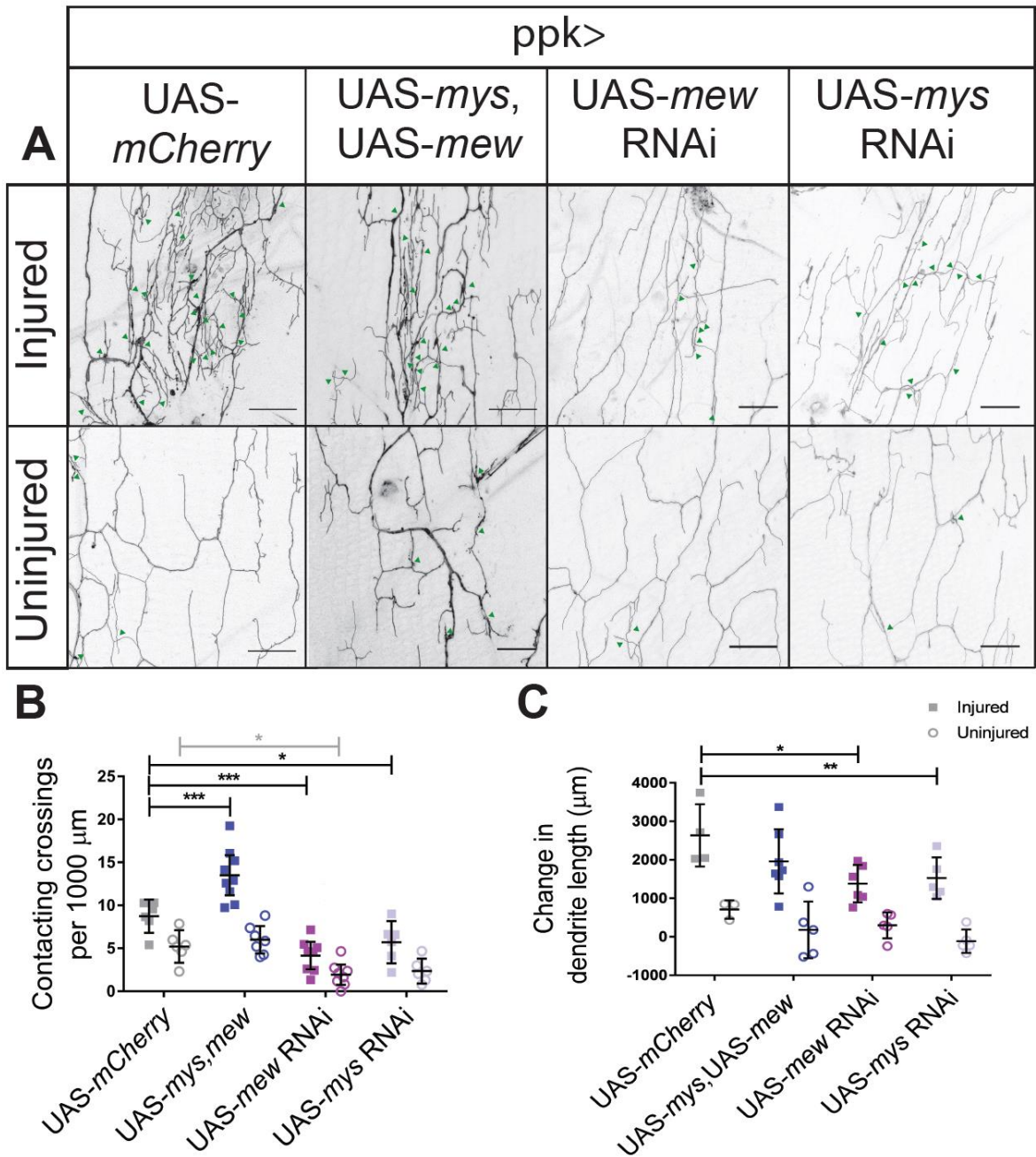


Figure 4.7. Integrin expression alters dendritic crossings and dendrite outgrowth of regenerated dendrites. A. Dendritic crossings of injured and uninjured neurons in neurons overexpressing integrin subunits (*mys* and *mew*), expressing *mew* RNAi, expressing *mys* RNAi and expressing *mCherry*. Scale bar represents 20 μm . Green arrows indicate contacting crossings. B. Contacting crossings events were analyzed by a two-way ANOVA. Injury, $F(1, 48) = 56.16$, $p < 0.0001$, integrin, $F(3, 48) = 33.32$, $p < 0.0001$, and interaction, $F(3, 48) =$

4.945, $p=0.0045$, were significant. Post hoc analysis using Dunnett's test for multiple comparisons demonstrated that overexpression of *mys*, *mew* increased contacting crossings in injured neurons (M=13.5; SD=3.0) compared to overexpression of *mCherry* (M=8.7; SD=1.8); knockdown of *mew* (M=4.1; SD=1.9) and *mys* (M=5.7; SD=2.3) decreased contacting crossings compared to *mCherry*. Knockdown of *mew* (M=1.9; SD=1.4) decreased contacting crossings compared to *mCherry* expression (M=5.2; SD=1.8) in uninjured neurons. $n=$ 9 injured, 7 uninjured *mys*, *mew*; 6 injured, 6 uninjured *mCherry*; 8 injured, 8 uninjured *mew* RNAi, 6 injured, 6 uninjured *mys* RNAi neurons. C. Change in dendrite length upon integrin manipulation. Change in dendritic length was analyzed by two-way ANOVA. Injury, $F(1,32) = 67.48$, $p < 0.0001$, and integrin, $F(3,32) = 3.95$, $p = 0.0166$. were significant. There was no interaction effect $F(3,32) = 0.9318$, $p = 0.4366$. Post hoc analysis using Sidak's multiple comparison test revealed that injured *mys* RNAi (M=1526; SD=539) and *mew* RNAi (M=1380, SD=487) had decreased changes in dendrite length compared to injured neurons expressing *mCherry* (M=2636, SD=808).



Figure 4.8. Images of disc for repeated imaging in adult *Drosophila*. Images of disc for repeated imaging in adult *Drosophila*. Disc is shown under a microscope. Underside of disc with connection to CO₂ is shown.

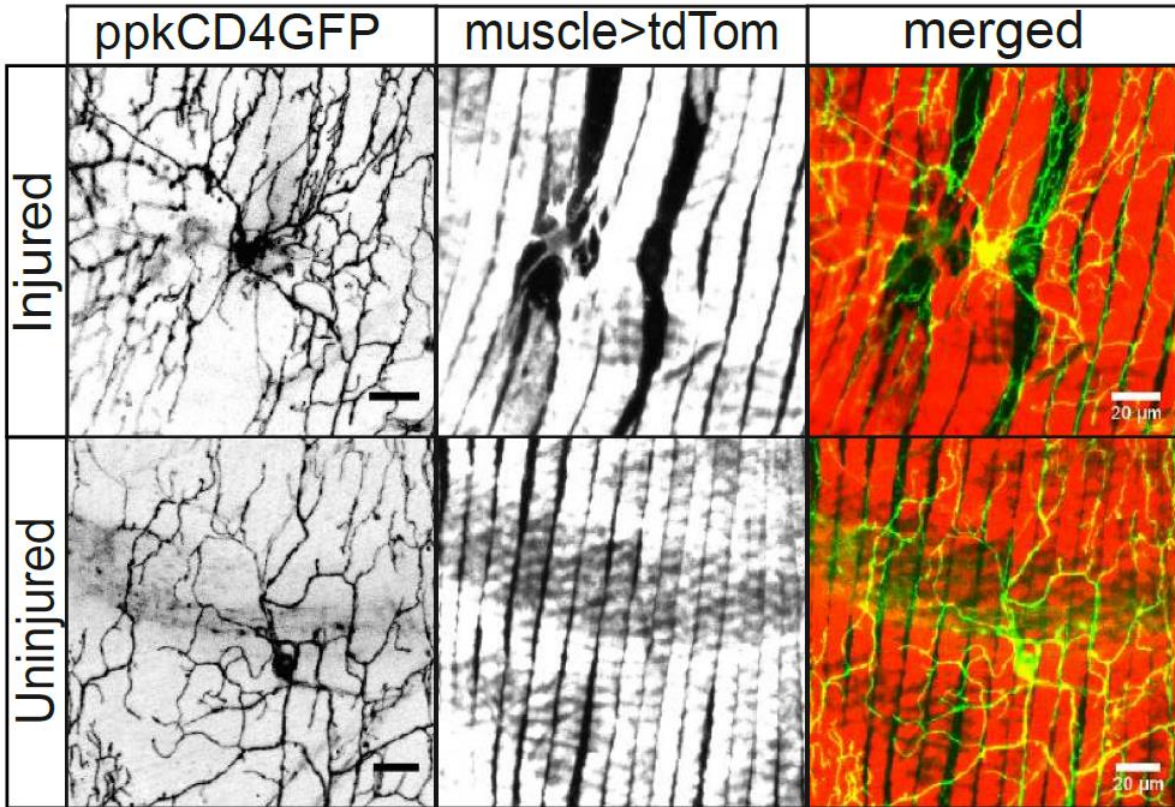


Figure 4.9. Muscle damage occurred during dendrite injury. Neurons are marked by *ppkCD4tdGFP*. Expression of UAS-tdTomato by Muscle Gal 4 (*Mef2*) marks the lateral abdominal muscles. Injury and degeneration are noted near location of scanning laser injury.

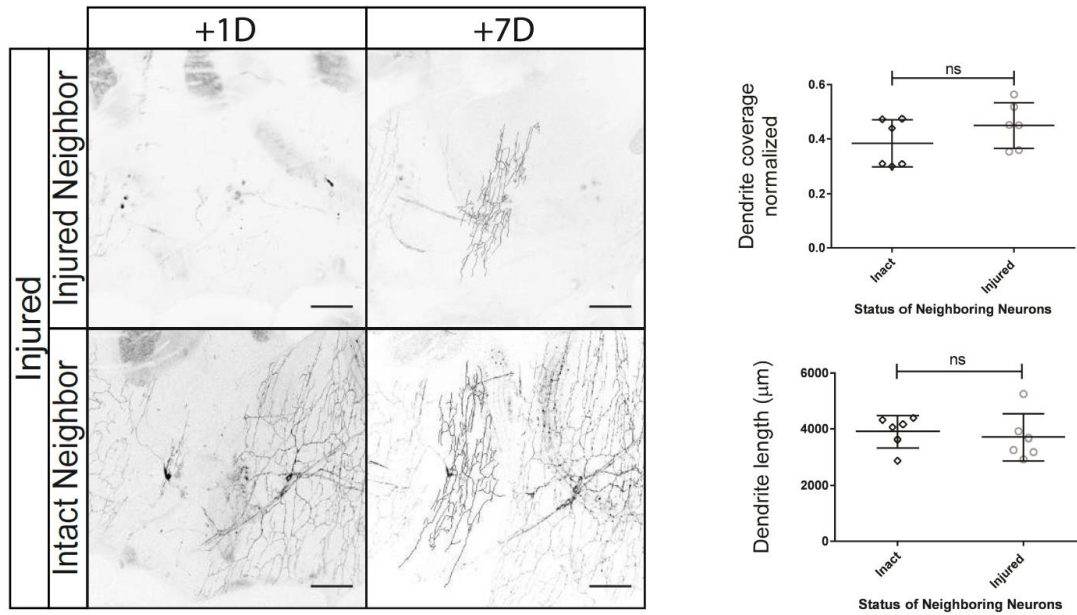


Figure 4.10. Effect of injured neighboring neurons on dendrite regrowth. Status of neighboring neurons does not effect dendrite regeneration. Dendrite coverage is not effected by status of neighboring neurons. Dendrite coverage was subject to a t-test. There was not a significant difference between regenerating neurons with injured neighbors ($M=0.4490$, $SD=0.0841$) and regenerating neurons with intact neighbors ($M=0.3834$, $SD=0.0870$) $t(10) = 1.329$, $p=0.2135$. Dendrite length of regenerating neurons was not effected by the status of neighboring neurons. Dendrite length was subject to a t-test. There was not a significant difference between regenerating neurons with injured neighbors ($M=3711$, $SD=834$) and regenerating neurons with intact neurons ($M=3911$, $SD=568$) $t(10) = 0.4862$, $p= 0.6373$. $n = 6$ intact neighboring neurons, 6 injured neighboring neurons.

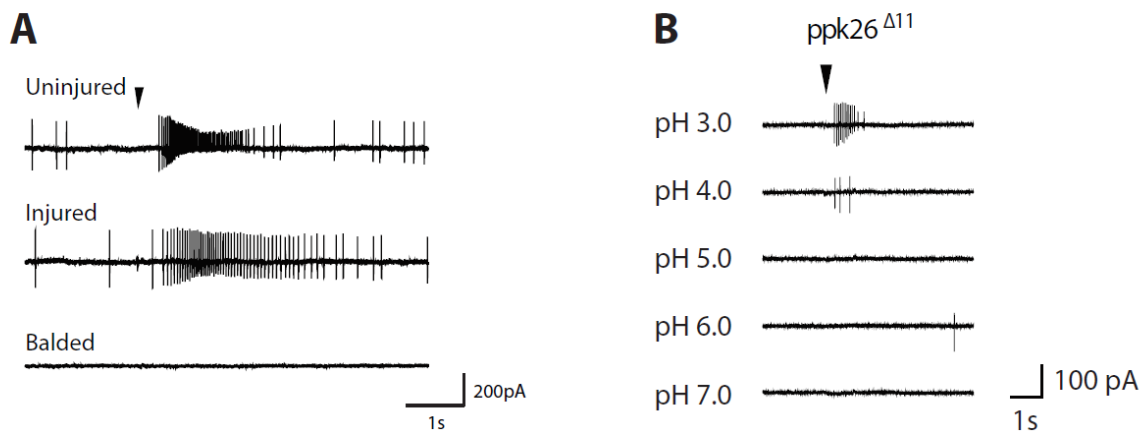


Figure 4.11. Electrophysiological response of c4da neurons. A. Sample traces for response to acidified solution at pH=3. Balded neurons show no response to stimulation with acidified solution n=10. B. Ppk26 is not required for response to acid stimuli. Flies null for Ppk26, *ppk26^{Δ11}/Df(3L) exel8104* responded to stimulation at pH=3.

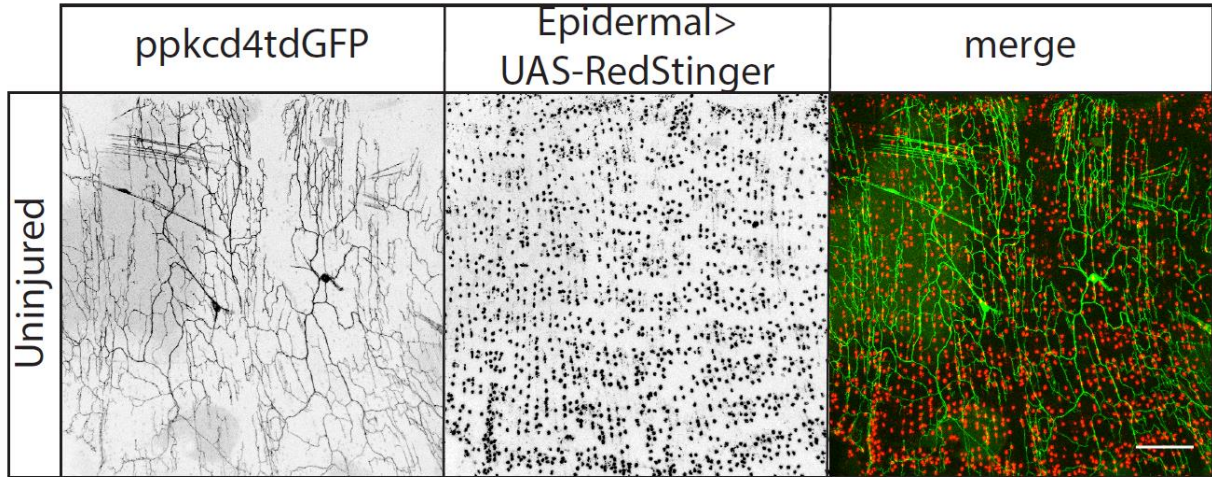


Figure 4.12. *GMR51F10 Gal4* is expressed in the epidermis of the abdomen. *UASRed-Stinger* is driven by *GMR51F10 Gal4* expression in the abdomen.

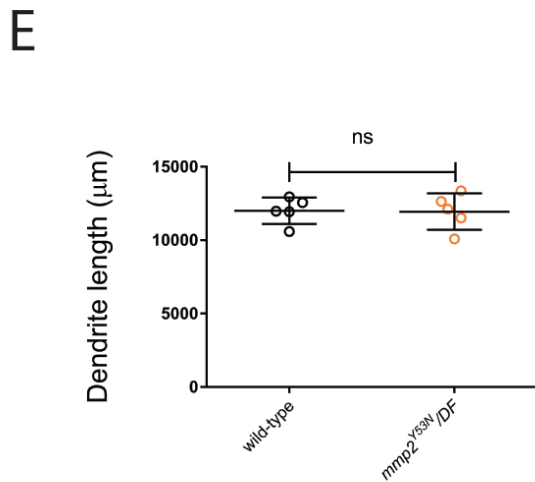
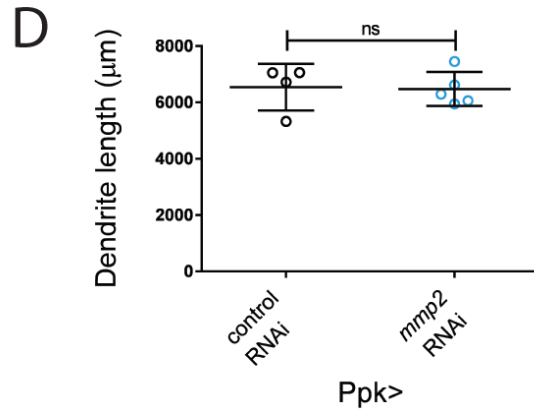
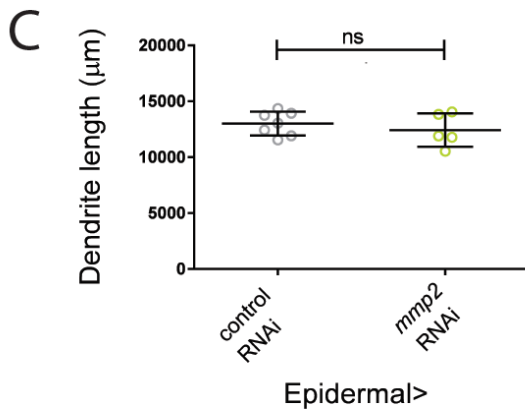
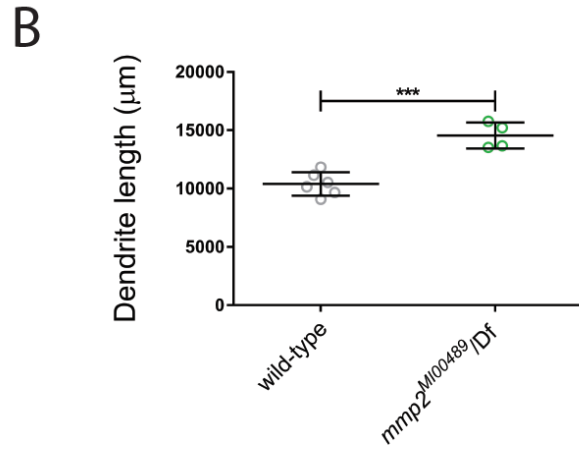
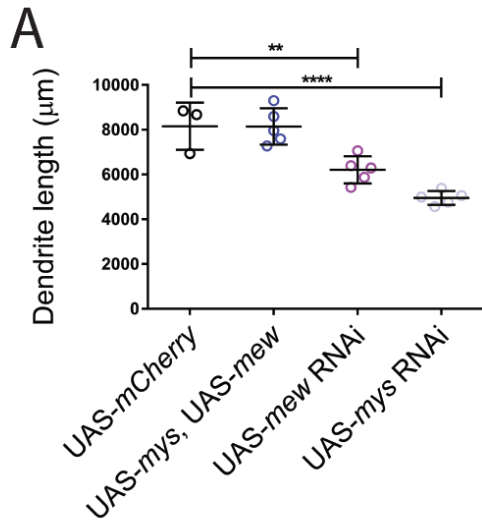


Figure 4.13. Dendrite length of uninjured neurons at 8 days after eclosion. A.

Knockdown of *mys* and *mew* decrease total dendrite length. Dendrite length was subject to a one-way ANOVA. There was a significant effect of integrin manipulation on dendrite length $F(3,14) = 23.07$, $p < 0.0001$. Tukey's posthoc test revealed that *mew* RNAi (M= 6211; SD=611) and *mys* RNAi (M=4957, SD=309) decreased dendrite length compared to *mCherry* expression (M= 8155; SD=1054) B. Mutants for *mmp2* ^{M100489}/*DF* (*2RBSC132*) had increased dendritic length compared to wild-type neurons. Dendritic length was subject to a t-test. There was a significant difference between wild-type and *mmp2*^{M100489}/*DF*(2*R*) *BSC132* neurons $t(8) = 6.150$, $p = 0.0003$. C. Epidermal knockdown of *mmp2* does not affect dendritic length in uninjured neurons. An unpaired t-test revealed no difference $t(10) = 0.7839$, $p = 0.4419$. D. Neuronal knockdown of *mmp2* does not affect dendrite length in uninjured neurons. An unpaired t-test reveal no difference $t(5) = 0.4433$, $p = 0.676$. E. At 29° mutants for *mmp2*^{Y53N}/*DF*(2*R*) *BSC132* did not have increased dendritic length compared to wild-type neurons. An unpaired t-test revealed no difference between *mmp2*^{Y53N}/*DF*(2*R*) *BSC132* (M=11950, SD=1242) and wild-type neurons (M=12007, SD=899) $t(8) = 0.0833$, $p = 0.9356$.

References

- Adams, C.M., Anderson, M.G., Motto, D.G., Price, M.P., Johnson, W.A., and Welsh, M.J. (1998). Ripped Pocket and Pickpocket, Novel *Drosophila* DEG/ENaC Subunits Expressed in Early Development and in Mechanosensory Neurons. *The Journal of Cell Biology* *140*, 143–152.
- Ainsley, J.A., Pettus, J.M., Bosenko, D., Gerstein, C.E., Zinkevich, N., Anderson, M.G., Adams, C.M., Welsh, M.J., and Johnson, W.A. (2003). Enhanced locomotion caused by loss of the *Drosophila* DEG/ENaC protein Pickpocket1. *Curr. Biol.* *13*, 1557–1563.
- Anderson, M.A., Burda, J.E., Ren, Y., Ao, Y., O’Shea, T.M., Kawaguchi, R., Coppola, G., Khakh, B.S., Deming, T.J., and Sofroniew, M.V. (2016). Astrocyte scar formation aids central nervous system axon regeneration. *Nature* *532*, 195–200.
- Andrews, M.R., Czvitkovich, S., Dassie, E., Vogelaar, C.F., Faissner, A., Blits, B., Gage, F.H., French-Constant, C., and Fawcett, J.W. (2009). Alpha9 integrin promotes neurite outgrowth on tenascin-C and enhances sensory axon regeneration. *J. Neurosci.* *29*, 5546–5557.
- Andries, L., Van Hove, I., Moons, L., and De Groef, L. (2017). Matrix Metalloproteinases During Axonal Regeneration, a Multifactorial Role from Start to Finish. *Mol. Neurobiol.* *54*, 2114–2125.
- Baas, P.W., and Lin, S. (2011). Hooks and Comets: The Story of Microtubule Polarity Orientation in the Neuron. *Dev Neurobiol* *71*, 403–418.
- Baas, P.W., Deitch, J.S., Black, M.M., and Banker, G.A. (1988). Polarity orientation of microtubules in hippocampal neurons: uniformity in the axon and nonuniformity in the dendrite. *Proc Natl Acad Sci U S A* *85*, 8335–8339.
- Badre, N.H., Martin, M.E., and Cooper, R.L. (2005). The physiological and behavioral effects of carbon dioxide on *Drosophila melanogaster* larvae. *Comp. Biochem. Physiol., Part A Mol. Integr. Physiol.* *140*, 363–376.
- Barnat, M., Benassy, M.-N., Vincensini, L., Soares, S., Fassier, C., Propst, F., Andrieux, A., von Boxberg, Y., and Nothias, F. (2016). The GSK3-MAP1B pathway controls neurite branching and microtubule dynamics. *Mol. Cell. Neurosci.* *72*, 9–21.
- Barnes, A.P., and Polleux, F. (2009). Establishment of axon-dendrite polarity in developing neurons. *Annu. Rev. Neurosci.* *32*, 347–381.
- Bartus, K., James, N.D., Didangelos, A., Bosch, K.D., Verhaagen, J., Yáñez-Muñoz, R.J., Rogers, J.H., Schneider, B.L., Muir, E.M., and Bradbury, E.J. (2014). Large-scale chondroitin sulfate proteoglycan digestion with chondroitinase gene therapy leads to reduced pathology and modulates macrophage phenotype following spinal cord contusion injury. *J. Neurosci.* *34*, 4822–4836.
- Bei, F., Lee, H.H.C., Liu, X., Gunner, G., Jin, H., Ma, L., Wang, C., Hou, L., Hensch, T.K.,

- Frank, E., Sanes, J.R., Chen, C., Fagiolini, M., He, Z. (2016). Restoration of Visual Function by Enhancing Conduction in Regenerated Axons. *Cell* 164, 219–232.
- Bischoff, M., and Cseresnyés, Z. (2009). Cell rearrangements, cell divisions and cell death in a migrating epithelial sheet in the abdomen of *Drosophila*. *Development* 136, 2403–2411.
- Boiko, N., Kucher, V., Stockand, J.D., and Eaton, B.A. (2012). Pickpocket1 is an ionotropic molecular sensory transducer. *J. Biol. Chem.* 287, 39878–39886.
- Brace, E.J., and DiAntonio, A. (2017). Models of axon regeneration in *Drosophila*. *Exp. Neurol.* 287, 310–317.
- Bunt, S., Hooley, C., Hu, N., Scahill, C., Weavers, H., and Skaer, H. (2010). Hemocyte-secreted type IV collagen enhances BMP signaling to guide renal tubule morphogenesis in *Drosophila*. *Dev. Cell* 19, 296–306.
- Busch, S.A., Horn, K.P., Silver, D.J., and Silver, J. (2009). Overcoming macrophage-mediated axonal dieback following CNS injury. *J. Neurosci.* 29, 9967–9976.
- Carter, L.M., McMahon, S.B., and Bradbury, E.J. (2011). Delayed treatment with chondroitinase ABC reverses chronic atrophy of rubrospinal neurons following spinal cord injury. *Exp. Neurol.* 228, 149–156.
- Chauvet, N., Prieto, M., and Alonso, G. (1998). Tanycytes present in the adult rat mediobasal hypothalamus support the regeneration of monoaminergic axons. *Exp. Neurol.* 151, 1–13.
- Chen, L., Stone, M.C., Tao, J., Rolls, M.M. (2012) Axon injury and stress trigger a microtubule-based neuroprotective pathway. *PNAS* 29, 11842-7.
- Chen, T., Wardill, T.J., Sun, Y., Pulver, S.R., Renninger, S.L., Baohan, A., Schreiter, E.R., Kerr, R.A., Orger, M.B., Jayaraman, V., Looger, L.L., Svoboda, K., Kim, D.S. (2013). Ultra-sensitive fluorescent proteins for imaging neuronal activity. *Nature* 499, 295-300.
- Cholas, R., Hsu, H.-P., and Spector, M. (2012). Collagen scaffolds incorporating select therapeutic agents to facilitate a reparative response in a standardized hemi section defect in the rat spinal cord. *Tissue Eng Part A* 18, 2158–2172.
- Christie, K.J., Webber, C.A., Martinez, J.A., Singh, B., and Zochodne, D.W. (2010). PTEN inhibition to facilitate intrinsic regenerative outgrowth of adult peripheral axons. *J. Neurosci.* 30, 9306–9315.
- Conde, C., and Cáceres, A. (2009). Microtubule assembly, organization and dynamics in axons and dendrites. *Nat. Rev. Neurosci.* 10, 319–332.
- Condic, M.L. (2001). Adult neuronal regeneration induced by transgenic integrin expression. *J. Neurosci.* 21, 4782–4788.
- Cregg, J.M., DePaul, M.A., Filous, A.R., Lang, B.T., Tran, A., and Silver, J. (2014). Functional

regeneration beyond the glial scar. *Exp. Neurol.* 253, 197–207.

Crest, J., Diz-Muñoz, A., Chen, D.-Y., Fletcher, D.A., and Bilder, D. (2017). Organ sculpting by patterned extracellular matrix stiffness. *Elife* 6.

Crozatier, M., and Vincent, A. (2008). Control of multidendritic neuron differentiation in *Drosophila*: the role of Collier. *Dev. Biol.* 315, 232–242.

Dansie, L.E., and Ethell, I.M. (2011). Casting a net on dendritic spines: the extracellular matrix and its receptors. *Dev Neurobiol* 71, 956–981.

Dantas, T.J., Carabalona, A., Hu, D.J.K., and Vallee, R.B. (2016). Emerging roles for motor proteins in progenitor cell behavior and neuronal migration during brain development. *Cytoskeleton (Hoboken)* 73, 566–576.

Das, R., Bhattacharjee, S., Patel, A.A., Harris, J.M., Bhattacharya, S., Letcher, J.M., Clark, S.G., Nanda, S., Iyer, E.P.R., Ascoli, G.A., Cox, D.N. (2017). Dendritic Cytoskeletal Architecture Is Modulated by Combinatorial Transcriptional Regulation in *Drosophila melanogaster*. *Genetics* 207, 1401–1421.

Del Castillo, U., Lu, W., Winding, M., Lakonishok, M., and Gelfand, V.I. (2015). Pavarotti/MKLP1 regulates microtubule sliding and neurite outgrowth in *Drosophila* neurons. *Curr. Biol.* 25, 200–205.

DeVault, L., Li, T., Izabel, S., Thompson-Peer, K.L., Jan, L.Y., and Jan, Y.N. (2018). Dendrite regeneration of adult *Drosophila* sensory neurons diminishes with aging and is inhibited by epidermal-derived matrix metalloproteinase 2. *Genes Dev.* 32, 402–414.

Dill, J., Wang, H., Zhou, F., and Li, S. (2008). Inactivation of glycogen synthase kinase 3 promotes axonal growth and recovery in the CNS. *J. Neurosci.* 28, 8914–8928.

Dong, X., Shen, K., and Bülow, H.E. (2015). Intrinsic and extrinsic mechanisms of dendritic morphogenesis. *Annu. Rev. Physiol.* 77, 271–300.

Duan, X., Qiao, M., Bei, F., Kim, I.-J., He, Z., and Sanes, J.R. (2015). Subtype-specific regeneration of retinal ganglion cells following axotomy: effects of osteopontin and mTOR signaling. *Neuron* 85, 1244–1256.

Edwards, T.J., and Hammarlund, M. (2014). Syndecan promotes axon regeneration by stabilizing growth cone migration. *Cell Rep* 8, 272–283.

Ekström, P.A.R., Mayer, U., Panjwani, A., Pountney, D., Pizzey, J., and Tonge, D.A. (2003). Involvement of alpha7beta1 integrin in the conditioning-lesion effect on sensory axon regeneration. *Mol. Cell. Neurosci.* 22, 383–395.

Ertürk, A., Hellal, F., Enes, J., Bradke, F. (2007) Disorganized microtubules underlie the formation of retraction bulbs and the failure of axonal regeneration. *J Neurosci.* 27, 9169-9180.

- Evans, T.A., Barkauskas, D.S., Myers, J.T., Hare, E.G., You, J.Q., Ransohoff, R.M., Huang, A.Y., and Silver, J. (2014). High-resolution intravital imaging reveals that blood-derived macrophages but not resident microglia facilitate secondary axonal dieback in traumatic spinal cord injury. *Exp. Neurol.* 254, 109–120.
- Falke, E., Nissanov, J., Mitchell, T.W., Bennett, D.A., Trojanowski, J.Q., and Arnold, S.E. (2003). Subicular dendritic arborization in Alzheimer's disease correlates with neurofibrillary tangle density. *Am. J. Pathol.* 163, 1615–1621.
- Ferreira, T., Ou, Y., Li, S., Giniger, E., and van Meyel, D.J. (2014). Dendrite architecture organized by transcriptional control of the F-actin nucleator Spire. *Development* 141, 650–660.
- Filous, A.R., and Schwab, J.M. (2018). Determinants of Axon Growth, Plasticity, and Regeneration in the Context of Spinal Cord Injury. *Am. J. Pathol.* 188, 53–62.
- Filous, A.R., Miller, J.H., Coulson-Thomas, Y.M., Horn, K.P., Alilain, W.J., and Silver, J. (2010). Immature astrocytes promote CNS axonal regeneration when combined with chondroitinase ABC. *Dev Neurobiol* 70, 826–841.
- Fischler, W., Kong, P., Marella, S., and Scott, K. (2007). The detection of carbonation by the *Drosophila* gustatory system. *Nature* 448, 1054–1057.
- Franker, M.A.M., and Hoogenraad, C.C. (2013). Microtubule-based transport - basic mechanisms, traffic rules and role in neurological pathogenesis. *J. Cell. Sci.* 126, 2319–2329.
- Fushiki, A., Zwart, M.F., Kohsaka, H., Fetter, R.D., Cardona, A., and Nose, A. (2016). A circuit mechanism for the propagation of waves of muscle contraction in *Drosophila*. *Elife* 5.
- Gallaher, Z.R., and Steward, O. (2018). Modest enhancement of sensory axon regeneration in the sciatic nerve with conditional co-deletion of PTEN and SOCS3 in the dorsal root ganglia of adult mice. *Exp. Neurol.* 303, 120–133.
- Ghosh-Roy, A., Wu, Z., Goncharov, A., Jin, Y., and Chisholm, A.D. (2010). Calcium and cyclic AMP promote axonal regeneration in *Caenorhabditis elegans* and require DLK-1 kinase. *J. Neurosci.* 30, 3175–3183.
- Girouard, M.-P., Bueno, M., Julian, V., Drake, S., Byrne, A.B., and Fournier, A.E. (2018). The molecular interplay between axon degeneration and regeneration. *Dev Neurobiol.*
- Gobrecht, P., Andreadaki, A., Diekmann, H., Heskamp, A., Leibinger, M., and Fischer, D. (2016). Promotion of Functional Nerve Regeneration by Inhibition of Microtubule Detyrosination. *J. Neurosci.* 36, 3890–3902.
- Goldberg, J.L. (2012). Role of electrical activity in promoting neural repair. *Neurosci. Lett.* 519, 134–137.
- Goldstein, A.Y.N., Jan, Y.-N., and Luo, L. (2005). Function and regulation of Tumbleweed (RacGAP50C) in neuroblast proliferation and neuronal morphogenesis. *Proc. Natl. Acad. Sci.*

U.S.A. *102*, 3834–3839.

Goodwin, P.R., Sasaki, J.M., and Juo, P. (2012). Cyclin-dependent kinase 5 regulates the polarized trafficking of neuropeptide-containing dense-core vesicles in *Caenorhabditis elegans* motor neurons. *J. Neurosci.* *32*, 8158–8172.

Gorczyca, D.A., Younger, S., Meltzer, S., Kim, S.E., Cheng, L., Song, W., Lee, H.Y., Jan, L.Y., and Jan, Y.N. (2014). Identification of Ppk26, a DEG/ENaC Channel Functioning with Ppk1 in a Mutually Dependent Manner to Guide Locomotion Behavior in *Drosophila*. *Cell Rep* *9*, 1446–1458.

Goshima, G., and Vale, R.D. (2003). The roles of microtubule-based motor proteins in mitosis: comprehensive RNAi analysis in the *Drosophila* S2 cell line. *J. Cell Biol.* *162*, 1003–1016.

Goulas, S., Conder, R., and Knoblich, J.A. (2012). The Par complex and integrins direct asymmetric cell division in adult intestinal stem cells. *Cell Stem Cell* *11*, 529–540.

Grueber, W.B., Jan, L.Y., and Jan, Y.N. (2002). Tiling of the *Drosophila* epidermis by multidendritic sensory neurons. *Development* *129*, 2867–2878.

Grueber, W.B., Ye, B., Moore, A.W., Jan, L.Y., and Jan, Y.N. (2003). Dendrites of distinct classes of *Drosophila* sensory neurons show different capacities for homotypic repulsion. *Curr. Biol.* *13*, 618–626.

Guardia, C.M., Farías, G.G., Jia, R., Pu, J., and Bonifacino, J.S. (2016). BORC Functions Upstream of Kinesins 1 and 3 to Coordinate Regional Movement of Lysosomes Along Different Microtubule Tracks. *Cell Rep* *17*, 1950–1961.

Guo, Y., Wang, Y., Wang, Q., and Wang, Z. (2014). The role of PPK26 in *Drosophila* larval mechanical nociception. *Cell Rep* *9*, 1183–1190.

Gysi, S., Rhiner, C., Flibotte, S., Moerman, D.G., and Hengartner, M.O. (2013). A network of HSPG core proteins and HS modifying enzymes regulates netrin-dependent guidance of D-type motor neurons in *Caenorhabditis elegans*. *PLoS ONE* *8*, e74908.

Hammarlund, M., Nix, P., Hauth, L., Jorgensen, E.M., and Bastiani, M. (2009). Axon regeneration requires a conserved MAP kinase pathway. *Science* *323*, 802–806.

Han, C., Wang, D., Soba, P., Zhu, S., Lin, X., Jan, L.Y., and Jan, Y.-N. (2012). Integrins regulate repulsion-mediated dendritic patterning of *Drosophila* sensory neurons by restricting dendrites in a 2D space. *Neuron* *73*, 64–78.

Han, S.M., Baig, H.S., and Hammarlund, M. (2016). Mitochondria Localize to Injured Axons to Support Regeneration. *Neuron* *92*, 1308–1323.

Hattori, Y., Sugimura, K., and Uemura, T. (2007). Selective expression of Knot/Collier, a transcriptional regulator of the EBF/Olf-1 family, endows the *Drosophila* sensory system with neuronal class-specific elaborated dendritic patterns. *Genes Cells* *12*, 1011–1022.

- Hawthorne, A.L., Hu, H., Kundu, B., Steinmetz, M.P., Wylie, C.J., Deneris, E.S., and Silver, J. (2011). The unusual response of serotonergic neurons after CNS Injury: lack of axonal dieback and enhanced sprouting within the inhibitory environment of the glial scar. *J. Neurosci.* *31*, 5605–5616.
- Hellal, F., Hurtado, A., Ruschel, J., Flynn, K.C., Laskowski, C. J., Umlauf, M., Kapitein, L.C., Strikis, D., Lemmon, V., Bixby, J., Hoogenraad, C.C., Bradke, F. (2011) Microtubule stabilization reduces scarring and causes axon regeneration after spinal cord injury. *Science* *331*, 928-931.
- Hill, S.E., Parmar, M., Gheres, K.W., Guignet, M.A., Huang, Y., Jackson, F.R., and Rolls, M.M. (2012). Development of dendrite polarity in *Drosophila* neurons. *Neural Dev* *7*, 34.
- Horn, K.P., Busch, S.A., Hawthorne, A.L., van Rooijen, N., and Silver, J. (2008). Another barrier to regeneration in the CNS: activated macrophages induce extensive retraction of dystrophic axons through direct physical interactions. *J. Neurosci.* *28*, 9330–9341.
- Horton, A.C., and Ehlers, M.D. (2003). Dual modes of endoplasmic reticulum-to-Golgi transport in dendrites revealed by live-cell imaging. *J. Neurosci.* *23*, 6188–6199.
- Horton, A.C., and Ehlers, M.D. (2004). Secretory trafficking in neuronal dendrites. *Nat. Cell Biol.* *6*, 585–591.
- Horton, A.C., Rácz, B., Monson, E.E., Lin, A.L., Weinberg, R.J., and Ehlers, M.D. (2005). Polarized secretory trafficking directs cargo for asymmetric dendrite growth and morphogenesis. *Neuron* *48*, 757–771.
- Hu, F., and Strittmatter, S.M. (2008). The N-terminal domain of Nogo-A inhibits cell adhesion and axonal outgrowth by an integrin-specific mechanism. *J. Neurosci.* *28*, 1262–1269.
- Huang, H., Du, G., Chen, H., Liang, X., Li, C., Zhu, N., Xue, L., Ma, J., and Jiao, R. (2011). *Drosophila* Smt3 negatively regulates JNK signaling through sequestering Hipk in the nucleus. *Development* *138*, 2477–2485.
- Hummel, T., Krukkert, K., Roos, J., Davis, G., and Klämbt, C. (2000). *Drosophila* Futsch/22C10 is a MAP1B-like protein required for dendritic and axonal development. *Neuron* *26*, 357–370.
- Huntwork-Rodriguez, S., Wang, B., Watkins, T., Ghosh, A.S., Pozniak, C.D., Bustos, D., Newton, K., Kirkpatrick, D.S., and Lewcock, J.W. (2013). JNK-mediated phosphorylation of DLK suppresses its ubiquitination to promote neuronal apoptosis. *J. Cell Biol.* *202*, 747–763.
- Hwang, R.Y., Zhong, L., Xu, Y., Johnson, T., Zhang, F., Deisseroth, K., and Tracey, W.D. (2007). Nociceptive neurons protect *Drosophila* larvae from parasitoid wasps. *Curr. Biol.* *17*, 2105–2116.
- Inman, D.M., and Steward, O. (2003). Ascending sensory, but not other long-tract axons, regenerate into the connective tissue matrix that forms at the site of a spinal cord injury in mice. *J. Comp. Neurol.* *462*, 431–449.

- Ivins, J.K., Yurchenco, P.D., and Lander, A.D. (2000). Regulation of neurite outgrowth by integrin activation. *J. Neurosci.* *20*, 6551–6560.
- Jaarsma, D., and Hoogenraad, C.C. (2015). Cytoplasmic dynein and its regulatory proteins in Golgi pathology in nervous system disorders. *Front Neurosci* *9*, 397.
- Jan, Y.-N., and Jan, L.Y. (2010). Branching out: mechanisms of dendritic arborization. *Nat. Rev. Neurosci.* *11*, 316–328.
- Jia, Q., Liu, Y., Liu, H., and Li, S. (2014). Mmp1 and Mmp2 cooperatively induce *Drosophila* fat body cell dissociation with distinct roles. *Sci Rep* *4*, 7535.
- Jin, D., Liu, Y., Sun, F., Wang, X., Liu, X., and He, Z. (2015). Restoration of skilled locomotion by sprouting corticospinal axons induced by co-deletion of PTEN and SOCS3. *Nat Commun* *6*, 8074.
- Jinushi-Nakao, S., Arvind, R., Amikura, R., Kinameri, E., Liu, A.W., and Moore, A.W. (2007). Knot/Collier and cut control different aspects of dendrite cytoskeleton and synergize to define final arbor shape. *Neuron* *56*, 963–978.
- Jones, W.D., Cayirlioglu, P., Kadow, I.G., and Vosshall, L.B. (2007). Two chemosensory receptors together mediate carbon dioxide detection in *Drosophila*. *Nature* *445*, 86–90.
- Kahn, O.I., Sharma, V., González-Billault, C., and Baas, P.W. (2015). Effects of kinesin-5 inhibition on dendritic architecture and microtubule organization. *Mol. Biol. Cell* *26*, 66–77.
- Kelliher, M.T., Yue, Y., Ng, A., Kamiyama, D., Huang, B., Verhey, K.J., and Wildonger, J. (2018). Autoinhibition of kinesin-1 is essential to the dendrite-specific localization of Golgi outposts. *J. Cell Biol.* *217*, 2531–2547.
- Keough, M.B., Rogers, J.A., Zhang, P., Jensen, S.K., Stephenson, E.L., Chen, T., Hurlbert, M.G., Lau, L.W., Rawji, K.S., Plemel, J.R., Koch, M., Ling, C.C., Yong, V.W. (2016). An inhibitor of chondroitin sulfate proteoglycan synthesis promotes central nervous system remyelination. *Nat Commun* *7*, 11312.
- Kern, J.V., Zhang, Y.V., Kramer, S., Brenman, J.E., and Rasse, T.M. (2013). The kinesin-3, unc-104 regulates dendrite morphogenesis and synaptic development in *Drosophila*. *Genetics* *195*, 59–72.
- Kerschensteiner, M., Schwab, M.E., Lichtman, J.W., and Misgeld, T. (2005). *In vivo* imaging of axonal degeneration and regeneration in the injured spinal cord. *Nat. Med.* *11*, 572–577.
- Kim, M.E., Shrestha, B.R., Blazeski, R., Mason, C.A., and Grueber, W.B. (2012). Integrins establish dendrite-substrate relationships that promote dendritic self-avoidance and patterning in *Drosophila* sensory neurons. *Neuron* *73*, 79–91.
- Koleske, A.J. (2013). Molecular mechanisms of dendrite stability. *Nat. Rev. Neurosci.* *14*, 536–550.

- Kravtsov, V., Oren-Suissa, M., and Podbilewicz, B. (2017). The fusogen AFF-1 can rejuvenate the regenerative potential of adult dendritic trees by self-fusion. *Development* *144*, 2364–2374.
- Krupp, J.J., and Levine, J.D. (2010). Dissection of oenocytes from adult *Drosophila melanogaster*. *J Vis Exp*.
- Krylova, O., Herreros, J., Cleverley, K.E., Ehler, E., Henriquez, J.P., Hughes, S.M., and Salinas, P.C. (2002). WNT-3, expressed by motoneurons, regulates terminal arborization of neurotrophin-3-responsive spinal sensory neurons. *Neuron* *35*, 1043–1056.
- Kuleesha, Y., Puah, W.C., and Wasser, M. (2016). Live imaging of muscle histolysis in *Drosophila* metamorphosis. *BMC Dev. Biol.* *16*, 12.
- Kuo, C.T., Jan, L.Y., and Jan, Y.N. (2005). Dendrite-specific remodeling of *Drosophila* sensory neurons requires matrix metalloproteases, ubiquitin-proteasome, and ecdysone signaling. *Proc. Natl. Acad. Sci. U.S.A.* *102*, 15230–15235.
- Kuo, C.T., Zhu, S., Younger, S., Jan, L.Y., and Jan, Y.N. (2006). Identification of E2/E3 ubiquitinating enzymes and caspase activity regulating *Drosophila* sensory neuron dendrite pruning. *Neuron* *51*, 283–290.
- Kusche-Gullberg, M., Garrison, K., MacKrell, A.J., Fessler, L.I., and Fessler, J.H. (1992). Laminin A chain: expression during *Drosophila* development and genomic sequence. *EMBO J.* *11*, 4519–4527.
- Kwon, J.Y., Dahanukar, A., Weiss, L.A., and Carlson, J.R. (2007). The molecular basis of CO₂ reception in *Drosophila*. *Proc. Natl. Acad. Sci. U.S.A.* *104*, 3574–3578.
- Lee, S.B., Bagley, J.A., Lee, H.Y., Jan, L.Y., and Jan, Y.-N. (2011). Pathogenic polyglutamine proteins cause dendrite defects associated with specific actin cytoskeletal alterations in *Drosophila*. *Proc. Natl. Acad. Sci. U.S.A.* *108*, 16795–16800.
- Lemons, M.L., and Condic, M.L. (2008). Integrin signaling is integral to regeneration. *Exp. Neurol.* *209*, 343–352.
- Lin, S., Liu, M., Mozgova, O.I., Yu, W., and Baas, P.W. (2012). Mitotic motors coregulate microtubule patterns in axons and dendrites. *J. Neurosci.* *32*, 14033–14049.
- Lipka, J., Kapitein, L.C., Jaworski, J., and Hoogenraad, C.C. (2016). Microtubule-binding protein doublecortin-like kinase 1 (DCLK1) guides kinesin-3-mediated cargo transport to dendrites. *EMBO J.* *35*, 302–318.
- Liu, K., Lu, Y., Lee, J.K., Samara, R., Willenberg, R., Sears-Kraxberger, I., Tedeschi, A., Park, K.K., Jin, D., Cai, B., Xu, B., Connolly, L., Steward, O., Zheng, B., He, Z. (2010). PTEN deletion enhances the regenerative ability of adult corticospinal neurons. *Nat. Neurosci.* *13*, 1075–1081.
- Liz, M.A., Mar, F.M., Santos, T.E., Pimentel, H.I., Marques, A.M., Morgado, M.M., Vieira, S., Sousa, V.F., Pemble, H., Wittmann, T., Sutherland, C., Woodgett, J.R., Sousa, M.M. (2014).

Neuronal deletion of GSK3 β increases microtubule speed in the growth cone and enhances axon regeneration via CRMP-2 and independently of MAP1B and CLASP2. *BMC Biol.* *12*, 47.

Llano, E., Adam, G., Pendás, A.M., Quesada, V., Sánchez, L.M., Santamariá, I., Noselli, S., and López-Otín, C. (2002). Structural and enzymatic characterization of *Drosophila* Dm2-MMP, a membrane-bound matrix metalloproteinase with tissue-specific expression. *J. Biol. Chem.* *277*, 23321–23329.

Losick, V.P., Fox, D.T., and Spradling, A.C. (2013). Polyploidization and cell fusion contribute to wound healing in the adult *Drosophila* epithelium. *Curr. Biol.* *23*, 2224–2232.

Lucas, F.R., Goold, R.G., Gordon-Weeks, P.R., and Salinas, P.C. (1998). Inhibition of GSK-3 β leading to the loss of phosphorylated MAP-1B is an early event in axonal remodeling induced by WNT-7a or lithium. *J. Cell. Sci.* *111 (Pt 10)*, 1351–1361.

Luo, X., and Park, K.K. (2012). Neuron-intrinsic inhibitors of axon regeneration: PTEN and SOCS3. *Int. Rev. Neurobiol.* *105*, 141–173.

Lyons, G.R., Andersen, R.O., Abdi, K., Song, W.-S., and Kuo, C.T. (2014). Cysteine proteinase-1 and cut protein isoform control dendritic innervation of two distinct sensory fields by a single neuron. *Cell Rep* *6*, 783–791.

Madhavan, M.M., and Madhavan, K. (1980). Morphogenesis of the epidermis of adult abdomen of *Drosophila*. *J Embryol Exp Morphol* *60*, 1–31.

Matsubayashi, Y., Louani, A., Dragu, A., Sánchez-Sánchez, B.J., Serna-Morales, E., Yolland, L., Gyöergy, A., Vizcay, G., Fleck, R.A., Heddleston, J.M., Chew, T.L., Siekhaus, D.E., Stramer, B.M. (2017). A Moving Source of Matrix Components Is Essential for De Novo Basement Membrane Formation. *Curr. Biol.* *27*, 3526-3534.e4.

Mauthner, S.E., Hwang, R.Y., Lewis, A.H., Xiao, Q., Tsubouchi, A., Wang, Y., Honjo, K., Skene, J.H.P., Grandl, J., and Tracey, W.D. (2014). Balboa binds to pickpocket *in vivo* and is required for mechanical nociception in *Drosophila* larvae. *Curr. Biol.* *24*, 2920–2925.

McKeon, R.J., Schreiber, R.C., Rudge, J.S., and Silver, J. (1991). Reduction of neurite outgrowth in a model of glial scarring following CNS injury is correlated with the expression of inhibitory molecules on reactive astrocytes. *J. Neurosci.* *11*, 3398–3411.

McLaughlin, C.N., Nechipurenko, I.V., Liu, N., Broihier, H.T. (2016). A Toll receptor-FoxO pathway represses Pavarotti/MKLP1 to promote microtubule dynamics in motoneurons. *J Cell Biol* *214*, 459-474.

Medina, P.M.B., Swick, L.L., Andersen, R., Blalock, Z., and Brenman, J.E. (2006). A novel forward genetic screen for identifying mutations affecting larval neuronal dendrite development in *Drosophila melanogaster*. *Genetics* *172*, 2325–2335.

Meltzer, S., Yadav, S., Lee, J., Soba, P., Younger, S.H., Jin, P., Zhang, W., Parrish, J., Jan, L.Y., and Jan, Y.-N. (2016). Epidermis-Derived Semaphorin Promotes Dendrite Self-Avoidance by

- Regulating Dendrite-Substrate Adhesion in *Drosophila* Sensory Neurons. *Neuron* 89, 741–755.
- Miller, C.M., Page-McCaw, A., and Broihier, H.T. (2008). Matrix metalloproteinases promote motor axon fasciculation in the *Drosophila* embryo. *Development* 135, 95–109.
- Moon, L.D.F., Asher, R.A., Rhodes, K.E., and Fawcett, J.W. (2002). Relationship between sprouting axons, proteoglycans and glial cells following unilateral nigrostriatal axotomy in the adult rat. *Neuroscience* 109, 101–117.
- Morrison, E.E., and Costanzo, R.M. (1995). Regeneration of olfactory sensory neurons and reconnection in the aging hamster central nervous system. *Neurosci. Lett.* 198, 213–217.
- Nechipurenko, I.V., and Broihier, H.T. (2012). FoxO limits microtubule stability and is itself negatively regulated by microtubule disruption. *J. Cell Biol.* 196, 345–362.
- Ninov, N., Chiarelli, D.A., and Martín-Blanco, E. (2007). Extrinsic and intrinsic mechanisms directing epithelial cell sheet replacement during *Drosophila* metamorphosis. *Development* 134, 367–379.
- Oren-Suissa, M., Gattegno, T., Kravtsov, V., and Podbilewicz, B. (2017). Extrinsic Repair of Injured Dendrites as a Paradigm for Regeneration by Fusion in *Caenorhabditis elegans*. *Genetics* 206, 215–230.
- Ori-McKenney, K.M., Jan, L.Y., and Jan, Y.-N. (2012). Golgi outposts shape dendrite morphology by functioning as sites of acentrosomal microtubule nucleation in neurons. *Neuron* 76, 921–930.
- Owen, R., and Gordon-Weeks, P.R. (2003). Inhibition of glycogen synthase kinase 3beta in sensory neurons in culture alters filopodia dynamics and microtubule distribution in growth cones. *Mol. Cell. Neurosci.* 23, 626–637.
- Pack-Chung, E., Kurshan, P.T., Dickman, D.K., and Schwarz, T.L. (2007). A *Drosophila* kinesin required for synaptic bouton formation and synaptic vesicle transport. *Nat. Neurosci.* 10, 980–989.
- Page-McCaw, A., Serano, J., Santé, J.M., and Rubin, G.M. (2003). *Drosophila* matrix metalloproteinases are required for tissue remodeling, but not embryonic development. *Dev. Cell* 4, 95–106.
- Park, K.K., Liu, K., Hu, Y., Smith, P.D., Wang, C., Cai, B., Xu, B., Connolly, L., Kramvis, I., Sahin, M., He, Z. (2008). Promoting axon regeneration in the adult CNS by modulation of the PTEN/mTOR pathway. *Science* 322, 963–966.
- Park, K.K., Liu, K., Hu, Y., Kanter, J.L., and He, Z. (2010). PTEN/mTOR and axon regeneration. *Exp. Neurol.* 223, 45–50.
- Park, K.W., Lin, C.-Y., Li, K., and Lee, Y.-S. (2015). Effects of Reducing Suppressors of Cytokine Signaling-3 (SOCS3) Expression on Dendritic Outgrowth and Demyelination after

Spinal Cord Injury. PLoS ONE 10, e0138301.

Parrish, J.Z., Xu, P., Kim, C.C., Jan, L.Y., and Jan, Y.N. (2009). The microRNA bantam functions in epithelial cells to regulate scaling growth of dendrite arbors in *Drosophila* sensory neurons. *Neuron* 63, 788–802.

Pastor-Pareja, J.C., and Xu, T. (2011). Shaping cells and organs in *Drosophila* by opposing roles of fat body-secreted Collagen IV and Perlecan. *Dev. Cell* 21, 245–256.

Plantman, S. (2012). Integrin manipulation to improve regeneration. *Cell Adh Migr* 6, 451–453.

Poe, A.R., Tang, L., Wang, B., Li, Y., Sapar, M.L., and Han, C. (2017) Dendrite space-filling requires a neuronal type-specific extracellular permissive signal in *Drosophila*. *Proc Natl Acad Sci U S A*. 114(38): E8062-E8071.

Puram, S.V., and Bonni, A. (2013). Cell-intrinsic drivers of dendrite morphogenesis. *Development* 140, 4657–4671.

Rao, A.N., and Baas, P.W. (2018). Polarity Sorting of Microtubules in the Axon. *Trends Neurosci.* 41, 77–88.

Rao, K., Stone, M.C., Weiner, A.T., Gheres, K.W., Zhou, C., Deitcher, D.L., Levitan, E.S., and Rolls, M.M. (2016). Spastin, atlastin, and ER relocalization are involved in axon but not dendrite regeneration. *Mol. Biol. Cell* 27, 3245–3256.

Rolls, M.M., Satoh, D., Clyne, P.J., Henner, A.L., Uemura, T., and Doe, C.Q. (2007). Polarity and intracellular compartmentalization of *Drosophila* neurons. *Neural Dev* 2, 7.

Ruschel J., Hellal, F., Flynn, K.C., Dupraz, S., Elliot, E.A., Tedeschi, A., Bates, M., Sliwinski, C., Brook, G., Dobrint, K., Peitz, M., Brustle, O., Norenberg, M.D., Blesch, A., Weidner, N., Bartlett Bunge, M., Bixby, J.L., Bradke, F. (2015) Systematic administration of Epothilone B promotes axon regeneration and functional recovery after spinal cord injury. *Science* 348, 347-352.

Saijilafu, Hur, E.-M., Liu, C.-M., Jiao, Z., Xu, W.-L., and Zhou, F.-Q. (2013). PI3K-GSK3 signaling regulates mammalian axon regeneration by inducing the expression of Smad1. *Nat Commun* 4, 2690.

Sanes, J.R., and Chiu, A.Y. (1983). The basal lamina of the neuromuscular junction. *Cold Spring Harb. Symp. Quant. Biol.* 48 Pt 2, 667–678.

Satoh, D., Suyama, R., Kimura, K., and Uemura, T. (2012). High-resolution *in vivo* imaging of regenerating dendrites of *Drosophila* sensory neurons during metamorphosis: local filopodial degeneration and heterotypic dendrite-dendrite contacts. *Genes Cells* 17, 939–951.

Sears, J.C., and Broihier, H.T. (2016). FoxO regulates microtubule dynamics and polarity to promote dendrite branching in *Drosophila* sensory neurons. *Dev. Biol.* 418, 40–54.

- Sharma, H.S., and Olsson, Y. (1990). Edema formation and cellular alterations following spinal cord injury in the rat and their modification with p-chlorophenylalanine. *Acta Neuropathol.* 79, 604–610.
- Sharma, K., Selzer, M.E., and Li, S. (2012). Scar-mediated inhibition and CSPG receptors in the CNS. *Exp. Neurol.* 237, 370–378.
- Shimono, K., Fujimoto, A., Tsuyama, T., Yamamoto-Kochi, M., Sato, M., Hattori, Y., Sugimura, K., Usui, T., Kimura, K., and Uemura, T. (2009). Multidendritic sensory neurons in the adult *Drosophila* abdomen: origins, dendritic morphology, and segment- and age-dependent programmed cell death. *Neural Dev* 4, 37.
- Shin, J.E., Cho, Y., Beirowski, B., Milbrandt, J., Cavalli, V., and DiAntonio, A. (2012). Dual leucine zipper kinase is required for retrograde injury signaling and axonal regeneration. *Neuron* 74, 1015–1022.
- Siebert, J.R., and Osterhout, D.J. (2011). The inhibitory effects of chondroitin sulfate proteoglycans on oligodendrocytes. *J. Neurochem.* 119, 176–188.
- Smith, P.D., Sun, F., Park, K.K., Cai, B., Wang, C., Kuwako, K., Martinez-Carrasco, I., Connolly, L., and He, Z. (2009). SOCS3 deletion promotes optic nerve regeneration *in vivo*. *Neuron* 64, 617–623.
- Snow, D.M., Atkinson, P.B., Hassinger, T.D., Letourneau, P.C., and Kater, S.B. (1994). Chondroitin sulfate proteoglycan elevates cytoplasmic calcium in DRG neurons. *Dev. Biol.* 166, 87–100.
- Soares, L., Parisi, M., and Bonini, N.M. (2014). Axon injury and regeneration in the adult *Drosophila*. *Sci Rep* 4, 6199.
- Soba, P., Han, C., Zheng, Y., Perea, D., Miguel-Aliaga, I., Jan, L.Y., and Jan, Y.N. (2015). The Ret receptor regulates sensory neuron dendrite growth and integrin mediated adhesion. *Elife* 4.
- Song, Y., Ori-McKenney, K.M., Zheng, Y., Han, C., Jan, L.Y., and Jan, Y.N. (2012). Regeneration of *Drosophila* sensory neuron axons and dendrites is regulated by the Akt pathway involving Pten and microRNA bantam. *Genes Dev.* 26, 1612–1625.
- Steinmetz, M.P., Horn, K.P., Tom, V.J., Miller, J.H., Busch, S.A., Nair, D., Silver, D.J., and Silver, J. (2005). Chronic enhancement of the intrinsic growth capacity of sensory neurons combined with the degradation of inhibitory proteoglycans allows functional regeneration of sensory axons through the dorsal root entry zone in the mammalian spinal cord. *J. Neurosci.* 25, 8066–8076.
- Stepanova, T., Slemmer, J., Hoogenraad, C.C., Lansbergen, G., Dortland, B., De Zeeuw, C.I., Grosveld, F., van Cappellen, G., Akhmanova, A., and Galjart, N. (2003). Visualization of microtubule growth in cultured neurons via the use of EB3-GFP (end-binding protein 3-green fluorescent protein). *J. Neurosci.* 23, 2655–2664.

- Stevens, L.J., and Page-McCaw, A. (2012). A secreted MMP is required for reepithelialization during wound healing. *Mol. Biol. Cell* 23, 1068–1079.
- Stone, M.C., Roegiers, F., and Rolls, M.M. (2008). Microtubules have opposite orientation in axons and dendrites of *Drosophila* neurons. *Mol. Biol. Cell* 19, 4122–4129.
- Stone, M.C., Albertson, R.M., Chen, L., and Rolls, M.M. (2014). Dendrite injury triggers DLK-independent regeneration. *Cell Rep* 6, 247–253.
- Suh, G.S.B., Wong, A.M., Hergarden, A.C., Wang, J.W., Simon, A.F., Benzer, S., Axel, R., and Anderson, D.J. (2004). A single population of olfactory sensory neurons mediates an innate avoidance behavior in *Drosophila*. *Nature* 431, 854–859.
- Sun, F., Park, K.K., Belin, S., Wang, D., Lu, T., Chen, G., Zhang, K., Yeung, C., Feng, G., Yankner, B.A., He, Z. (2011). Sustained axon regeneration induced by co-deletion of PTEN and SOCS3. *Nature* 480, 372–375.
- Tan, C.L., Kwok, J.C.F., Patani, R., Ffrench-Constant, C., Chandran, S., and Fawcett, J.W. (2011). Integrin activation promotes axon growth on inhibitory chondroitin sulfate proteoglycans by enhancing integrin signaling. *J. Neurosci.* 31, 6289–6295.
- Tan, C.L., Andrews, M.R., Kwok, J.C.F., Heintz, T.G.P., Gumy, L.F., Fässler, R., and Fawcett, J.W. (2012). Kindlin-1 enhances axon growth on inhibitory chondroitin sulfate proteoglycans and promotes sensory axon regeneration. *J. Neurosci.* 32, 7325–7335.
- Tas, R.P., Chazeau, A., Cloin, B.M.C., Lambers, M.L.A., Hoogenraad, C.C., and Kapitein, L.C. (2017). Differentiation between Oppositely Oriented Microtubules Controls Polarized Neuronal Transport. *Neuron* 96, 1264-1271.e5.
- Tedeschi, A., and Bradke, F. (2013). The DLK signaling pathway--a double-edged sword in neural development and regeneration. *EMBO Rep.* 14, 605–614.
- Terenzio, M., Schiavo, G., and Fainzilber, M. (2017). Compartmentalized Signaling in Neurons: From Cell Biology to Neuroscience. *Neuron* 96, 667–679.
- Thompson-Peer, K.L., DeVault, L., Li, T., Jan, L.Y., and Jan, Y.N. (2016). *In vivo* dendrite regeneration after injury is different from dendrite development. *Genes Dev.* 30, 1776–1789.
- Tracey, W.D., Wilson, R.I., Laurent, G., and Benzer, S. (2003). Painless, a *Drosophila* gene essential for nociception. *Cell* 113, 261–273.
- Valakh, V., Frey, E., Babetto, E., Walker, L.J., and DiAntonio, A. (2015). Cytoskeletal disruption activates the DLK/JNK pathway, which promotes axonal regeneration and mimics a preconditioning injury. *Neurobiol. Dis.* 77, 13–25.
- Valenzuela, J.I., and Perez, F. (2015). Diversifying the secretory routes in neurons. *Front Neurosci* 9, 358.

- Van De Bor, V., Zimniak, G., Papone, L., Cerezo, D., Malbouyres, M., Juan, T., Ruggiero, F., and Noselli, S. (2015). Companion Blood Cells Control Ovarian Stem Cell Niche Microenvironment and Homeostasis. *Cell Rep* 13, 546–560.
- Vickers, J.C., Mitew, S., Woodhouse, A., Fernandez-Martos, C.M., Kirkcaldie, M.T., Canty, A.J., McCormack, G.H., and King, A.E. (2016). Defining the earliest pathological changes of Alzheimer’s disease. *Curr Alzheimer Res* 13, 281–287.
- Vogelezang, M.G., Liu, Z., Relvas, J.B., Raivich, G., Scherer, S.S., and French-Constant, C. (2001). Alpha4 integrin is expressed during peripheral nerve regeneration and enhances neurite outgrowth. *J. Neurosci.* 21, 6732–6744.
- Wang, X., and Page-McCaw, A. (2014). A matrix metalloproteinase mediates long-distance attenuation of stem cell proliferation. *J. Cell Biol.* 206, 923–936.
- Wang, X., Zhang, M.W., Kim, J.H., Macara, A.M., Sterne, G., Yang, T., and Ye, B. (2015). The Krüppel-Like Factor Dar1 Determines Multipolar Neuron Morphology. *J. Neurosci.* 35, 14251–14259.
- Wasserman, S., Salomon, A., and Frye, M.A. (2013). *Drosophila* tracks carbon dioxide in flight. *Curr. Biol.* 23, 301–306.
- Wehner, D., Tsarouchas, T.M., Michael, A., Haase, C., Weidinger, G., Reimer, M.M., Becker, T., and Becker, C.G. (2017). Wnt signaling controls pro-regenerative Collagen XII in functional spinal cord regeneration in zebrafish. *Nat Commun* 8, 126.
- Williams, D.W., and Truman, J.W. (2005a). Remodeling dendrites during insect metamorphosis. *J. Neurobiol.* 64, 24–33.
- Williams, D.W., and Truman, J.W. (2005b). Cellular mechanisms of dendrite pruning in *Drosophila*: insights from *in vivo* time-lapse of remodeling dendritic arborizing sensory neurons. *Development* 132, 3631–3642.
- Williams, P.R., Marincu, B.-N., Sorbara, C.D., Mahler, C.F., Schumacher, A.-M., Griesbeck, O., Kerschensteiner, M., and Misgeld, T. (2014). A recoverable state of axon injury persists for hours after spinal cord contusion *in vivo*. *Nat Commun* 5, 5683.
- Winding, M., Kelliher, M.T., Lu, W., Wildonger, J., and Gelfand, V.I. (2016). Role of kinesin-1–based microtubule sliding in *Drosophila* nervous system development. *Proc Natl Acad Sci U S A* 113, E4985–E4994.
- Xiang, Y., Yuan, Q., Vogt, N., Looger, L.L., Jan, L.Y., and Jan, Y.N. (2010). Light-avoidance-mediating photoreceptors tile the *Drosophila* larval body wall. *Nature* 468, 921–926.
- Yan, D., Wu, Z., Chisholm, A.D., and Jin, Y. (2009). The DLK-1 kinase promotes mRNA stability and local translation in *C. elegans* synapses and axon regeneration. *Cell* 138, 1005–1018.

- Yan, Z., Zhang, W., He, Y., Gorczyca, D., Xiang, Y., Cheng, L.E., Meltzer, S., Jan, L.Y., and Jan, Y.N. (2013). *Drosophila* NOMPC is a mechanotransduction channel subunit for gentle-touch sensation. *Nature* 493, 221–225.
- Yasothornsrikul, S., Davis, W.J., Cramer, G., Kimbrell, D.A., and Dearolf, C.R. (1997). viking: identification and characterization of a second type IV collagen in *Drosophila*. *Gene* 198, 17–25.
- Yasunaga, K., Tezuka, A., Ishikawa, N., Dairyo, Y., Togashi, K., Koizumi, H., and Emoto, K. (2015). Adult *Drosophila* sensory neurons specify dendritic territories independently of dendritic contacts through the Wnt5-Drl signaling pathway. *Genes Dev.* 29, 1763–1775.
- Yau, K.W., Schätzle, P., Tortosa, E., Pagès, S., Holtmaat, A., Kapitein, L.C., and Hoogenraad, C.C. (2016). Dendrites *In Vitro* and *In Vivo* Contain Microtubules of Opposite Polarity and Axon Formation Correlates with Uniform Plus-End-Out Microtubule Orientation. *J. Neurosci.* 36, 1071–1085.
- Ye, B., Zhang, Y., Song, W., Younger, S.H., Jan, L.Y., and Jan, Y.N. (2007). Growing dendrites and axons differ in their reliance on the secretory pathway. *Cell* 130, 717–729.
- Ye, S., Fowler, T.W., Pavlos, N.J., Ng, P.Y., Liang, K., Feng, Y., Zheng, M., Kurten, R., Manolagas, S.C., and Zhao, H. (2011). LIS1 regulates osteoclast formation and function through its interactions with dynein/dynactin and Plekhm1. *PLoS ONE* 6, e27285.
- Yick, L.-W., So, K.-F., Cheung, P.-T., and Wu, W.-T. (2004). Lithium chloride reinforces the regeneration-promoting effect of chondroitinase ABC on rubrospinal neurons after spinal cord injury. *J. Neurotrauma* 21, 932–943.
- Zhang, J., Yang, D., Huang, H., Sun, Y., Hu, Y. (2018). Coordination of necessary and permissive signals by PTEN inhibition for CNS axon regeneration. *Front Neurosci* 12, 558.
- Zhang, Y.V., Hannan, S.B., Stapper, Z.A., Kern, J.V., Jahn, T.R., and Rasse, T.M. (2016). The *Drosophila* KIF1A Homolog unc-104 Is Important for Site-Specific Synapse Maturation. *Front Cell Neurosci* 10, 207.
- Zhao, R.-R., and Fawcett, J.W. (2013). Combination treatment with chondroitinase ABC in spinal cord injury--breaking the barrier. *Neurosci Bull* 29, 477–483.
- Zheng, Y., Wildonger, J., Ye, B., Zhang, Y., Kita, A., Younger, S.H., Zimmerman, S., Jan, L.Y., and Jan, Y.N. (2008). Dynein is required for polarized dendritic transport and uniform microtubule orientation in axons. *Nat. Cell Biol.* 10, 1172–1180.
- Zhou, F.C., Azmitia, E.C., and Bledsoe, S. (1995). Rapid serotonergic fiber sprouting in response to ibotenic acid lesion in the striatum and hippocampus. *Brain Res. Dev. Brain Res.* 84, 89–98.
- Zhou, W., Chang, J., Wang, X., Savelieff, M.G., Zhao, Y. and Ye, B. (2014). GM130 is required for compartmental organization of dendritic Golgi outposts. *Curr. Biol.* 24, 1227–1233.
- Zong, W., Wang, Y., Tang, Q., Zhang, H., Yu, F. (2018). Prd1 associates with the clathrin

adaptor α -Adaptin and the kinesin-3 Imac/Unc-104 to govern dendrite pruning in *Drosophila*. *PLoS Biol* 16(8).

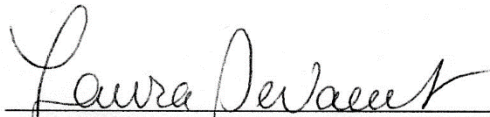
Zukor, K., Belin, S., Wang, C., Keelan, N., Wang, X., and He, Z. (2013). Short hairpin RNA against PTEN enhances regenerative growth of corticospinal tract axons after spinal cord injury. *J. Neurosci.* 33, 15350–15361.

Publishing Agreement

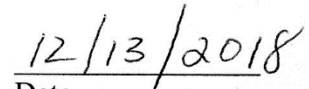
It is the policy of the University to encourage the distribution of all theses, dissertations, and manuscripts. Copies of all UCSF theses, dissertations, and manuscripts will be routed to the library via the Graduate Division. The library will make all theses, dissertations, and manuscripts accessible to the public and will preserve these to the best of their abilities, in perpetuity.

Please sign the following statement:

I hereby grant permission to the Graduate Division of the University of California, San Francisco to release copies of my thesis, dissertation, or manuscript to the Campus Library to provide access and preservation, in whole or in part, in perpetuity.



Author Signature



Date